LBL-13309

Lawrence Berkeley Laboratory
UNIVERSITY OF CALIFORNIA

Materials & Molecular
Research Division

THE EFFECT OF VIBRATIONAL EXCITATION ON THE DYNAMICS OF ION-MOLECULE REACTIONS

Scott Law Anderson
(Ph.D. thesis)

November 1981

Prepared for the U.S. Department of Energy under Contract W-7405-ENG-48

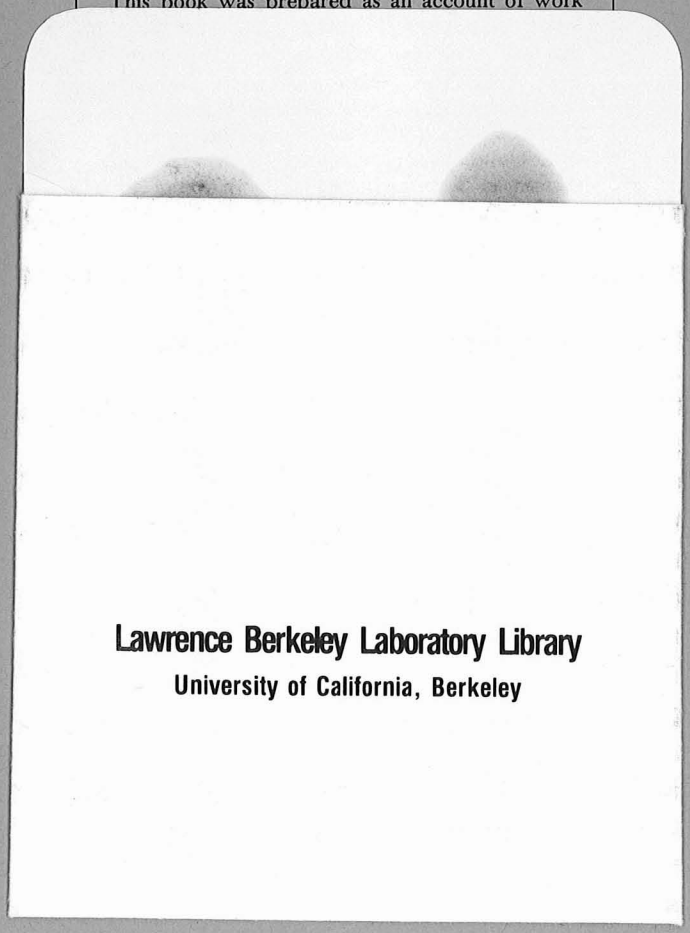

THE EFFECT OF VIBRATIONAL EXCITATION ON THE DYNAMICS OF ION-MOLECULE REACTIONS

Scott Law Anderson

Materials and Molecular Research Division
Lawrence Berkeley Laboratory
and Department of Chemistry
University of California
Berkeley, CA 94720

ABSTRACT

A new experimental technique for the study of vibrational effects on ion-molecule reaction cross sections is described. Vibrational and collision energy dependent cross sections are presented for proton and H atom transfer, charge transfer and collision induced dissociation reactions in various isotopic $H_2^+ + H_2$ systems. Charge and proton transfer cross sections are presented for the reactions of H_2^+ and D_2^+ with Ar, N_2, CO, and O_2. All the reactions are shown to be highly influenced by avoided crossings between the ground and first excited potential energy surfaces. Because of the nature of the crossings, vibrational motion of the systems can cause both adiabatic and non-adiabatic behavior of the system. This makes the vibrational dependences of the various cross sections a very sensitive probe of the dynamics of the collisions particularly, their behavior in the region of the crossings. Evidence is seen for charge transfer between reagents as they approach each other, transition to and in some cases reactions on excited potential energy surfaces, competition between different channels, and strong coupling of proton and charge transfer

channels which occurs only for two of the systems studied (H_2^+ + Ar, N_2). Oscillatory structure is observed in the collision energy dependence of the endoergic H_2^+ (v = 0) + Ar charge transfer reaction for the first time, and a simple model which is commonly used for atom-atom charge transfer is used to fit the peaks. Finally a simple model is used to assess the importance of energy resonance and "Franck-Condon" effects on molecular charge transfer.

THE EFFECT OF VIBRATIONAL EXCITATION ON THE DYNAMICS OF ION-MOLECULE REACTIONS

Contents

ACKNOWLEDGMENTS

My thanks go to my co-workers on this experiments. Dieter Gerlich designed a fair fraction of the machine and contributed new technology and many design tricks which have proved essential in some cases and highly convenient in others. His experience and patience made the experiment possible, and his friendship made the work very enjoyable. Frances Houle shared many frustrating moments and aided in collecting a lot of data. Tom Turner worked hard taking and analyzing a mound of data and with Odile Dutuit will presumably keep pushing the experiment along.

I owe a great deal to Yuan Lee for trusting me and my co-workers enough to provide a great deal of support for the experiment, and for using his knowledge and skills, both personal and scientific, to smooth out many of the rough edges we ran into.

While on the subject of rough edges, I should thank the other members of the Lee group for teaching me many things, most of them useful, and for making my graduate career most entertaining.

Ann Weightman was extremely helpful in circumventing many bureaucratic obstacles, and in deciphering and preparing manuscripts. Her knowledge of how to get things done at LBL has saved me and my cohorts many hours of beating our heads on the walls, and her tolerance (enjoyment ?) of our ways of having fun does much to make life pleasant for the group.

The number of other helpful people who I have run into on campus and at LBL precludes mentioning them individually. I hope their feelings toward me are just as warm as mine are for them.

Finally, I thank Donna for putting up with me, and for making and helping me see that life is more pleasant and full than it has seemed at times.

I would like to acknowledge the support of a National Science Foundation Graduate Fellowship.

This work was supported by the Director, Office of Energy Research, Office of Basic Energy Sciences, Chemical Sciences Division of the U. S. Department of Energy under Contract Number W-7405-ENG-48.

I. GENERAL INTRODUCTION

The study of vibrational effects on reactivity and on the dynamics of reactions has been pursued for many years. In neutral reactions, the observed effects are generally well understood. Polanyi[1] has shown for example, that in reactions which have barriers in the exit channel (typical of endoergic reactions) vibrational motion increases the probability of surmounting the barrier. Experimental evidence[2] shows that at least near threshold, vibrational energy indeed is very effective in promoting endoergic reactions. In general it seems that most vibrational effects on neutral reactions are primarily due to the increased nuclear motion.

The effects of vibration on ion-molecule reactions are more complicated. While many neutral reactions are governed by a single potential energy surface (PES), nearly all ion-molecule systems have at least two low lying potential surfaces corresponding to $A^+ + B$ and $A + B^+$, and possibly several more. These surfaces have crossings and avoided crossings, and except for cases like $H_2^+ + He$, where the first excited PES lies far above the $H_2^+ + He$ ground PES, transitions between different surfaces and different electronic configurations of the systems are likely. Consider $A^+ + BC$, where A and BC have similar ionization potentials. In this case there are two electronic states of the system ($A^+ + BC$ and $A + BC^+$) lying very close together. Figure 1a shows a cut along the BC stretch coordinate through the entrance channel of an $A^+ + BC$ collision. The reaction coordinate is into the plane of the figure. At infinite reagent separation, the

two PES cross and there is no mixing between charge states. As the reagents come together, the two charge states, which are of the same symmetry, begin to mix and the crossing becomes avoided. Initially the interaction is weak and the motion of the system, including the BC vibration remains on the diabatic $A^+ + BC$ potential surface (1b). As the reagent separation decreases, the mixing becomes stronger (1c) and the splitting between the two new adiabatic surfaces created by the avoided crossing becomes larger. At this point, motion of the system through the avoided crossing seam (the surface of intersection between the two multi-dimensional PES's) can be either diabatic (retaining the same electronic configuration or adiabatic (remaining on the same PES). This allows the possibility of transitions between the two reagent charge states and between the ground PES and the excited adiabatic PES. Figure 1d shows the potential curves when the reagents are close together. Here the motion is again strictly on a single PES, since the surface splitting is too large to allow transitions. Thus as the reagents approach each other through the entrance channel, vibrational motion couples the two charge states and also can cause hopping to the excited PES. These electronic effects induced by the vibrational motion can far outweigh the simple nuclear motion effects.

This type of behavior has been studied theoretically for $H_2^+ + H_2$ (Ref. 3) and $A_r^+ + H_2$ (Ref. 4). Measurements of the effects of both collision and vibrational energy on reaction cross sections

and branching ratios for H_2^+ and H_2 and H_2^+ + Ar provide a very sensitive probe of the above picture and can be used in conjunction with theory to map out the reaction dynamics in some detail.

In ion-molecule reactions, quite frequently one or more of the reagents is vibrationally excited. This is because the most common method of ion preparation, electron impact, leaves the ion in a roughly Franck-Condon distribution of vibrational states, and except for favorable cases like N_2 and CO, many vibrational states are populated. In H_2^+, for instance, ions are formed in vibrational states from v = 0 to the dissociation limit (V = 17), with the distribution peaking at V = 2.[5] Many studies have been carried out in which some attempt is made at studying vibrational effects by varying the ionizing electron energy and thus the distribution of vibrational states formed.[6] These studies, while interesting, have not been able to provide much dynamical information.

The use of photoionization to prepare partially state selected ions and study their reactions has been more successful in this respect. This technique was pioneered by Chupka et al.[7] Current research in this field by Tanaka et al.[8] and Campbell et al.[9] as well as the present work has considerably extended Chupka's original work and promises to increase our understanding of ion-molecule reaction dynamics.

The experimental design used in our study will be explained in detail and then results for each reactive system will be presented. Background information for the individual systems will be discussed in the introduction to each chapter.

Chapter I

REFERENCES

1. D. S. Perry, J. C. Polanyi, C. W. Wilson, Jr., Chem. Phys. 3, 317 (1974); J. C. Polanyi, N. Sathyamurthy, Chem. Phys. 33, 287 (1978); J. C. Polanyi, N. Sathyamurthy, Chem. Phys. 37, 259 (1979); A. M. G. Ding, L. J. Kirsh, D. S. Perry, J. C. Polanyi, J. L. Schreiber, Faraday Disc. Chem. Soc. 55, 252 (1973).
2. J. G. Pruett, F. R. Grabiner, P. R. Brooks, J. Chem. Phys. 63, 1173 (1975); H. H. Dispert, M. W. Geis, P. R. Brooks, J. Chem. Phys. 70, 5317 (1979); D. J. Douglas, J. C. Polanyi, J. J. Sloan, Chem. Phys. 13, 15 (1976); A. Gupta, D. S. Perry, R. N. Zare, J. Chem. Phys. 72, 6250 (1980).
3. J. R. Krenos, K. K. Lehman, J. C. Tully, P. M. Hierl, G. P. Smith, Chem. Phys. 16, 109 (1976); J. R. Stine, J. T. Muckerman, J. Chem. Phys. 68, 185 (1978).
4. S. Chapman and R. K. Preston, J. Chem. Phys. 60, 650 (1974); M. Baer, J. A. Beswick, Phys. Rev. A 19, 1559 (1979).
5. Franck-Condon distribution from J. A. R. Sampson J. Elec. Spec. 8, 123 (1976).
6. For an excellent review see T. O. Tiernan, C. Lifshitz in The Excited State in Chemical Physics Part 2, Wiley, New York, p. 82 (1981).
7. W. A. Chupka in Ion Molecule Reactions, J. Franklin ed Plenum, New York, 1972.
8. I. Koyano, K. Tanaka, J. Chem. Phys. 72, 4858 (1980).
9. F. M. Campbell, R. Browning, C. J. Latimer, J. Phys. B 13, 4257 (1980).

Chapter I

FIGURE CAPTIONS

Fig. 1. Cuts through a typical ion-molecule reaction entrance channel. (a) Infinite reagent separation, (b) R(A-BC) ≅ 5Å, (c) R(A-BC) ≅ 3Å, (d) small reagent separation.

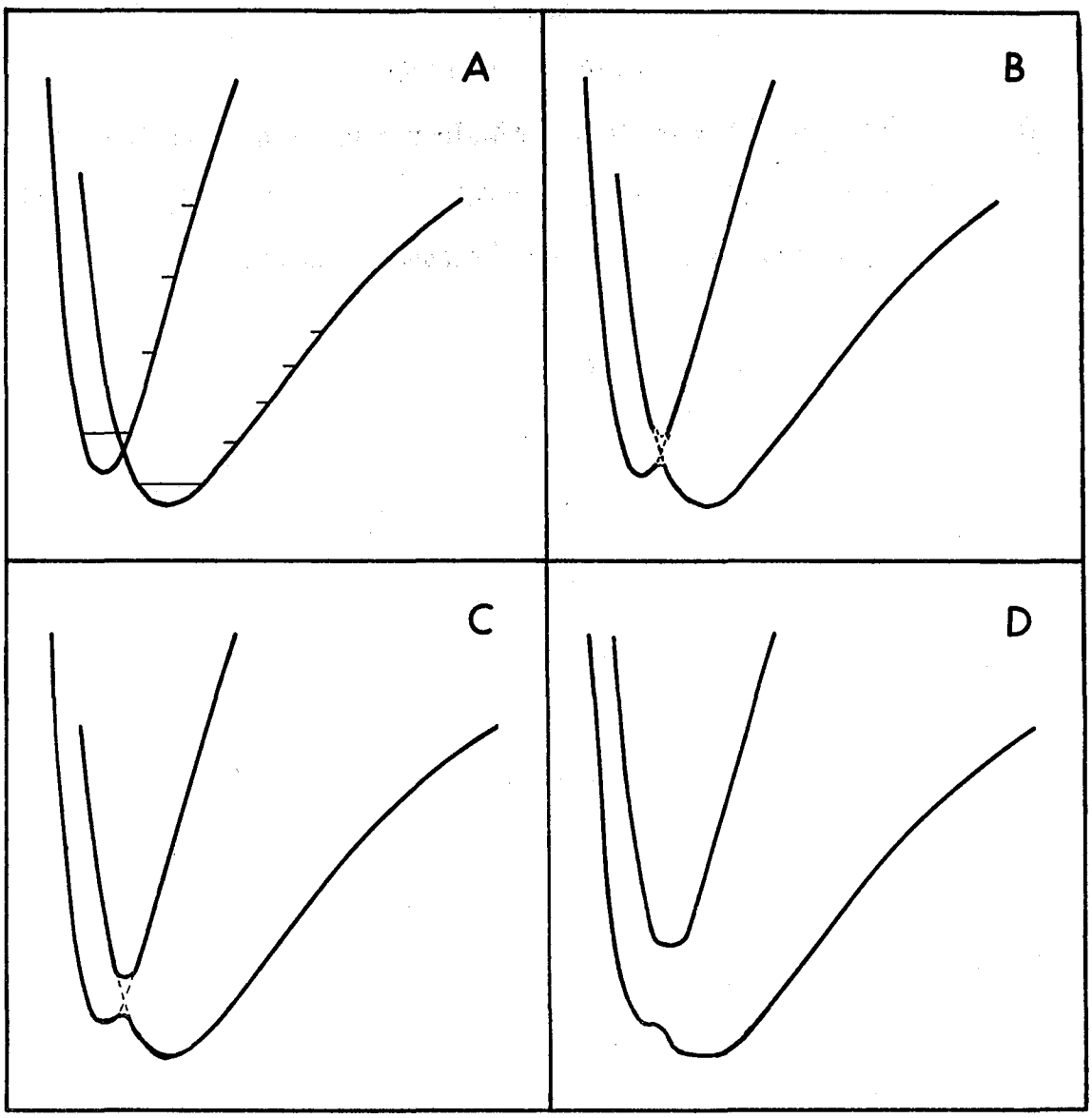

XBL 8110-11886

Fig. 1

II. EXPERIMENTAL

The apparatus, which consists of a photoionization source, radio frequency ion optics and a mass spectrometric detector is shown schematically in Figure 1.

The heart of the machine is the photoionization source, which allows us to prepare ions with well defined translational and internal energy. Photoionization in general allows one to control the maximum internal energy of the ions. The actual internal energy distribution is determined by autoionization selection rules and direct ionization Franck-Condon factors at the photon energy used, all of which are usually unknown. Fortunately, for some ions (NO, NH_3, Ar, etc.)[1] it is possible to determine the distribution of ion internal energy states as a function of photoionizing wavelength. This allows the measurement of state dependent properties of these ions by difference techniques.

The ideal case is H_2, for which we can prepare fairly pure "single vibrational state" selected ion beams. This is possible because photoionization of H_2 near threshold occurs almost entirely by vibrational autoionization.[2]

This process consists of exciting the H_2 to a state which is a member of a Rydberg series converging on a vibrationally excited ion core. Ionization is then possible by vibrational to electronic energy transfer, leaving an ion in some lower vibrational state. In H_2, autoionization occurs, where possible, by a $\Delta v = 1$ process; and even when this is not energetically possible, the ions are still formed

predominately (>75 percent) in the highest possible vibrational state.[3] Thus, by tuning the photon energy to excite autoionizing states which lie between the H_2^+ (v = n) and H_2^+ (v = n + 1) ionization limits we obtain H_2^+ predominately in the v = n state.

To obtain an estimate of the actual vibrational distribution as a function of photoionizing energy, it is necessary to take into account both the dominant autoionization and smaller direct ionization contributions. The very high resolution H_2^+ spectrum of Dehmer and Chupka[2] was used to estimate the ratio of direct to autoionization at the photon energies which we use to prepare the various vibrational states of H_2^+. Franck-Condon factors obtained by photoelectron spectroscopy[4] are used to calculate the vibrational distribution of ions formed by direct ionization. This is combined with the autoionization contribution (assumed to yield only the highest possible v state), to obtain the distributions shown in Table 1. The same procedure was used for D_2^+, except that since no very high resolution photoionization spectra have appeared for it in the literature, the direct/autoionization ratios determined for H_2 were used.

The rotational distribution of the ions is not selected. It consists of J = 0 to 4, and with our photon band width, the distribution cannot vary significantly from vibrational state to vibrational state. Chupka[5] has shown that at least for $H_2^+ + H_2$ reactions, any rotational effects are small (<10 percent).

Table 1. Estimated vibrational distributions.

Actual vibrational distribution	$H_2^{\ddagger}$ v nominal					$D_2^{\ddagger}$ v nominal				
	0	1	2	3	4	0	1	2	3	4
0	1	0.11	0.08	0.08	0.07	1	0.10	0.06	0.06	0.04
1		0.89	0.16	0.17	0.14		0.90	0.14	0.13	0.10
2			0.76	0.19	0.16			0.80	0.20	0.15
3				0.56	0.15				0.61	0.17
4					0.48					0.55

The source of vacuum UV photons is a 9 in. capillary discharge lamp. Depending on the photon wavelength desired, we use either a d.c. discharge in H_2 (900-1650Å), or in the present case, a pulsed discharge in helium (650-900Å).[6] The wavelength is selected by a 1 meter near normal incidence monochromator (McPherson 225) set to 4Å resolution. The light beam emerges from the monochromator and passes through a collimating slit and into the ionization chamber (Figure 1).

The neutral precursor molecules are formed into a supersonic beam (beam 1). Typical conditions are 50 psig H_2 (80 psig D_2) behind a 20μ, room temperature nozzle. The nozzle chamber is pumped by a 10 in. diffusion pump.

In addition to the collimated supersonic beam, there is an effusive gas flow through the skimmer which is pumped away in the small, wedge shaped chamber between the source and the ionization chamber. The beam then passes through the ionization chamber and into a beam catcher. The ions are formed in the intersection of the photon and molecular beams. The use of a molecular beam to create a small volume of high density ($>10^{-4}$ torr) gas in a chamber evacuated to $\sim 10^{-7}$ torr is essential--this avoids ion-molecule reactions in the source. The ion beam contains less than 2 percent H_3^+ reaction product. In addition, the ions are formed translationally cold. The combination of photoionization and molecular beams makes an exceedingly clean but inefficient ion source due to limited photon intensity. Typically, ion beam intensities are about 2×10^4 ions/second (three femtoamps).

Another novel feature of our experiment is the use of radio frequency ion guide optics instead of more conventional d.c. optics. This technique was developed by Teloy and Gerlich.[7] The octapole ion guides which we use are constructed of 8, one eigth inch molybdenum rods arranged around the circumference of a one inch dia. circle (Figure 2). Alternate poles are connected to opposite ends of a coil made of .100" diameter copper wire. The octapole (capacitor) and the coil (inductor) thus make up a resonant circuit, which will oscillate when stimulated. The coil size is adjusted to give a resonant frequency within the tuning range of our homemade rf generator (14-16 MHz), and the circuit is stimulated by a small coil connected to the output of the rf generator which is placed inside the resonant circuit coil. The actual ion guide system we use consists of 5 octapoles. These each have their own coil attached and are all adjusted to approximately the same resonant frequency. Rather than stimulating each resonant circuit separately, we simply stimulate one and force the other circuits to oscillate by coupling them together with capacitors. This insures that the amplitude on each octapole is the same, and also allows each octapole to be floated at different d.c. potentials. The d.c. potentials are introduced on center taps on the coil for each octapole, and are necessary for controlling the ion translational energy.

The principle that governs the operation of the guides is discussed in detail in Mechanics by Landau and Lifschitz.[8] Basically if an ion is placed in a field which varies rapidly compared to the time it

takes the ion to move a significant distance through the field, then the particle's average motion can be described by its motion in an effective potential proportional to the square of the amplitude of the high frequency field.

For the case of a cylindrical n-pole field

$$Veff(R) = \frac{(q\ V_o^{rf}\ )^2}{4m\ \omega^2\ R_o^{\ 2}} \left(\frac{R}{R_o}\right)^{n-2}$$

where q is the charge on the ion, V_o^{rf} is the amplitude of the rf field, ω is the rf frequency, R_o is the pole radius of the field and R is the distance from the field axis. The shape of the effective potential is shown for octapole and quadrupole symmetries in Figure 3. Note that the 8-pole field is much closer to the ideal square well potential, and that the center region is relatively field free. The condition of rapid oscillation of the rf field requires that ω_{rf} be greater than the ion velocity perpendicular to the axis of the trap divided by the pole spacing. For protons, $\omega_{rf} >$ 2.3 MHz for a transverse velocity corresponding to leV, which for our conditions is much faster than normal. The operating frequency we used in these experiments was 30 MHz for the $H_2^+ + H_2$ work (Chapter III) and 15 MHz for the remainder.

To avoid problems with injecting ions into the guide, the ions are actually formed in the first segment of the guide. Since the vertical exit slit of the monochromator results in an oblong ionization volume,

this first segment has been expanded by addition of 4 poles to produce an oval 12 pole geometry. This insures that the ions will be produced in the field-free center of the ion guide. The next segment is shaped and d.c. biased to accelerate and focus the ions into a beam, collinear to the guide axis. In order to facilitate forming an ion beam with minimal accelerating voltage, the molecular beam axis has been tilted 15 degrees from the vertical. The poles of the second segment are bent so that the guide smoothly transforms from 12 pole to cylindrical octapole symmetry. In the long, third guide segment the ions pass through a differential wall and enter the reaction chamber. By varying the d.c potential of the fourth segment with respect to the potential of the 12 pole segment in which the ions are formed, the ions can be accelerated to the desired collision energy at J_3.

Ion-molecule reactions can be carried out in two ways. For high collision energy resolution, experiments may be performed by passing a supersonic molecular beam of the neutral reactant through the octapole (Beam Source 2). Because of the narrow angular and velocity spread of the neutral beam, the collision energy resolution is limited mainly by the energy spread (<50 meV as measured by time-of-flight) and transverse velocity component of the ion beam. This results in approximately 60 meV fwhm laboratory collision energy resolution for the crossed beam mode. The signal intensity is very low (~0.1 count/sec), and measurements lasting several hundred hours are necessary.

All the work reported here was done at low resolution. Here the ion-molecule reactions are carried out by passing the ions through a scattering cell. This gives much higher signal levels, limited only by the pressure in the cell. In order to minimize secondary reactions and keep well within the range where we can take a linear approximation to the primary beam attenuation, we keep the total attenuation below 5 percent. This typically involves scattering gas pressures between 2 and 6 x 10^{-5} torr as measured by a Baratron capacitance manometer. This also insures that elastic scattering will not significantly perturb the collision energy distribution. Beam-gas experiments have inherently lower kinetic energy resolution due to target gas thermal motion. The resolution in the case of negligible ion beam spread has been shown to be[9]

$$E_{fwhm} = (11.1\ (m/(M+m))\ kT\ E_{cm})^{1/2} \quad ;$$

where m is the ion mass, M is the target mass, and E_{cm} is the nominal center of mass collision energy. Because it is necessary to heat the ion guides to maintain surface cleanliness, the target gas temperature is ~400K. At this temperature the spread ranges from $(0.26\ E_{cm})^{1/2}$eV for $D_2^+ + H_2$ to $(0.018\ E_{cm})^{1/2}$eV for $H_2^+ + Ar$. Thus only for the $H_2^+ + H_2$ system is this a real problem. Note that the collision energy spread increases with increasing collision energy.

The product ions formed in either the beam or gas cell are formed inside the ion guide and can only escape into the d.c. collection optics at the end of the last octapole. The ions are focussed and injected into a quadrupole mass spectrometer (QPMS) and the mass selected primary or product ions are counted by a Daly detector.[10] This consists of a high negative voltage target which emits electrons on ion impact, and a scintillator-PMT combination which detects the secondary electrons. Measurements of detection efficiency versus target voltage for the various mass ions showed that the efficiency saturated at voltages larger than 40 kV. This is assumed to be near unit detection efficiency. All experiments were performed at this voltage.

The detection efficiency is limited primarily by the transmission of the ions through the QPMS. For the study of $H_2^+ + H_2$ reactions the QPMS was set up at low enough resolution ($M/\Delta M \sim 10$) that essentially all ions are transmitted. This is substantiated by the fact that when the QPMS is tuned to the primary ion mass, and then switched to the non-mass selective mode the signal remains constant. For the study of H_2^+ reacting with CO, N_2, O_2 and Ar it was necessary to go to much higher resolution, and under these conditions the transmission of all the ions is less than 100 percent. It is necessary to correct for this when attempting to obtain absolute cross sections.

Experimental data have been obtained under computer control in two different modes. In one of these, the ionizing photon wavelength is

kept fixed while the ion kinetic energy is varied, typically from 0–10 eV in 0.1 eV steps. The other mode involves scanning the monochromator at fixed ion kinetic energy. The wavelength step size is chosen such that the same set of wavelengths is used in both the variable energy and variable wavelength experiments. It is for these photon energies that vibrational distributions of H_2^+ were estimated. In both modes cross sections are determined in the following manner. Since the scattering cell is not sealed, gas leakage establishes a constant background pressure of the neutral reagent throughout the reaction chamber, allowing some reactions to take place outside the scattering cell. This background signal as well as any detector noise is corrected for as follows. The scattering cell is filled to the desired pressure through a leak valve, and the product ion intensity is measured. The computer then diverts the gas flow to a second inlet which dump the gas into the reaction chamber itself, thus filling it to the same background pressure which exists when the scattering cell is filled ($\sim 5 \times 10^{-7}$ torr). Product ion intensity is again measured and subtraction of the two measurements gives the product ion intensity resulting from reactions in the scattering cell itself (S). Measurement of the unattenuated primary beam intensity, I_0, the target gas density, n, and knowledge of the length of the scattering cell, L, allow calculation of the absolute reaction cross section according to the relation $\sigma = S/(I_0 nL)$. Ion intensities as a function of energy or wavelength are scanned repetitively until the desired signal-to-noise ratio is obtained. Typical experiments last 8–15 hours each.

Data analysis is relatively simple. Having obtained cross sections as a function of collision energy at fixed vibrational state and as a function of vibrational state at fixed collision energy, the data is checked for internal consistency. For the $H_2^+ + H_2$ system, where the QPMS can be operated at low resolution and the transmission is near 100 percent, the two types of measurements typically agree within 5 percent. In cases of discrepancy, the experiment in doubt was repeated, and thus a complete set of vibrational and collision energy dependent cross sections were obtained.

For the other systems ($H_2^+ + CO$, Ar, N_2, O_2), the same sort of procedure is followed. Here, because of non-unit QPMS transmission, the scale of the raw cross sections is somewhat arbitrary, and due to small differences in QPMS tuning and resolution from run to run, sometimes the values of the vibrational dependent and collision energy dependent cross sections differ. In this case, the cross sections are scaled, using the collision energy dependence from the fixed vibrational state scans and vice versa. This in no way changes the relative vibrational or collision energy dependence observed.

These reactions ($H_2^+ + CO$, N_2, O_2, Ar) are much more sensitive than those of the $H_2^+ + H_2$ system to surface contamination in the final section of the ion guide. This is presumably due to the very low product laboratory scattering energies for light ion plus heavy target systems. This manifests itself as a loss of low energy proton and charge transfer products due to poor collection. In cases where data appeared to be bad because of this problem, those runs were rejected in favor of data taken when the ion guides were freshly cleaned.

This procedure results in a set of relative cross sections as a function of collision energy and vibrational state. In order to assign absolute values to the cross sections corrections must be made for non-unit QPMS transmission. This was done by lowering the QPMS resolution as far as possible and turning off the d.c. bias on the QPMS. This gives very low resolution; approximately $M/\Delta M \sim 0.8$. This is still enough to separate the primary and product ions but results in a single peak for the products. The cross section for product formation as a function of collision energy was measured. This is assumed to be the sum of the absolute cross sections for the two predominate product channels (proton and charge transfer). By comparing the known energy dependences of the two channels and the energy dependence of the low resolution measurement we obtain the proper factor with which to scale our relative cross sections to obtain absolute cross sections.

The error in absolute cross sections is hard to estimate. The above procedure certainly is not perfect, but probably gives the correct value to within 10 percent. A larger error in the absolute cross sections comes from our lack of knowledge of the exact distribution of gas pressure within the scattering cell. Because we can only estimate the effective "length" of the gas cloud in the cell and adjoining regions of the ion guides, the absolute cross section may be in error by as much as ±25 percent. Nevertheless, our data is in good agreement with work of other groups on these reactions.[11]

The relative error bars in the raw data are much smaller, typically a few percent. Because they vary somewhat from reaction to reaction

the actual error estimates will be presented along with the experimental results.

After obtaining raw absolute cross sections, we then use our estimates of the actual vibrational distributions present in our state selected ion beams to correct the vibrational dependence of the cross sections. This is done by starting with the cross sections for v = 0 and working up to v = 4, iteratively subtracting out the contributions from the lower vibrational states. This procedure gives our best estimates for the actual vibrational dependences. Any errors in our estimates of the vibrational distributions will propagate through the set of data. Because the purity of the vibrational state selection is high for v = 0 and v = 1 and falls off to only ~50 percent for v = 4, this error is small for v = 0, 1, 2 and gets worse for 3 and 4. Although it is impossible for us to give error bars here, it is very important to point out that all of the vibrational effects we report are present in the raw data, and are merely amplified by the unfolding process. Our estimates of vibrational state purity are necessarily upper bounds. This is because for want of a better assumption, we have assumed that <u>all</u> autoionization leaves ions in the highest possible vibrational state. To the degree which this is wrong, the actual vibrational state purity calculated at each photon energy is too high. The effect of the error is to <u>understate</u> the magnitudes of the various vibrational effects observed. Comparison of our data on H_2^+ + Ar (Chapter IV) with that of Koyano and Tanaka[11c] suggests that this may be true to a small extent, primarily with v = 4.

Chapter II

REFERENCES

1. W. A. Chupka in Ion Molecule Reactions, J. Franklin, ed. Plenum, New York, 1942.
2. P. M. Dehmer, W. A. Chupka, J. Chem. Phys. 65, 2243 (1976).
3. P. M. Dehmer, W. A. Chupka, J. Chem. Phys. 66, 1972 (1977).
4. J. A. R. Samson, J. Elec. Spec. 8, 123 (1976).
5. W. A. Chupka, M. E. Russel, K. Refaey, J. Chem. Phys. 48, 1518 (1968).
6. Techniques of Vacuum Ultraviolet Spectroscopy, J. A. R. Samson, Wiley and Sons, New York, 1967, and Cheuck Ng, Ph. D. Thesis, University of California.
7. E. Teloy, D. Gerlich, Chem. Phys. 4, 417 (1974).
   D. Gerlich, Diplomarbeit, Fakultat fur Physik der Universitat, Frieburg i/Br, W. Germany (1971).
8. Mechanics, L. D. Landau and E. Lifschitz, Pergamon Press, Oxford, 1960, p. 93.
9. P. J. Chantry, J. Chem. Phys. 55, 2746 (1971).
10. N. R. Daly, Rev. Sci. Inst. 31, 264 (1960).
11. (a) C. H. Douglass, D. J. McClure, W. R. Gentry, J. Chem. Phys. 67, 4931 (1977).
    (b) W. A. Chupka, M. E. Russell, K. Refaey, J. Chem. Phys. 48, 1378 (1968).
    (c) I. Koyano, K. Tanaka, J. Chem. Phys. 72, 4858 (1980).
    I. Koyano, K. Tanaka, submitted to J. Chem. Phys.

Chapter II

FIGURE CAPTIONS

Fig. 1. Schematic of Experiment

Fig. 2. Geometry of octapole ion guide showing a calculated ion trajectory.

Fig. 3. Radial dependence of V_{eff} for octapole and quadrupole fields.

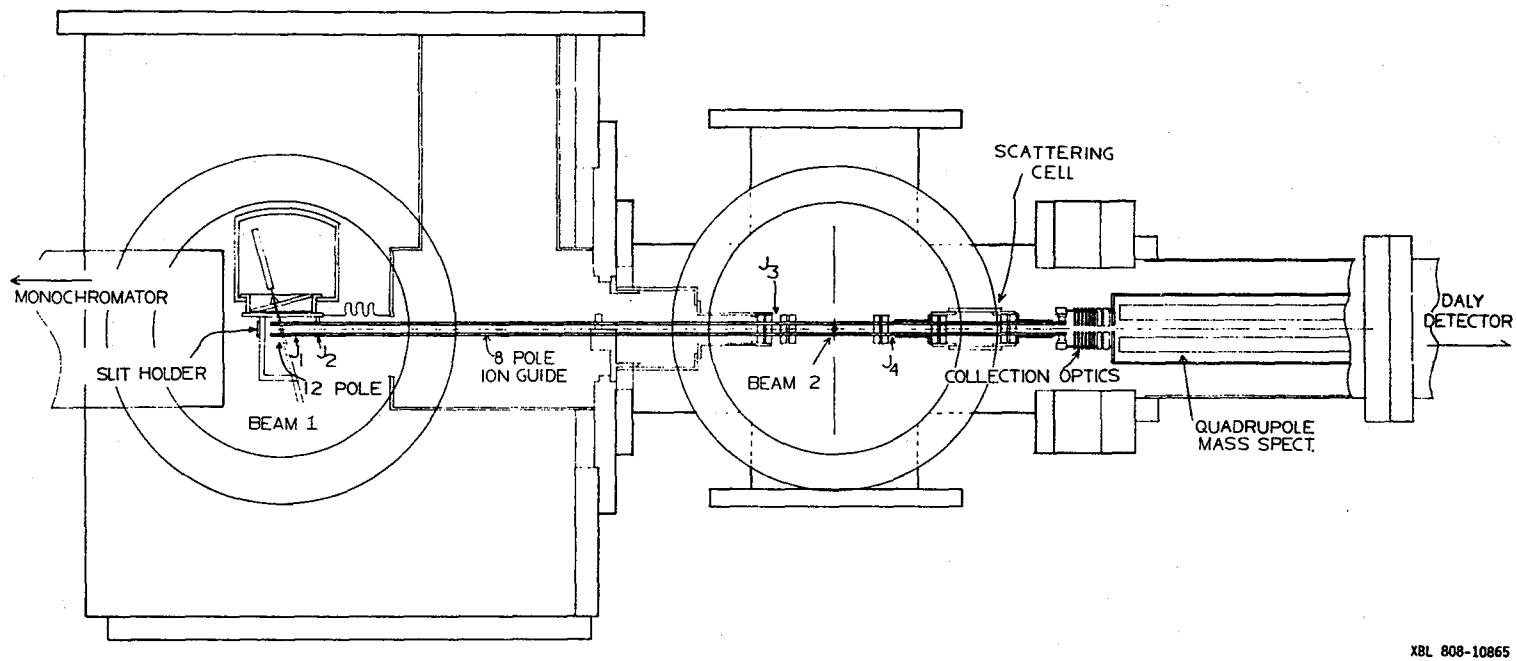
MONOCHROMATOR
SLIT HOLDER
BEAM 1
2 POLE
8 POLE
ION GUIDE
BEAM 2
SCATTERING
CELL
COLLECTION OPTICS
QUADRUPOLE
MASS SPECT.
DALY
DETECTOR
XBL 808-10865

Fig. 1

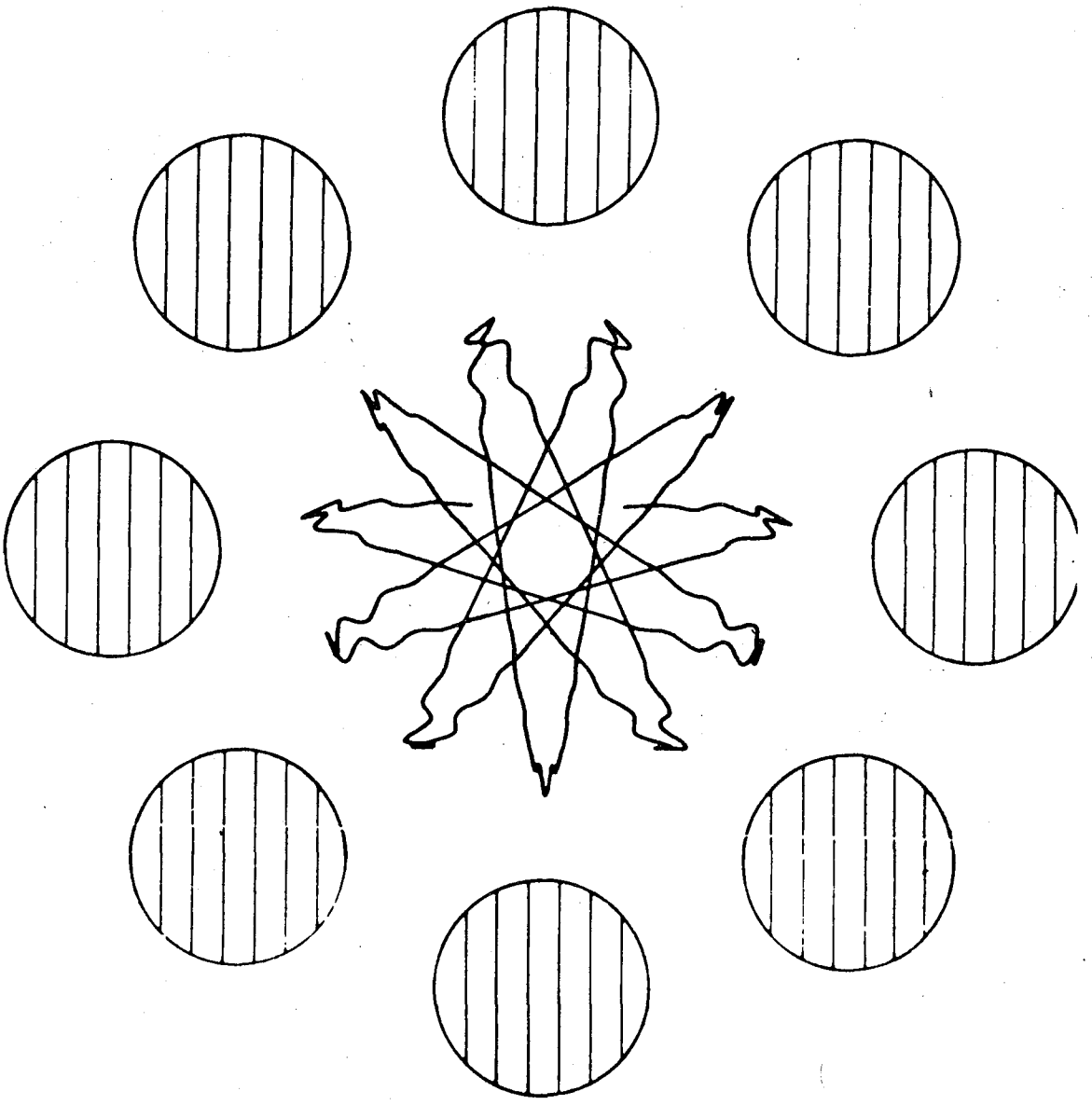

XBL 802-8326

Fig. 2

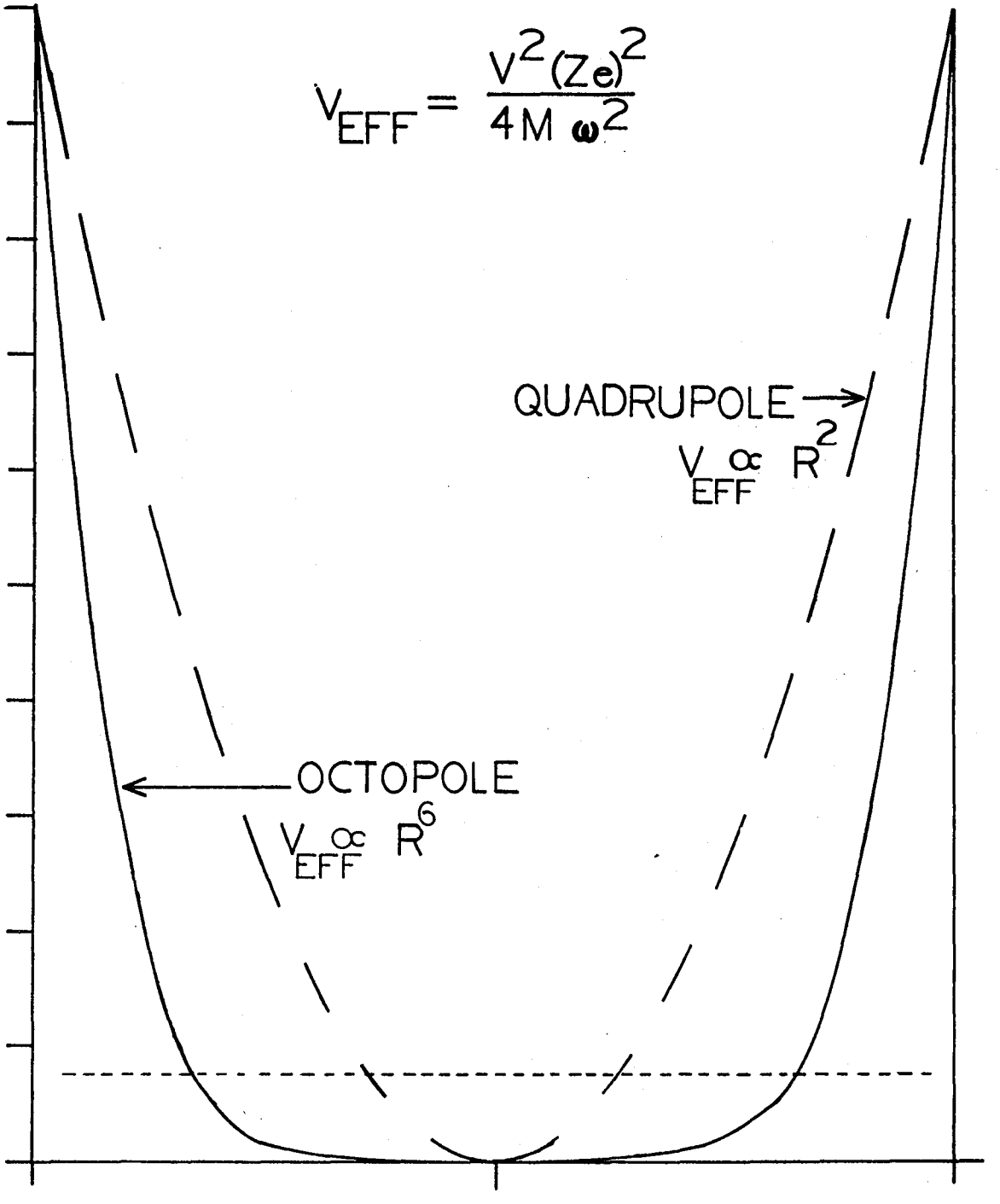

XBL 808-10863

Fig. 3

III. $H_2^+ + H_2$

Introduction

The reaction $H_2^+ + H_2 \rightarrow H_3^+ + H$ has been extensively studied over the years. The interest in this reaction stems partly from its importance in interstellar[1] and atmospheric[2] chemistry, and partly because of its suitability for rigorous theoretical treatment. Experimentally it has been studied by crossed beam,[3] mass spectrometric,[4] merged beam,[5,6] photoionization,[7] ICR,[8] and ion beam-gas cell[9] techniques. The experiments have provided a reasonably clear picture of the gross reaction dynamics. The reaction is exoergic by 1.7 eV and, contrary to early speculation, appears to proceed almost entirely by a direct mechanism[3,5] without any observable barrier.[5,6] Studies of $(H_2)_2$ photoionization in our laboratory also indicate that H_4^+ is indeed unstable with respect to $H_3^+ + H$, demonstrating the lack of a barrier to reaction.[10] The reaction cross section is very large (ca. 100 $Å^2$) at thermal energies, and falls off rapidly with increasing collision energy.[5,6]

In the available experimental work, there are two observations that indicate the existence of complexities in this apparently simple reaction. In the $H_2^+ + H_2 \rightarrow H_3^+ + H$ reaction, H_3^+ may in principle, be formed by proton or H atom transfer mechanisms. The proton transfer involves breaking the H_2^+ bond ($D^\circ \simeq 2.6$ eV), while H atom transfer requires H_2 neutral bond rupture ($D^\circ \simeq 4.5$ eV). One might expect that the two channels would have very different dynamics, and in particular, that proton transfer would predominate. In trajectory

calculations by Muckerman[11] it is found in fact, that only proton transfer occurs. Experimentally, by using isotopic substitution, it is found that products corresponding to both nominal H atom and proton transfer reactions occur with comparable cross sections and similar dynamics.[3,5] This appears to be the consequence of extensive charge transfer between the reagents.[3,5,11]

Secondly, in pioneering work by Chupka, et al.,[7] and more recently by Koyano and Tanaka,[12] using photoionization to prepare vibrationally state selected H_2^+, it is observed that at low collision energies ($E_{cm} < 1$ eV), H_3^+ formation is inhibited by vibrational excitation of the H_2^+ reagent, and that at higher energies, there is some vibrational enhancement. These two aspects of the reaction have been linked to the interaction of several potential energy surfaces.[3,13]

There have been a number of good calculations of the H_4^+ ground state potential energy surface (PES).[14] These calculations show quite clearly the absence of a barrier for the $H_2^+ + H_2 \rightarrow H_3^+ + H$ reaction, thus supporting the experimental observation of direct reaction dynamics. If it exists at all, H_4^+ appears to be stable only as a weakly bound $H_3^+....H$ complex in the PES exit channel, but not as $H_2^+ - H_2$. There have also been DIM (diatomics-in-molecules) calculations by Krenos et al.[3] and Stine and Muckerman.[13] This work shows that there is considerable interaction between the ground and excited PES's, and in particular there are a number of avoided crossings. These not only distort the ground state surface, but allow the

possibility of repeated surface hoppings, opening up a number of excited pathways for reaction.

This set of interacting PES's allows an explanation of the above mentioned experimental observations. Consider two sets of $H_2^+ + H_2$ isotopic reagents, $H_2^+ + D_2$ and $D_2^+ + H_2$, which are just the two reagent charge states of the $(H_2 + D_2)^+$ system. Assuming that reaction is exclusively by proton transfer, different triatomic ions will be produced from the two sets of reagents:

$$H_2^+ + D_2 \rightarrow D_2H^+ + H$$
$$D_2^+ + H_2 \rightarrow H_2D^+ + D \quad .$$

At infinite reagent separation, the two reagent charge states are described by two different potential energy surfaces, which cross at points where the ion and neutral bond lengths are equal.[3,14] As the reagents approach, however, the surface crossing becomes avoided, and the two sets of reagents correspond simply to two different entrance valleys on the ground PES. The barrier between the two decreases with decreasing reagent separation, until at ~8-10 bohr the barrier becomes smaller than the reagent zero point energy. At this point rapid interconversion (charge hopping) between $H_2^+ + D_2$ and $D_2^+ + H_2$ may occur, eliminating the experimental ability to distinguish between the two reagent charge states. This would also allow production of both the D_2H^+ and H_2D^+ product ions from each set of reagents, explaining the experimental similarity of the nominal "atom" and "proton" transfer reactions. The charge hopping is induced by reagent vibration, and

the mixing of the two reagent charge status might be expected to be somewhat dependent on reagent vibrational state.

Krenos et al.[3] also suggested an explanation for the vibrational inhibition of the formation of H_3^+ at low collision energies. They suggest that reagent vibration promotes hopping of the system from the ground surface ($H_2^+(^2\Sigma_g)+H_2$) to the first excited surface ($H_2^+(^2\Sigma_u)+H_2$). Since DIM calculations show a large barrier to reaction on the excited surface, this hopping decreases reaction probability.

It appears that due to the multiple surface nature of the H_4^+ system, the detailed reaction dynamics including reagent charge transfer and surface hopping are likely to be strongly influenced by reagent vibration. Unfortunately, in all existing experiments with the exception of the photoionization studies,[7,11] the H_2^+ reagent is prepared using electron bombardment. This populates an approximately Franck-Condon distribution of vibrational states[3,5,6] which ranges from v = 0 up to the H_2^+ dissociation limit (ca. v = 16), with a peak at v = 2.[15] Thus it is possible that the dynamics observed in the crossed[3] and merged beam[5,6] experiments may reflect greater involvement with all accessible potential energy surfaces than would occur for reagents in their ground vibrational state. In particular, charge exchange and the involvement of excited potential surfaces may be much more important.

Previous photoionization work by Chupka,[7] et al. and Koyano and Tanaka[12] has provided interesting data on vibrational effects in the

$H_2^+ + H_2$ reaction over a kinetic energy range of 0-1 eV. Above ~1 eV experimental complications in the use of a single chamber for ion production and reaction have allowed only qualitative data to be obtained. Also, their single chamber arrangement makes it difficult to use isotopic substitution to distinguish between different initial reagent charge states leading to the same products (e.g., D_2H^+ from $H_2^+ + D_2$ and $D_2^+ + H_2$). It would be especially desirable to extend the measurement of the effects of reagent vibration and collision energy on other channels, and interchannel branching ratios for various isotopic systems. This detailed mapping of the reaction vibrational and translational energy dependence certainly would yield some dynamical insight, and in particular, would provide a very sensitive test of any theoretical modelling of the scattering of $H_2^+ + H_2$.

Results

Several processes are possible in the $H_2^+ + H_2$ system: H_3^+ formation, collision-induced dissociation, and charge transfer. Although the present experiments focus on the reactive channel, limited data were also obtained for the collision-induced dissociation and charge transfer channels in order to investigate competition between these processes.

Triatomic Ion Production. Cross sections have been measured for the reactions:

$$H_2^+ + D_2 \rightarrow D_2H^+ + H \qquad (1)$$

$$D_2^+ + H_2 \rightarrow D_2H^+ + H \qquad (2)$$

The other reaction product, DH_2^+ can not be distinguished mass spectrometrically from D_2^+ which is the charge transfer product in $H_2^+ + D_2$ and the reagent in $D_2^+ + H_2$. In both cases the collision energy was varied from E_{cm} = 0 to 6 eV, and the ion vibrational state from v = 0 to 4. A typical example of raw data for reaction 1 is shown in Figure 1. The cross section falls rapidly with collision energy, as expected for an exoergic ion-molecule reaction. Since all the cross sections measured for reactions 1 and 2 have the same gross shape, they have been plotted in Figure 2 in a way that emphasizes the effects of reagent vibration. For selected collision energies (right margins), cross sections for ion vibrational states 0-4 are compared for reactions (1) and (2). Results of both wavelength and kinetic energy scans were used to obtain these data.

For $H_2^+ + D_2 \rightarrow D_2H^+ + H$, the nominal proton transfer reaction, vibrational energy inhibits reaction at low collision energy, but enhances it at energies above ~1.4 eV. For the $D_2^+ + H_2 \rightarrow D_2H^+ + H$ "atom" transfer reaction there is essentially no vibrational effect at low energies, substantial vibrational enhancement from $E_{cm} \simeq 1$ to 3 eV, and a sharp, vibrational energy dependent fall off at energies greater than 3 eV.

The earlier observations[7,12] of vibrational inhibition of the $H_2^+ + H_2 \rightarrow H_3^+ + H$ reaction at low collision energy are compatible with the sum of the "proton" transfer and "atom" transfer reactions, since both lead to H_3^+ product. Here "proton" and "atom" transfer are being used only as labels for the two reactions, and do not imply anything about the microscopic dynamics of the reactions.

At a given E_{cm}, the error in comparing the cross sections for different vibrational states ranges from ~±0.5 $Å^2$ at low E_{cm} to ~±0.25 $Å^2$ at the highest E_{cm}. Since the cross sections fall quite rapidly with increasing E_{cm}, this decrease in absolute error actually constitutes an increase in percent error. Thus for example, the oscillatory behavior at 0.77 eV for the atom transfer channel is real, while that at 4.1 eV probably is not. The relationship of the data at different values of E_{cm}, was taken from scans of E_{cm} for fixed vibrational states. This error is also ~±0.25 $Å^2$, except at the very lowest energy, where problems with transmission of the slow primary and product ions may cause errors as large as ±1.5 $Å^2$. Relative error in comparison of the two sets of internally consistent data for reactions 1 and 2, arises from the difference in the ratio of reagent ion mass to target mass. This introduces a possibility of error in defining the zero of the CM energy scale for reactions 1 and 2, which in turn introduces an error in comparing cross sections at a given E_{cm}. Due to the shape of the cross section, this effect is worst at low E_{cm} (±1.5 $Å^2$), and is negligible at energies above ~2 eV.

Collision Induced Dissociation (CID). Because of possible interplay between CID and the chemical reaction channels at higher collision energies, we have studied the effects of vibrational and collision energy on CID in $D_2^+ + HD$. This isotopic combination was chosen so that dissociation of the primary ion and the dissociation of secondary ions formed by charge exchange could be distinguished. Figures 3 and 4 show the cross sections obtained for D^+ and H^+ production. The thresholds shift to lower energy with increasing vibrational state, as expected, and there is sharp rise from threshold, followed by a leveling off at $E_{cm} \sim 5$ eV. The thresholds are consistent with the dissociation energy of D_2^+ (2.69 eV) when consideration is made of the broadening in the E_{cm} distribution induced by target gas motion. The curves shown result from averaging of the raw data, which was taken at 0.1 eV laboratory energy intervals, and subtraction of a small background signal which results from reactions of hot ions created by photoelectron bombardment in the ion source. The magnitude of this background corresponds to a cross section of 0.15Å and that is also the magnitude of the estimated relative error.

Figure 5 shows the ratio of the D^+ production to the H^+ production. Although there are large variations in the ratio as a function of D_2^+ reagent vibrational state at low energies, for energies above 5 eV, where the cross sections level off, the ratio is 3 within experimental error. This is just the ratio of D atoms to H atoms in the reagents. We have also measured cross sections for CID of $H_2^+ + D_2$. Here we can only measure the H^+ production channel since D^+ cannot be distinguished

from H_2^+. It is interesting to note that the H^+ production cross sections have a magnitude which is 2/3 that of the D^+ production cross sections in D_2^+ + HD. This suggests that CID is relatively free of isotope effects at high energy, and that the various isotopic ions are produced with equal probability. Our results are at variance with those of Futrell et al.[18] who failed to observe H^+ production in CID of D_2^+ + HD.

Charge Transfer (CT). Figure 6 shows our measured cross section for the reaction D_2^+ (v = 0) + H_2 → D_2 + H_2^+. The cross section is large, and relatively independent of collision energy, except at very low energies. CT cross sections are difficult to measure in this experimental arrangement because the H_2^+ product ions are produced with little laboratory kinetic energy. These slow ions can then react with the H_2 in the scattering cell to form H_3^+. In principle one can obtain the correct charge transfer cross section by merely adding the mass 2 and mass 3 production cross sections. In practice there are two additional problems. One is the contamination of the D_2^+ ion beam with approximately 2 percent HD^+. Because our charge transfer cross sections are sensitive only to the net change in the mass 2 plus mass 3 ion intensity when the scattering cell is filled, only the reaction $HD^+ + H_2 \rightarrow DH_2^+ + H$ has an effect (negative) on the cross section. Since the HD^+ is only 2 percent of the reagent beam, and reagent ion attenuation is only ~5 percent, and only one of the three major $HD^+ + H_2$ reactions has any net effect; the error introduced is small and we have not made any corrections for it.

A more serious problem is that some of the scattering gas (H_2), diffuses back into the ionization chamber and contaminates the D_2^+ beam with ~4 percent H_2^+. Since reactions of H_2^+ with H_2 only yield mass 2 and 3, and the CT cross section is only sensitive to net change in m/e 2 and 3 signal when the scattering cell is filled, this component would have no effect on the measured CT cross sections as long as there is no change in the H_2^+ primary ion intensity when the scattering cell is filled. Unfortunately, filling the cell sends an effusive beam of H_2 into the ionizer. Because of the large separation (~50 cm) between the scattering cell and the ionizer, this only increases the H_2^+ intensity by ~3 percent (of 4 percent). We have corrected for this small but significant artifact by turning off the D_2 molecular beam and measuring the H_2^+ production and attenuation cross sections, which are then subtracted from the $D_2^+ + H_2$ CT cross section. Because this procedure is very time consuming, we have only carefully measured the CT cross section for D_2^+ v = 0. However, comparison of uncorrected cross sections indicates very little effect of reagent ion vibration on $D_2^+ + H_2$ charge transfer. Similar behavior is seen in $H_2^+ + D_2$ CT.

Discussion

One of the most interesting features of the D_2H^+ production cross sections (Figure 2) in reaction of $H_2^+ + D_2$ and $D_2^+ + H_2$ is the similarity between them. At low collision energy, the magnitudes of the "proton" and "atom" transfer reactions are very similar. Even more striking is the similarity of the pronounced vibrational effects in the energy range around 2 eV, which suggests that the two reactions

may proceed through a common mechanism. This result is certainly consistant with the idea of rapid charge hopping in the reaction entrance channel,[3,13] which was discussed in the introduction. Reaction at low energies proceeds via proton transfer,[11] producing either $D_2H^+ + H$, or $DH_2^+ + D$, depending on the reagent charge state at the time of reaction. It appears that this charge hopping is quite facile, even for ground vibrational state reagents. The idea of efficient, long range charge hopping is certainly supported by the large, translational energy independent cross section for $D_2^+(v = 0) + H_2$ charge transfer (Figure 6). The 20 $Å^2$ cross section implies an average range for the CT process of ~2.5 Å, or ~3.5 Å if we allow for the possibility of multiple charge hops. This behavior is in good agreement with the calculations of Krenos et al.[3] which show that charge hopping becomes likely at reagent separations ~4 Å. A prediction of Stine and Muckerman[13] that net CT of ground vibrational state reagents would be unlikely due to competition with the reactive channel appears to be correct only at collision energies below 0.2 eV. The decrease in CT cross section at low collision energies, which we see for all reagent ion vibrational states, is almost certainly due to this competition, but the competition is not sufficient to eliminate CT altogether.

Although our data indicates extensive interconversion between the $H_2^+ + D_2$ and $D_2^+ + H_2$ charge states, there remain differences in the production of D_2H^+ from them. At very low collision energy, the reaction $H_2^+ + D_2 \rightarrow D_2H^+ + H$ shows vibrational inhibition, while on the other hand D_2H^+ formation from $D_2^+ + H_2$, which has a similar cross section,

shows no vibrational effect. In $H_2^+ + H_2 \rightarrow H_3^+ + H$, the reaction is supressed by vibrational energy at low collision energy.[7,12] Krenos et al.[3] suggested that the inhibition results from a vibrationally enhanced probability of hopping to the first excited PES. Since there is a barrier to reaction on this excited PES, collisions on it are non-reactive at low collision energies, and thus vibrationally enhanced surface hopping would lead to vibrational inhibition of the reaction at low collision energies. This vibrationally enhanced surface hopping would be expected to result in vibrational inhibition of both the $H_2^+ + D_2$ and $D_2^+ + H_2 \rightarrow D_2H^+ + H$ reactions. In order to explain the observed vibrational pattern, other effects must be considered.

$H_2^+ + D_2$ forms D_2H^+ simply by proton transfer. But the formation of D_2H^+ from $D_2^+ + H_2$, at least at low energies when other reaction mechanisms are inefficient, must proceed by a charge transfer-proton transfer mechanism. Since charge hopping between the two reagent charge states is vibrationally induced,[3,14] one might expect that the $H_2^+ + D_2 \rightarrow D_2H^+ + H$ reaction would show vibrational inhibition with concomitant vibrational enhancement of H_2D^+ production, while $D_2^+ + H_2 \rightarrow D_2H^+ + H$ would be vibrationally enhanced at the expense of the H_2D^+ channel. The similarity in magnitude of the low energy reaction cross sections for the $H_2^+ + D_2$ and $D_2^+ + H_2$ charge states suggests that this charge transfer is very efficient at mixing the reagent charge states. This would result in there being only a small residual vibrational inhibition in D_2H^+ formation from $H_2^+ + D_2$ and a small

enhancement for $D_2^+ + H_2$. Combining these two possible effects may explain the observed behavior. The reaction $H_2^+ + D_2 \rightarrow D_2H^+ + H$ is vibrationally inhibited by both surface hopping and charge transfer resulting in appreciable net vibrational inhibition. The $D_2^+ + H_2 \rightarrow D_2H^+ + H$ reaction on the other hand, is vibrationally inhibited by surface hopping and vibrationally enhanced by charge transfer. If the magnitudes of the two opposing effects are similar, they would cancel and no vibrational effect would be observed.

Hopping to an upper PES may also explain why both reactions show a strong vibrational enhancement in the intermediate collision energy range (1 to 3 eV). It may be that the system hops to the first excited PES as discussed above, but now has sufficient collision energy to surmount the barrier to reaction on the upper surface. If the excited PES reaction mechanism is more efficient than the ground state reaction, then we would expect to see net vibrational enhancement. If this mechanism is responsible for the observed enhancement, our data would yield a value of ~1 eV for the barrier.

As the collision energy increases above 1 eV the magnitude of the cross section of $D_2^+ + H_2 \rightarrow D_2H^+ + H$ (atom transfer) reaction begins to drop below that of the $H_2^+ + D_2 \rightarrow D_2H^+ + H$ (proton transfer) reaction, as shown in Figure 2. Up to about E_{cm} = 3 eV the translational energy dependence and vibrational effects are very similar for both the "proton" and "atom" transfer cross sections, with simply a slow decrease in the relative magnitude of the "atom transfer" cross section. Above E_{cm} = 3 eV the decrease in relative cross section of

the $D_2^+ + H_2 \rightarrow D_2H^+ + H$ ("atom transfer") reaction becomes much faster. Then at E_{cm} ~5 eV the fall off stabilizes. Over this same energy range, the vibrational effect on the "atom transfer" reaction changes from enhancement to strong inhibition, while for the $H_2^+ + D_2$ ("proton transfer") reaction the enhancement is only weakened.

It seems likely that the initial slow fall off of the $D_2^+ + H_2 \rightarrow D_2H^+ + H$ cross section relative to the $H_2^+ + D_2$ reaction is due simply to a breakdown of the entrance channel charge hopping which effectively mixes the two reagent charge states at low energy. Since proton transfer appears to be the dominant reaction mechanism at least at low collision energies, this breakdown would decrease the amount of D_2H^+ formed from $D_2^+ + H_2$ reagents. The fact that the CT cross sections (Figure 6) remain large at high collision energies suggests that the breakdown of efficient charge hopping occurs only for the small impact parameter collisions which lead to reactive scattering.

While this breakdown mechanism is no doubt partly responsible for the large difference between the $H_2^+ + D_2 \rightarrow D_2H^+ + H$ and $D_2^+ + H_2 \rightarrow D_2H^+ + H$ reactions at energies above 3 eV, there seems to be another effect which is important. From E_{cm} = 3 to 5 eV, the $D_2^+ + H_2 \rightarrow D_2H^+ + H$ cross sections show a pronounced, vibrationally enhanced fall-off. This fall-off then stabilizes at energies above 5 eV. This general shape is very similar to what is observed for the CID cross sections for $D_2^+ + HD$ (Figs. 3, 4). This strongly suggests that competition between D_2H^+ product formation and CID is occurring. Over the same energy range the $H_2^+ + D_2 \rightarrow D_2H^+ + H$ reaction cross section also shows a decrease in the degree of vibrational enhancement, some competition with CID is again suggested in this case.

Durup and Durup[17] have studied CID of $D_2^+ + D_2$, and suggested that CID occurs through a long lived intermediate. Our results on CID of $D_2^+ + HD$ and $H_2^+ + D_2$ show that in all cases CID is strongly vibrationally enhanced. Also, comparison of the results of H^+ and D^+ formation from $D_2^+ + HD$ and H^+ formation from $H_2^+ + D_2$ shows two important observations. First, of the four hydrogen (deuterium) atoms in the reactants, each one is equally likely to emerge as the detected proton (deuteron) at higher collision energies. This is shown for $D_2^+ + HD$ in Figure 5. For E_{cm} below 5 eV, the ratio depends strongly on the reagent ion vibrational state, while above 5 eV, the $D^+:H^+$ ratio is just 3 ± 0.5, for all D_2^+ reagent vibrational states. This is just the D atom:H atom ratio in the reagents. In addition, H^+ production cross section in CID of $H_2^+ + D_2$ are very similar in shape to those for $D_2^+ + HD$ and the magnitudes are just 2/3 those for D^+ production from $D_2^+ + HD$ which is again the ratio of H atoms in the two systems. This suggests that, at least at high collision energies, CID proceeds by a mechanism in which the reagent mass ratio is unimportant, and which randomizes the outcome of the dissociation. This certainly suggests that CID proceeds through some sort of intermediate, in which all four atoms involved become equivalent.

There are a number of possible mechanisms for the isotopic scrambling which is observed in our CID results. One possibility is that during those $D_2^+ + HD$ collisions which eventually lead to CID, a fleeting D_3H^+ species is formed whicn lives long enough for isotopic scrambling to occur. Isotopic scrambling in the D_3H^+ could occur

either by nuclear motion or by an electronic rearrangement in which all four atoms and bonds become equivalent. Another mechanism involves reaction to form a triatomic (D_2H^+,D_3^+) product, which is internally excited enough to unimolecularly decompose, yielding net CID. Other mechanisms such as direct dissociation of the D_2^+ primary ion are hard to reconcile with both our and Durup and Durup's results.

For collision energies below 5 eV, the D^+:H^+ production ratio in CID of $D_2^+ + H_2$ varies widely from the high energy value of 3. The variation is smooth with collison energy, but is very strongly dependent on D_2^+ reagent vibrational state (Figure 5). This suggests that at collision energies near the CID threshold kinematic effects involving different isotopes and the variation in entrance channel charge hopping with reagent vibrational state might be important. For example, if charge hopping between D_2^+ (v = 0) + HD is not efficient at small impact parameter, HD_2^+ will be the product species, and further decomposition of some of the excited HD_2^+ give a D^+/H^+ ratio of less than 3. On the other hand for D_2^+ in higher vibrationally excited states, charge hopping might be fascile and produce excited D_3^+ and HD_2^+ intermediates in a statistical ratio. But because of the mass ratio, D_3^+ is likely to contain higher excitation energy and a larger fraction of D_3^+ could dissociate and give a D^+/H^+ ratio greater than 3.

In any case, it is possible that at least part of the observed CID occurs through triatomic product decomposition, and thus competition between CID and D_2H^+ formation is not unreasonable. At high

collision energies, both channels have similar magnitude cross sections, and both involve substantial rearrangement of the collision partners.

Examination of Figure 2 shows that while the formation of D_2H^+ product from both the $H_2^+ + D_2$ and $D_2^+ + H_2$ reagents is suppressed by reagent vibrational and collision energy to some extent, the effect is much more dramatic for the $D_2^+ + H_2 \rightarrow D_2H^+ + H$ ("atom transfer") reaction. Part of this is no doubt due to the fact that the cross section for "atom transfer" is smaller than that for "proton transfer," and thus appears to be more strongly effected by the competition with CID. The size of the differences in cross sections and vibrational effects between the two reactions suggest however, that if competition between D_2H^+ formation and CID is the primary effect responsible for the differences, then D_2H^+ formed from $D_2^+ + H_2$ reagents must dissociate more than that formed from $H_2^+ + D_2$. This suggests that D_2H^+ product is formed with different degrees of internal excitation depending on the starting reagents. This could be a kinematic effect. But since kinematic effects do not seem to be very important in CID, it seems more likely that at E_{cm} greater than ~3 eV the $D_2^+ + H_2 \rightarrow D_2H^+ + H$ reaction proceeds at least in part, by a mechanism other than the low energy charge exchange-proton transfer process. This second, high energy mechanism yields more excited D_2H^+ product, which then dissociates with higher probability than D_2H^+ formed by proton transfer from $H_2^+ + D_2$ reagents. This high energy mechanism could include atom transfer or a number of excited PES reaction paths. If

this is true, then if one could measure the H_2D^+ production cross sections from $H_2^+ + D_2$ and $D_2^+ + H_2$, the large depletion of product formation at collision energies above 3 eV should appear in the $H_2^+ + D_2 \rightarrow H_2D^+ + D$ reaction.

Conclusions

Examination of the data presented here with previous work on the H_4^+ system has provided new information and new insights into the detailed dynamics of this "simple" chemical system. The present results add to the evidence for a direct mechanism for triatomic (H_3^+) ion formation. Extensive long range charge transfer is seen to be important. Evidence for both adiabatic and diabatic reactions has been discussed. A model for the reaction, which takes into account the multi-PES nature of the problem as well as competition between different reactive channels, seems to explain the experimental results satisfactorily.

We have also shown that in contrast to neutral reactions where reagent vibration appears to be important primarily in surmounting the potential energy barrier to reaction; in ion-molecule systems, especially when reagent charge transfer is near resonant, reagent vibration is very important in influencing such effects as charge transfer and surface hopping. In the H_4^+ system the electronic effects induced by vibrational excitation overshadow the effect of enhanced nuclear motion.

Our data has clearly shown the sensitivity of the vibrational dependence of reaction cross sections on the detailed nature of the

reaction PES. It has been shown to be a useful probe for understanding multipotential energy effects like surface hopping and charge state mixing. It also has allowed us to examine the competition effects between triatomic ion formation and collision induced dissociation.

By examining the competition between reaction, CID, and charge transfer, we can infer something about the range of impact parameters which contribute to each process. As discussed previously, the large magnitude, collision energy independent cross section for charge transfer (Figure 7) implies that this is a process which is effective even with a large impact parameter. At very low collision energies, the reaction cross section is quite large, leading to some competition with the charge transfer process which can be seen in Figure 7. As the collision energy increases, the range of impact parameters leading to reaction becomes smaller, and reaction ceases to compete with CT, although in reactive collisions, CT may still occur at long range in the entrance channel. Above 3 eV the CID process begins to compete with reaction. Although, both processes occur at small impact parameters, comparison of Figure 2-6 suggest that the competition is very complicated, with strong dependence on collision energy and reagent vibrational state. This again indicates that the competition between product formation and collisional dissociation is not a simple branching of some common intermediates. There must be some basic difference in the nature of collisions leading to the two processes; perhaps orientation, or whether charge transfer occurred in the reaction entrance channel.

Many questions still remain concerning competition between various processes, excited state dynamics, etc. More detailed theoretical investigation will be required before the detailed reaction dynamics will be understood. The H_4^+ system is clearly a useful paradigm for more complex multisurface problems, and the new detailed data available should provide a sensitive test for the development of new theoretical models.

Chapter III

REFERENCES

1. E. Herbst, W. Klemperer, Ap. J. 185, 505 (1973), W. D. Watson, Ap. J. 183, 117 (1973).
2. S. S. Prasad and A. Tan, Geophys. Res. Lett. 1, 337 (1979).
3. J. R. Krenos, K. K. Lehman, J. C. Tully, P. M. Hierl, G. P. Smith, Chem. Phys. 16, 109 (1976). P. M. Hierl, Z. Herman, Chem. Phys. 50, 249 (1980).
4. D. W. Vance, T. L. Bailey, J. Chem. Phys. 44, 486 (1966). J. H. Futrell, F. P. Abramson, Adv. Chem. Ser. 58
5. C. H. Douglass, D. J. McClure, and W. R. Gentry, J. Chem. Phys. 67, 4931 (1977).
6. A. B. Lees and P. K. Rol, J. Chem. Phys. 61, 4444 (1974).
7. W. A. Chupka, M. E. Russell, K. Refaey, J. Chem. Phys. 48, 1518 (1968).
8. W. T. Huntress, D. D. Elleman, M. T. Bowers, J. Chem. Phys. 55, 5413 (1971).
9. L. D. Doverspike, R. L. Champion, J. Chem. Phys. 46, 4718 (1967).
10. S. L. Anderson, T. Hirooka, P. W. Tiedemann, B. H. Mahan, Y. T. Lee, J. Chem. Phys. 73, 4779 (1980).
11. J. T. Muckerman, private communication.
12. I. Koyano, K. Tanaka, J. Chem. Phys. 72, 4858 (1980).
13. J. R. Stine, J. T. Muckerman, J. Chem. Phys. 68, 185 (1978).

14. S. Sakai, S. Kato, K. Morokuma, Ann. Rev. Institute for Molecular Science, Okazaki, Japan, 1979.

R. F. Borkman and M. Cobb, preprint 1980.

M. Cobb, T. F. Moran, R. F. Borkman, R. Childs, Chem. Phys. Lett. 57, 326 (1978).

R. D. Poshusta, and D. F. Zetik, J. Chem. Phys. 58, 118 (1973).

16. J. Futrell, F. Abramson in ion Molecule Reactions in the Gas Phase. ACS Pub., Washington, 1966, p. 123.

17. J. Durup and M. Durup, J. Chim. Phys. 64, 386 (1967).

Chapter III

FIGURE CAPTIONS

Fig. 1. Typical quality data. Upper trace is the transmission function of the primary ions. The two lower traces are cross sections for D_2H^+ formation from H_2^+ (v = 0,4) + D_2.

Fig. 2. Vibrational and translational energy dependence of D_2H^+ formation reactions.

Fig. 3. D^+ formation cross sections from $D_2^+(v)$ + HD.

Fig. 4. H^+ formation cross sections from D_2^+ + HD.

Fig. 5. D^+:H^+ ratio in CID of D_2^+ + HD.

Fig. 6. D_2^+ (v = 0) + H_2 charge transfer cross section.

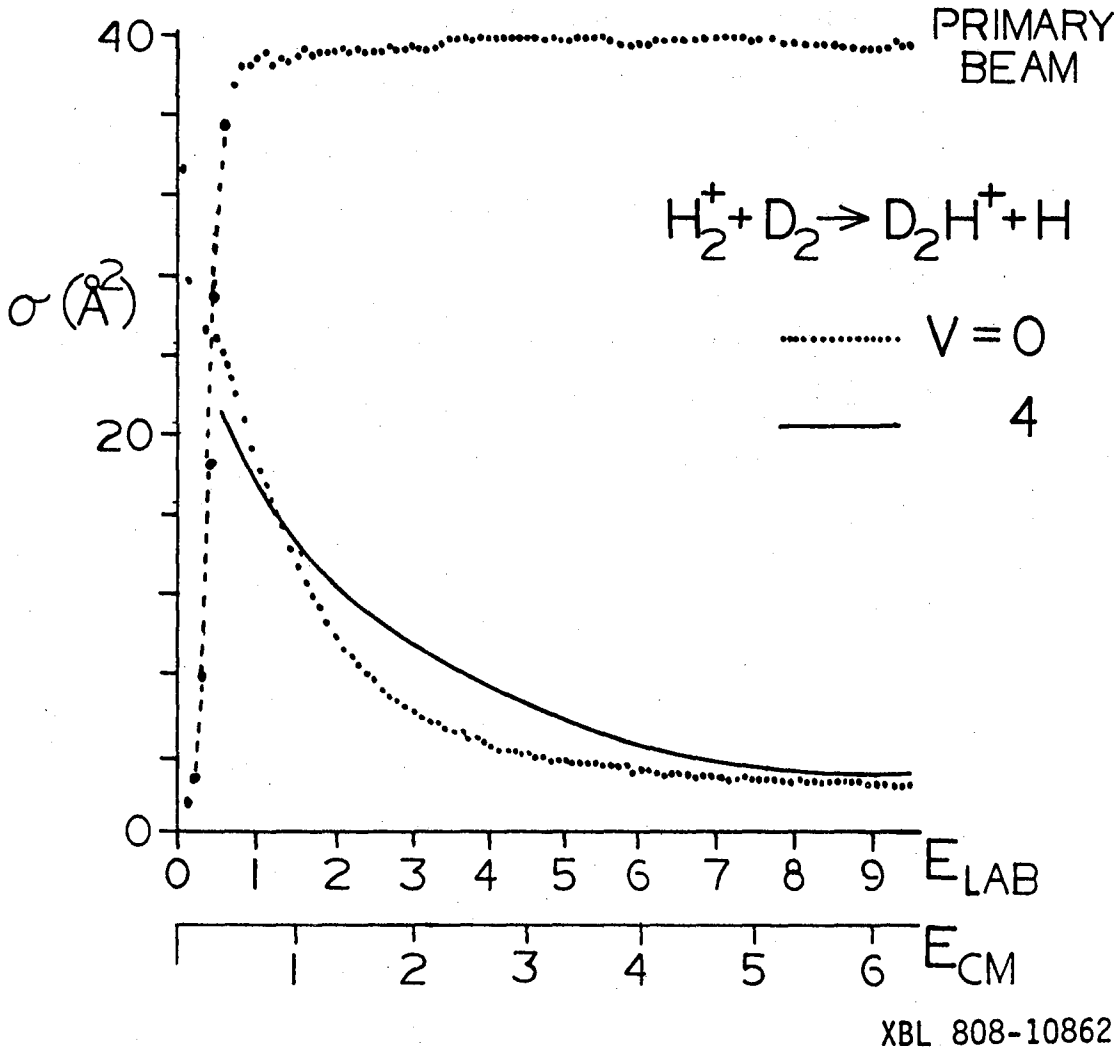
40
20
0
σ (Å²)
PRIMARY BEAM
H₂⁺ + D₂ → D₂H⁺ + H
V = 0
4
0 1 2 3 4 5 6 7 8 9
E_LAB
1 2 3 4 5 6
E_CM
XBL 808-10862

Fig. 1

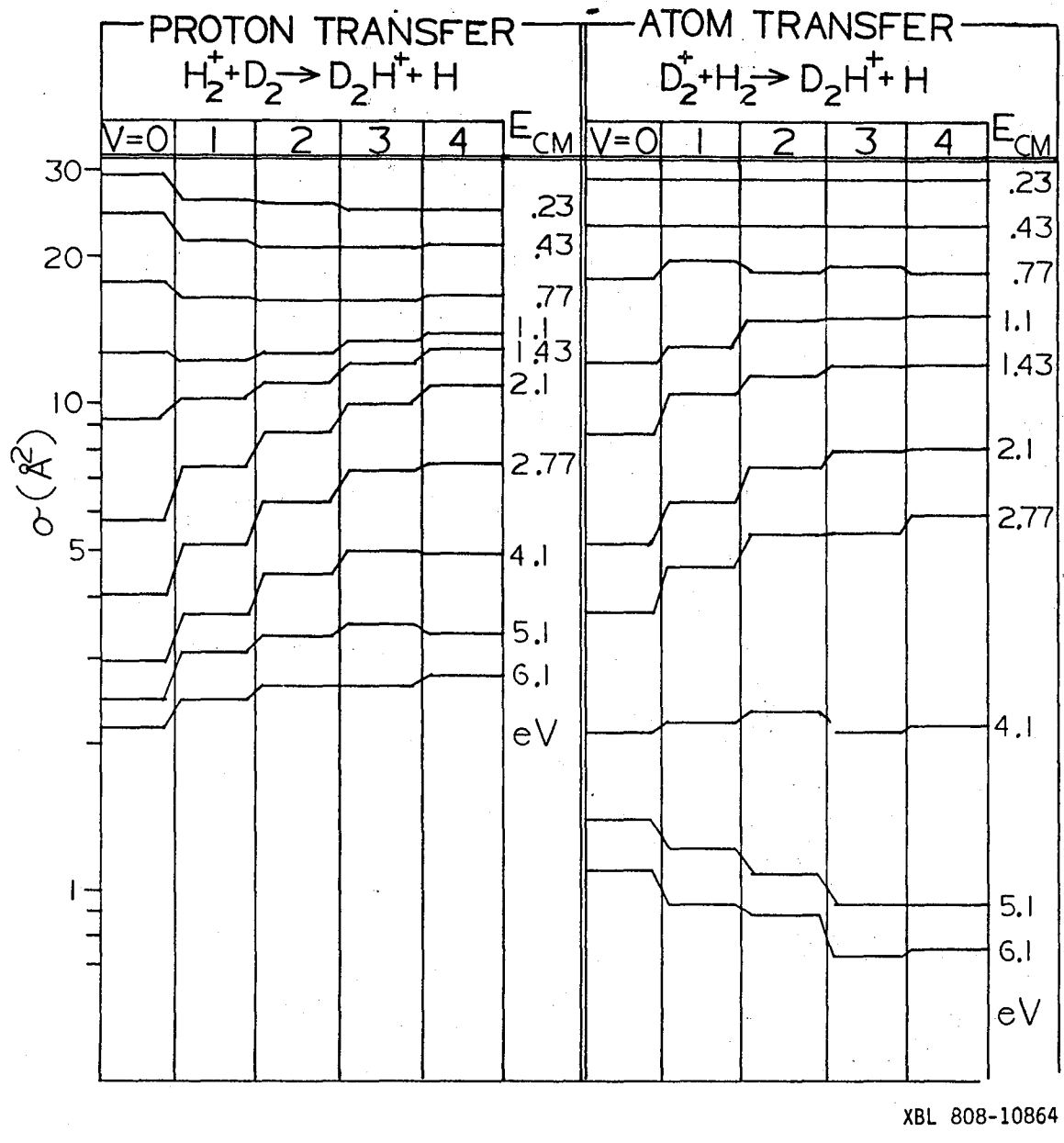
PROTON TRANSFER
$H_2^+ + D_2 \rightarrow D_2H^+ + H$
ATOM TRANSFER
$D_2^+ + H_2 \rightarrow D_2H^+ + H$
V=0
1
2
3
4
E_{CM}
30
20
10
5
1
σ (Å^2)
.23
.43
.77
1.1
1.43
2.1
2.77
4.1
5.1
6.1
eV
XBL 808-10864

Fig. 2

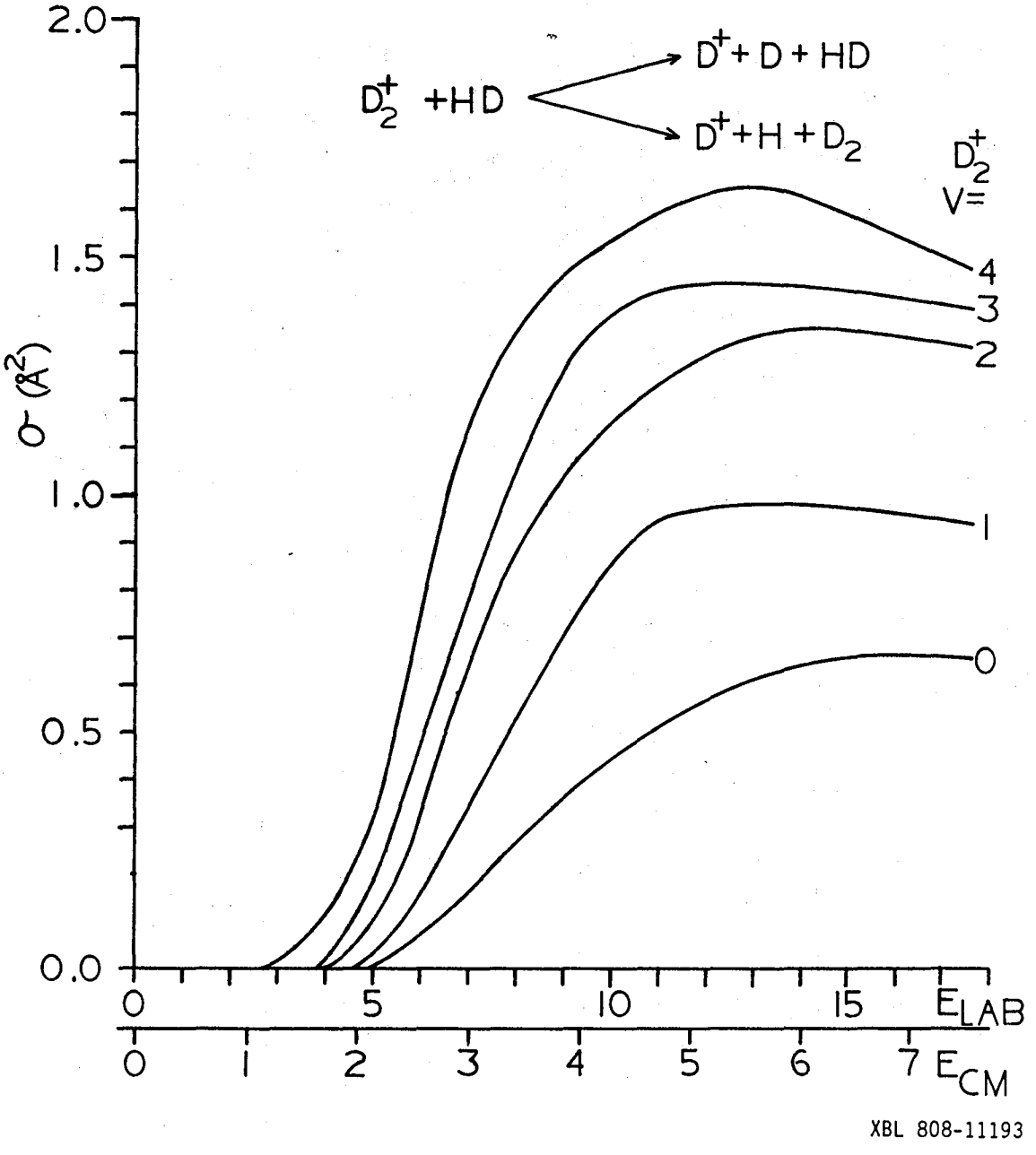
2.0
1.5
1.0
0.5
0.0
σ (Å²)
D₂⁺ +HD
D⁺+ D + HD
D⁺+H + D₂
D₂⁺ V=
4
3
2
1
0
0
5
10
15
E_LAB
0
1
2
3
4
5
6
7
E_CM
XBL 808-11193

Fig. 3

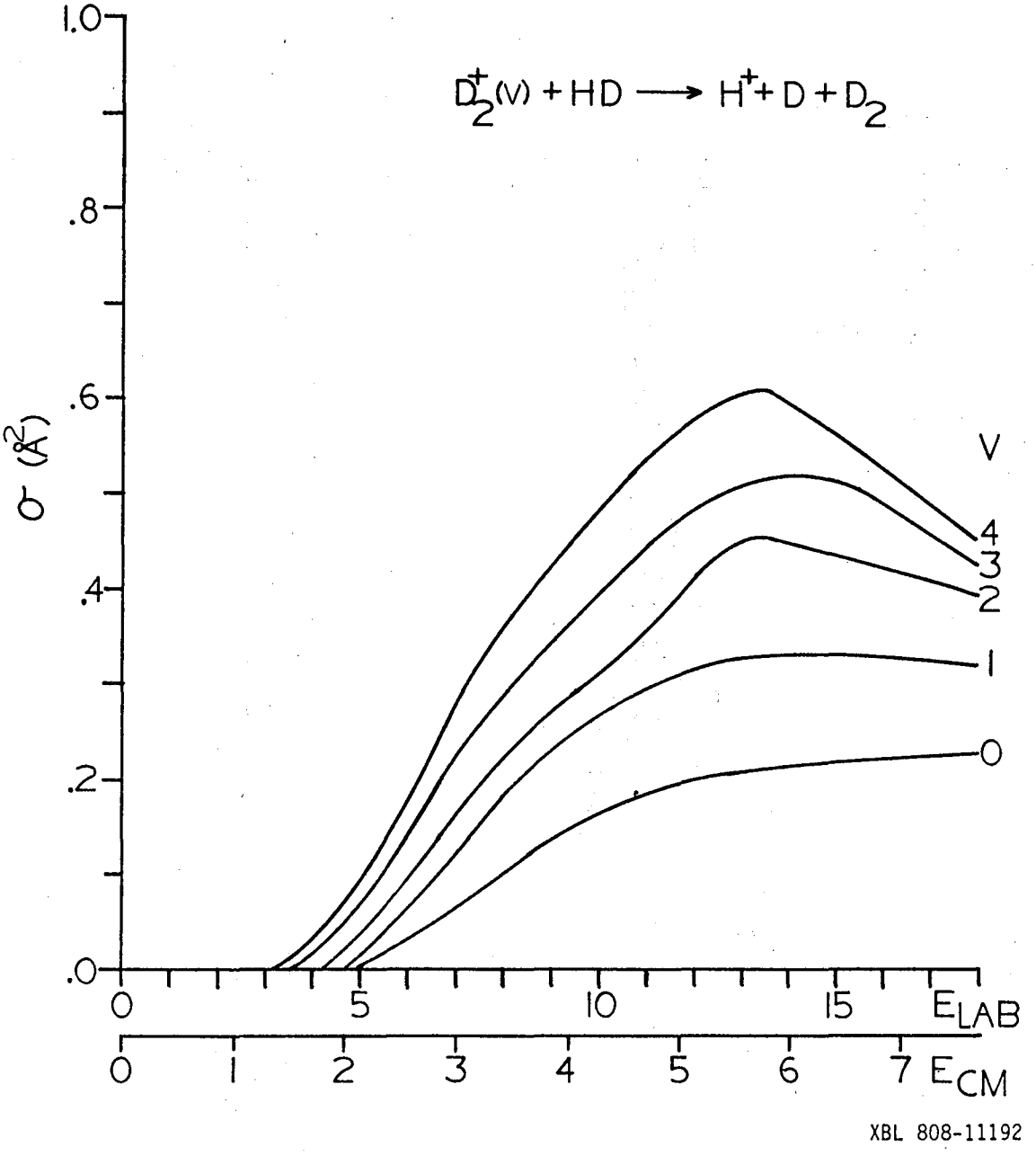
$D_2^+(V) + HD \longrightarrow H^+ + D + D_2$
1.0
.8
.6
.4
.2
.0
σ (Å²)
V
4
3
2
1
0
0
5
10
15
E_{LAB}
0
1
2
3
4
5
6
7
E_{CM}
XBL 808-11192

Fig. 4

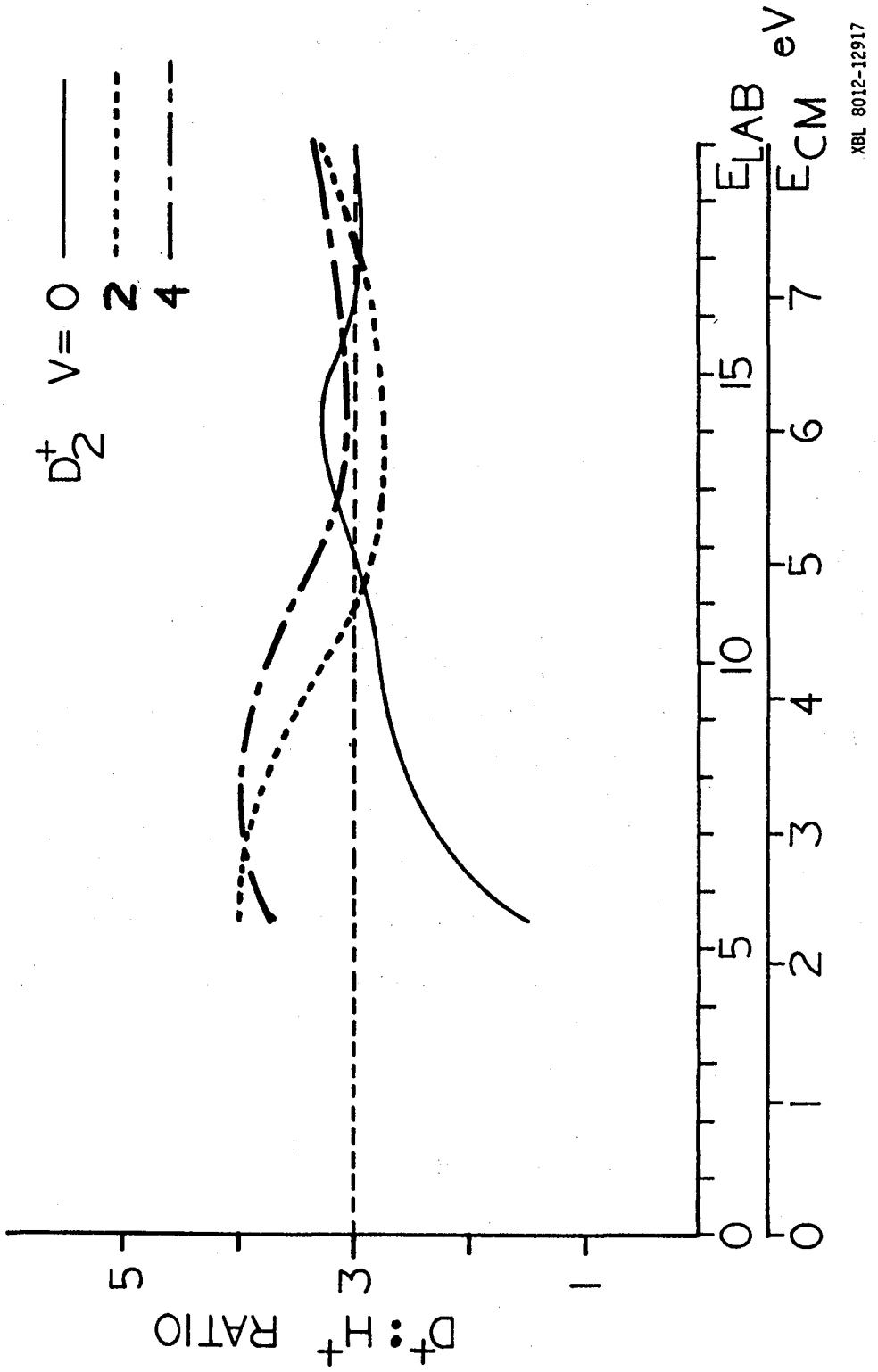
D_2^+ V= 0
2
4
$D^+ : H^+$ RATIO
5
3
1
0
1
2
5
3
4
10
5
6
15
7
E_{LAB}
E_{CM}
eV
XBL 8012-12917

Fig. 5

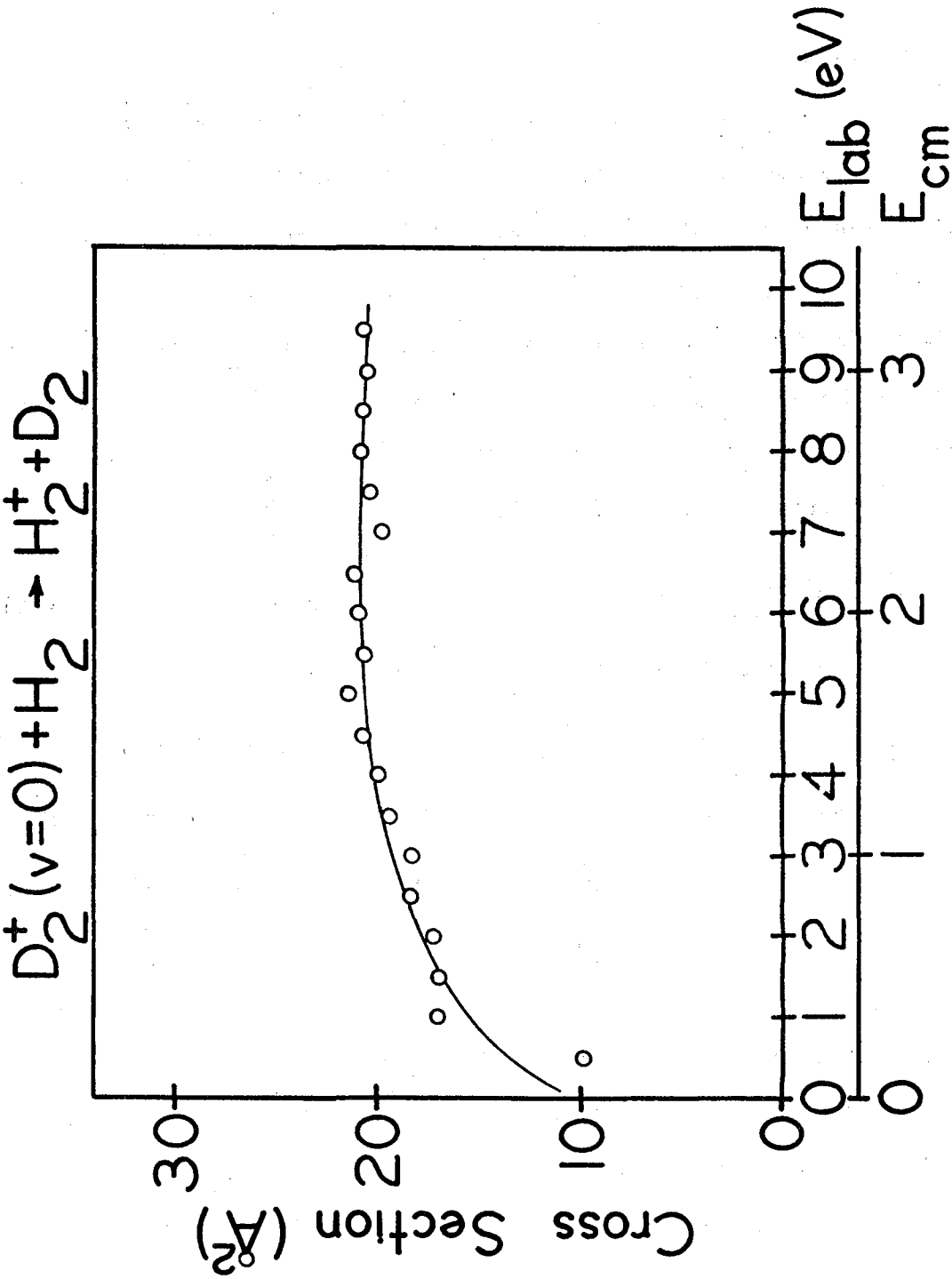

XBL 8012-12857

Fig. 6

IV. $H_2^+ + Ar$

Introduction

The $H_2^+ + H_2$ system is an example of a system where resonant or near resonant CT is always possible, coupling the different reagent charge states together effectively, especially at low collision energies. In $(H_2 + Ar)^+$, this near resonant CT is only possible for selected initial vibrational states and the system is highly asymmetric. This may be expected to result in striking vibrational effects on the dynamics of proton and charge transfer in $H_2^+ + Ar$.

The major reactive channels in $(H_2 + Ar)^+$ are:

$$H_2 + Ar^+(^2P_{3/2}) \rightarrow H_2^+ + Ar \qquad \Delta E = -0.33 \text{ eV} \qquad (1a)$$

$$H_2 + Ar^+(^2P_{1/2}) \rightarrow H_2^+ + Ar \qquad \Delta E = -0.51 \text{ eV} \qquad (1b)$$

$$H_2 + Ar^+ \rightarrow ArH^+ + H \qquad \Delta E = -1.61 \text{ eV} \qquad (2)$$

$$H_2^+ + Ar \rightarrow Ar^+(^2P_{3/2}) + H_2 \qquad \Delta E = +0.33 \text{ eV} \qquad (3a)$$

$$H_2^+ + Ar \rightarrow Ar^+(^2P_{1/2}) + H_2 \qquad \Delta E = +0.51 \text{ eV} \qquad (3b)$$

$$H_2^+ + Ar \rightarrow ArH^+ + H \qquad \Delta E = -1.30 \text{ eV} \qquad (4)$$

Theoretical investigations of the $(H_2Ar)^+$ system have provided a clear picture of some aspects of the dynamics of these reactions.[1-4] Mahan has shown that the initial charge state $Ar^+ + H_2$ does not correlate to ground state ArH^+, but $H_2^+ + Ar$ does. This implies that charge transfer must take place prior to proton transfer in order for reaction (2) to occur. Calculations of Diatomics-in-Molecules (DIM) potential surfaces[2], and trajectory studies[3] of reactions (1) and

(2) on them confirm this mechanism. There is an avoided crossing (Figure 1) between the surfaces corresponding to $H_2^+ + Ar$ and $Ar^+ + H_2$, which is located in the entrance valley, which begins to couple the charge states when the reagents are approximately 4Å apart. Trajectories show that, in the case where Ar^+ reacts with H_2, charge transfer does precede proton transfer, and that the occurrence of charge transfer is strongly influenced by vibrational motion of H_2. Furthermore, reactions (1) and (2) are predicted to be direct in nature: a long-lived ArH_2^+ intermediate is not likely to be involved.

A recent set of exact and approximate one dimensional scattering calculations for reactions (1)-(4) using DIM surfaces has focussed on the role of vibration in proton transfer[4]. The total energy range was 0.5-0.8 eV. It was found that proton transfer to Ar can occur on a single surface for H_2^+ (v=0,1) and no potential barriers are involved. Avoided crossings make barriers to reaction for H_2^+ (v>1) and all states of $Ar^+ + H_2$ (v). The primary effect of these barriers is on the shape of the reaction cross section function at very low kinetic energies. Also, evidence for formation of quasi-bound states at about 0.1 eV was found. It was suggested that these states were likely to be formed in the turning region rather than in one of the wells formed at an avoided crossing. Although these one dimensional theoretical calculations provide some insight on reaction dynamics, they are not expected to have significant relation to what one observes in the experiments.

Experimental work using mass spectroscopy, crossed molecular beams and photoionization have served to confirm various aspects of the theory.[5-12] Owing to the difficulty of producing H_2 and H_2^+ in known vibrational states, much of the published work has been restricted to reactions of electronic state-selected Ar^+ ($^2P_{1/2}$, $^2P_{3/2}$) with ground state H_2. Recently, several studies of reactions (3) and (4) using crossed molecular beams have appeared.[6-8] In those experiments, beams of H_2^+, presumably in a Franck-Condon distribution of vibrational states, were produced by electron impact. The proton transfer reaction was found to be direct, but the dynamics were more complex than a simple stripping process. Arguments were made based on some assumptions that high ArH^+ rotational excitation allowed formation of product with internal energy well above the dissociation limit[7]. In a separate experiment, the H_2^+ beam was partially state-selected, leaving ions of v=0-2. It was found that, at fixed collision energy, change in reagent vibrational state beyond v=2 had little or no effect on the reaction[8].

The crossed beam work suggested that charge transfer between H_2^+ and Ar occurs by two mechanisms:[6] a long-range process involving grazing collisions at all energies, and an intimate collision process at low energy (<1 eV). Both mechanisms were translationally endoergic, i.e., relative translation was converted to product vibration at all energies although only for H_2^+ (v=0 and 1) is the charge transfer to Ar endoergic. The observation of two mechanisms was also made in crossed beam studies of the other reagent charge state, $H_2 + Ar^{+9}$. However, in that work little or no translational energy was transferred

during the long range charge transfer collisions. The intimate collisions were found to involve a small conversion of translation to vibration in the products. The probability for long range charge transfer was found to depend strongly on the existence of resonant or near-resonant states of the products. This effect was masked in the H_2^+ + Ar work because of the distribution of reagent vibrational states.

Three studies have appeared in which photoionization has been used to select the initial H_2^+ vibrational state.[10-12] Data were obtained for kinetic energies of 1 eV and ~20 eV. As found in the beam experiments, at low relative translational energies (<1 eV), vibrational energy has little or no effect on the proton transfer reaction.[10-12] The charge transfer reaction, on the other hand, has a very strong vibrational dependence which follows a model in which charge transfer is most probable between two states that are near-resonant in energy, and have favorable Franck-Condon factors for the transition.[12-13] This is consistent with the observation of a long-range mechanism in crossed beams experiments.

Several of the experimental studies have addressed the question of competition between proton and charge transfer as a function of kinetic energy. Using crossed beams and non-state selected reagents, it was found that the two processes are about equally probable at low kinetic energy, while charge transfer becomes increasingly more important as kinetic energy increases[6]. This is in agreement with photoion-photoelectron coincidence experiments at 1 eV, if the strong

variation in charge transfer cross section with vibrational state is taken into account.[11] A very interesting observation was made in that work of a resonant enhancement of charge transfer at the expense of proton transfer at very low kinetic energy. With the exception of this result, the two channels do not appear to be linked in any general way at low energies, as evidenced by the great difference between their vibrational dependence.

The data presented here confirm the general conclusions reached in earlier studies. The range of kinetic energies used, 0-10 eV, bridges those of previous photoionization experiments, providing new information on the interaction of proton and charge transfer in this system. Isotopic substitution allows examination of the relative importance of resonance and Franck-Condon factors in determining the vibrational dependence of charge transfer cross sections. Finally, oscillatory structures in the kinetic energy dependence of charge transfer from ground vibrational state ions have been observed for the first time.

Results

Absolute charge transfer and proton transfer cross sections were obtained for center-of-mass kinetic energies of 0-10 eV, and for H_2^+ and D_2^+ vibrational states 0-4. The data are presented in Figures 2-6.

Charge Transfer. Figure 2 shows the collision energy dependence of H_2^+ + Ar CT cross sections for H_2^+ v = 0-2. Cross sections for the two isotopic systems are similar in magnitude. For each vibrational state, the kinetic energy dependences of the two isotopes are quite similar. At each kinetic energy, the vibrational dependence is also similar, peaking at v=2. In the D_2^+ system, however, the

enhancement of v=1 relative to v=0 is not as strong, and the decrease from v=2 to v=3 is not as great.

In general, the kinetic energy dependence of charge transfer for a single vibrational state is found to be quite smooth, and relatively flat. This is not the case for the v=0 state of both H_2^+ and D_2^+, as can be seen in Figure 5. Clear, reproducible structure is seen in the cross section functions. To our knowledge, this observation has not been reported previously.

Our results can be compared with previous photoionization studies of H_2^+ + Ar at two energies (Table 1). At low kinetic energy, 1 eV, Tanaka and co-workers[11] have found the vibrational dependence to be qualitatively similar to that shown in Figure 3. The cross section is a maximum at v=2, but the magnitude of the cross section for v=1 relative to v=2 is smaller than that found in the present work. The absolute values are in poor agreement: for v=2 we obtain σ = 50 Å^2, while their value is about 25 Å^2. Although we did not obtain charge transfer data at 20 eV, trends apparent in the data at 9 eV can be compared to results of Tanaka and Campbell[12]. Peaking of the cross section at v=2 is maintained, in agreement with Tanaka, but not with Campbell, who observed a maximum at v=1. An increase in the relative magnitude of the v=1 cross section with increasing kinetic energy is evident in our data, as is also observed by Tanaka. Both Tanaka and Campbell obtain absolute cross sections of about 5 Å^2 at 20 eV. This reflects a strong dropoff in cross section with kinetic energy. As shown in both Figures 3 and 4, such a trend is not observed in our data up to 9 eV.

Proton Transfer. Figure 6 shows the collision energy dependence for H_2^+ proton transfer to Ar. As is found in the charge transfer data, the magnitudes of the proton transfer cross sections for the two isotopes are similar, although in the D_2^+ system the cross sections fall off much more sharply with kinetic energy. The vibrational dependences (Figs. 3 and 4) are similar in shape, those of the D_2^+ system being slightly weaker, in general, than those of the H_2^+ system. In both systems, the cross sections rise gently with increasing vibrational energy at 1 eV. As the kinetic energy increases, however, the vibrational enhancement for v=0-2 becomes much more pronounced, and the dependence bears a strong resemblance to that observed for the charge transfer channel.

These data can only be compared to previous experiments on H_2^+ + Ar at ~1 eV. The vibrational dependence found by Tanaka[11] is in good agreement with ours, showing a weak increase with vibrational state (Table 1). Chupka[10] also reported that proton transfer has little or no vibrational dependence at thermal energies. The absolute cross sections in Figure 3 are in disagreement with those of Tanaka, ours being about a factor of three higher. This may be due to the superior collection efficiency which our experiment has for slow product ions. In any case ratio of PT/CT found by Tanaka agrees reasonably well with our data at low collision energies.

Sources of error in the relative cross sections reported for H_2^+ + Ar are essentially the same as for H_2^+ + H_2 (Chapter III). It has been noted that back-diffusion of gas from the scattering cell into

Table 1. Comparison of vibrational effects of this work and those of Tanaka et al.[11]

	Charge Transfer			
	A	B	C*	D
V	Tanaka et al.[11] 1.24 eV	Present work 1 eV	Tanaka scaled to v=2 = 47.7	Ratio B/C
0	2.0 ± 3.5 Å^2	3.06 ± 0.3 Å^2	3.3 ± 5.8	0.93
1	6.8 ± 3.5	17.7 ± 0.9	11.2 ± 5.8	1.6
2	29.0 ± 3.5	47.7 ± 2	47.7 ± 5.8	1.0
3	16.8 ± 3.5	28.4 ± 1.6	27.6 ± 5.8	1.02
4	9.45 ± 3.5	24.4 ± 2.2	15.5 ± 5.8	1.5

	Proton Transfer			
	A	B	C*	D
V	Tanaka et al.[11] 1.24 eV	Present work 1.0 eV	Tanaka scaled to v=2 = 69.1	Ratio B/C
0	21.5 ± 5.4	51.8 ± 2	57.1 ± 14	0.91
1	23.6 ± 5.4	66.1 ± 2.2	62.7 ± 14	0.94
2	26.0 ± 5.4	69.1 ± 2.3	69.1 ± 14	1.00
3	31.8 ± 5.4	67.7 ± 2.4	84.5 ± 14	0.80
4	25.4 ± 5.4	73.4 ± 3.0	67.5 ± 14	0.92

*Scaling factor for CT = 1.64.

Scaling factor for PT = 2.66.

the ionization region introduces a background signal that is difficult to correct for into the charge transfer cross sections. This problem was largely eliminated by changing the location of a differential wall in the instrument, but could not be eliminated completely. In the case of H_2^+ and D_2^+ charge transfer with Ar, the nature of the error is as follows. The photoionization efficiency curve for Ar is not constant over the wavelength range used because of the formation of two spin-orbit states of the ion[13]. If it were constant, the Ar^+ back-diffusion signal would be constant, introducing a uniform error into the CT cross sections. Instead, no Ar^+ is formed at the wavelengths used for H_2^+ and D_2^+ (v=0,1), small amounts are present for H_2^+ (v=2,3) and D_2^+ (v=2-4), and a larger quantity is formed with H_2^+ (v=4). Control experiments have allowed the following error limits to be placed on the charge transfer data: ±5 percent for H_2^+ and D_2^+ (v=0,1), ± 7 percent for H_2^+ (v=2,3) and D_2^+ (v=2-4), and ±15 percent for H_2^+ (v=4). The appropriate error limits for the proton transfer cross sections are ± 5 percent.

Comparison of our results with those of Tanaka[11] suggest that we may be overestimating the vibrational purity of our ion beam at the higher vibrational states. This has the effect of causing us to <u>understate</u> the magnitude of the vibrational effects observed. Table 1 compares our low energy CT results with Tanaka's, and shows that our v=4 cross section appears to be too high. This is not the ase for Proton Transfer. The large discrepancy for v=1 cannot be explained this way, however. Since the error bars on the combined measurements are fairly large, we have elected to continue to use our estimates for

vibrational purity. Table 2 shows the raw data and may be used to generate better vibrationally corrected cross sections if in the future we obtain better estimates of our vibrational state purity.

Discussion

The present results are in qualitative agreement with previous work. However, measurement of reaction cross sections over a wide energy range as a function of vibrational and kinetic energy has provided important new information concerning the interplay of charge transfer and proton transfer in $H_2^+ + Ar$, and hence on the role of the potential energy surfaces in the reaction.

Long-range charge transfer involves motion of the system through an avoided crossing region. When the system reaches the crossing seam, it can either remain on the original surface, undergoing charge transfer, or hop to the other surface, remaining in the initial charge state. If the system does hop to the upper surface, CT may occur there on subsequent vibrations. In general, vibrational motion, rather than relative translation is effective in carrying the system through the seam, thus playing a crucial role in determining whether or not and how charge transfer occurs.[3] Other factors are also important. When vibronic levels belonging to the two charge states of the system are close in energy, they will interact strongly, and their crossing will be more avoided than if their energies were not so close. In this case, charge transfer occurs more readily since the system is more likely to remain on the original potential energy surface which leads to two charge states in two asymptotic regions. The Franck-Condon

Table 2. Raw and vibrationally corrected cross sections for charge and proton transfer of H_2^+ and D_2^+ with Ar.

Reaction	E_{cm}	Corrected					Raw				
		v=0	1	2	3	4	v=0	1	2	3	4
H_2^+ + Ar, CT	1	3.06	17.7	47.2	28.4	24.4	3.06	16.1	38.9	28.1	26.2
	3	1.64	20.6	44.9	30.0	24.4	1.64	18.5	37.5	29.0	26.4
	6	1.51	24.8	38.9	30.1	27.8	1.51	22.2	33.6	28.6	27.7
	9	2.06	26.3	38.3	29.9	22.8	2.06	23.6	33.5	28.6	25.4
H_2^+ + Ar, PT	1	51.8	66.1	69.1	67.7	73.4	51.8	64.5	67.2	66.4	69.3
	3	12.3	30.4	44.6	38.9	45.3	12.3	28.4	39.7	36.4	39.8
	6	4.95	12.5	18.2	14.6	14.0	4.95	11.7	16.2	14.2	13.9
	9	3.17	8.9	12.1	10.8	7.24	3.17	8.27	10.9	10.1	8.5
O_2^+ + Ar, CT	1	2.32	13.3	32.8	30.0	25.5	2.32	12.2	28.2	26.7	25.4
	3	3.0	13.3	38.0	35.9	27.9	3.0	12.3	32.4	31.4	28.5
	6	1.89	15.1	36.5	32.0	25.4	1.89	13.8	31.4	28.9	26.4
	9	1.59	16.3	34.3	29.9	22.2	1.59	14.8	29.8	27.3	24.1
D_2^+ + Ar, PT	1	50.7	57.2	60.8	57.1	58.1	50.7	56.5	59.7	57.49	56.5
	3	9.74	17.5	27.1	26.5	24.4	9.74	10.7	24.7	24.4	23.7
	6	3.03	5.1	9.0	8.24	8.2	3.03	4.89	8.8	7.67	7.77
	9	1.55	3.15	4.64	4.8	3.0	1.55	2.99	4.25	4.36	3.48

overlap between the initial and final charge states also affects the probability of electron transfer at the avoided crossing. Thus, vibrational motion, resonance between energy levels, and favorable Franck-Condon factors are all expected to play a role in determining the magnitude of long-range charge transfer cross sections. Translational energy is not likely to be as critical.

Schematics of the energy levels for reaction (3) are presented in Figs. 7 and 8. The reason for the low H_2^+, D_2^+ (v=0) cross sections is evident from these diagrams. Reaction of these states is endoergic, and only substantial translational energy conversion will enable it to occur. Such transfer is inefficient except at short range, and thus the cross sections are low. The endoergicity for charge transfer to H_2^+ and D_2^+ (v=1) is smaller than from v=0. This is likely to be a major reason for the enhanced reaction cross sections of these states compared to those of v=0. The ordering $\sigma(H_2^+, v=1) > \sigma(D_2^+, v=1)$ may be due to the fact that the reaction of D_2^+ is more endoergic. For v=2 in both systems, exoergic charge transfer to near-resonant energy levels is possible, and the cross sections are high. While near-resonant levels also exist for v=3 and 4, they are endoergic for H_2^+ and exoergic for D_2^+. The cross sections, while remaining high, are seen to drop off more rapidly for H_2^+ above v=2 than for D_2^+.

The kinetic energy dependence of the cross sections are consistent with these trends. For v=0, translational energy transfer plays an important and interesting role in promoting charge transfer. For H_2^+ and D_2^+ (v=1), the cross sections are observed to increase with

kinetic energy. This is consistent with the fact that translational energy is required in order to overcome a rather modest endoermicity. For $v \geq 2$, the kinetic energy dependences are found to be rather flat, within experimental error.

Massey[14] proposed an adiabatic model to predict the location of maxima in the kinetic energy dependence of long range non-resonant charge transfer cross sections. These maxima are expected to occur when the following relation is satisfied:

$$\frac{\Delta E\ a}{\hbar\ V_{rel}} = 1$$

where ΔE is the asymptotic energy difference between the initial and final charge states of the system, a is a parameter which is related to the relative distance at which charge transfer occurs, and v_{rel} is the relative velocity of the ion and neutral. The maxima will only be pronounced for systems having relatively few accessible charge states that are not near-resonant in energy. This implies that structure would not be observable in the charge transfer cross sections of systems having many vibronic levels that are closely spaced in energy. A theory like that proposed by Bates,[15] which explicitly takes contributions from all possible transitions into account in calculating charge transfer cross sections, is more appropriate for such systems. In general charge transfer involving more than two atoms falls into the latter category--indeed, the kinetic energy dependence of charge

transfer for H_2^+ and D_2^+ ($v > 0$) shows the data to be quite smooth. H_2^+ and D_2^+ ($v = 0$) can be considered to be a system amenable to the Massey hypothesis, however. Table 3 shows a comparison between the positions of the peaks observed in the charge transfer function for H_2^+ and D_2^+ ($v = 0$) in Figure 5, and those calculated by using Massey's equation for the peak position and fitting one peak to obtain the parameter a. The parameter depends slightly on which peak is used, which is reasonable in light of its physical significance. The accuracy of the fit is good, indicating that this simple model may be used to describe charge transfer between an atom and a molecule under certain conditions. To our knowledge this is the first observation of this type of structure in charge transfer cross sections for polyatomic systems. Of course, it is dangerous to make assumptions based on fitting on two or three peaks. the peak positions occur at nearly the same collision energy for H_2^+ and D_2^+. This may result from some completely different effect and the apparent scaling may be coincidental. It is interesting to note that the "a" parameter used to fit the H_2^+ data is 2 times that used to fit the D_2^+ results. The reason for this is not clear from Massey's theory.

As noted above, overlaps of the nuclear wavefunctions should also be considered in a discussion of the vibrational effects. Franck-Condon factors for neutralization of H_2^+ and D_2^+ are obtained from calculations.[16] For H_2^+ and D_2^+ neutralization, the Franck-Condon

Table 3. Maxima in H_2^+ and D_2^+ (v=0) charge transfer cross sections.

Transition	$E(\sigma_{max})$ Observed (eV)	$E(\sigma_{max})$ Calculated (eV)
$\rightarrow H_2(v=0)+Ar^+(^2P_{3/2})$	1.2	1.49
$\rightarrow H_2(v=0)+Ar^+(^2P_{1/2})$ [a]	3.65	3.65
$\rightarrow D_2(v=0)+Ar^+(^2P_{3/2})$	1.1	1.47
$\rightarrow D_2(v=0)+Ar^+(^2P_{1/2})$ [a]	3.77	3.77
$\rightarrow D_2(v=1)+Ar^+(^2P_{3/2})$	7.6	7.32

a Transition used to obtain the a parameter (see text).

distributions are quite broad, in that regardless of the initial ion vibrational level, none of the transitions to low-lying neutral vibrational levels is strongly forbidden. Because of this and because of the fact that the $Ar \rightarrow Ar^+(^2P_{3/2,1/2})$ transition probabilities differ only by the statistical weight (2:1); wavefunction overlap between $H_2^+ + Ar$ and $Ar^+ + H_2$ states is less important in determining the magnitudes of the CT cross sections, than the CT energetics (exo or endoergic) and energy resonance effects. This is not the case with CT of H_2^+ with N_2 and CO. This data and a model calculation which crudely assesses the relative importance of various effects on CT will be presented in Chapter V.

Crossed molecular beams experiments have suggested that charge transfer between H_2^+ and Ar is predominately long-range, but that a fraction of the collisions are intimate in nature.[6] Kinetic energy analysis of the scattered products indicated that the reaction was substantially (up to several eV) translationally endoergic at all relative energies. This is surprising in view of the fact that the ion beam used was internally excited, and thus all vibrational levels greater than zero can undergo near-resonant charge transfer and the corresponding energy defects are only on the order of a few meV. Such a large transfer of kinetic energy would suggest that the charge transfer cross sections should have a strong translational energy dependence since the efficiency of energy transfer varies with relative velocity. This is not what we observe, however. The weak dependence of the charge transfer cross sections on kinetic energy found in our experiments is incompatible with

substantial energy conversion during the collision. Rather, we conclude that charge transfer in H_2^+ + Ar is mainly long range in nature and involves states that are very close in energy. One partial explanation for the inconsistency of the two sets of data is that the beam used by Farrar might be substantially lower in internal energy than is assumed due to partial relaxation. This does not account for the translational endoergicity quantitatively, however.

Proton transfer to Ar is a direct, exoergic process, and the reaction cross sections in Figs. 3, 4, and 6 have a typical kinetic energy dependence. The falloff for proton transfer compared to deuteron transfer is slower, however. Simple kinematic considerations account for the direction of the effect, but cannot account for the magnitude of the falloff. The origin of the difference in kinetic energy dependence of the two isotopic systems is not clear.

One-dimensional calculations by Baer and Beswick[4] predict the existence of a barrier to proton transfer of 0.7 eV for H_2^+ ($v = 2$). As can be seen in Figure 6, there is no downturn of the cross section at low kinetic energy, and thus no evidence for a barrier high enough to influence the reaction.

The vibrational dependence of the proton transfer process is particularly interesting. The data show that at all kinetic energies the reaction cross section for ground state ions is smaller than that for vibrationally excited ions, with relatively little variation for $v \geq 2$ in agreement with crossed molecular beams results. This is is the opposite of what would be expected on the basis of the potential

surfaces alone. Because H_2^+ (v=0) + Ar is substantially lower in energy than the $Ar_4^+ + H_2$ ground state, it does not mix significantly with the Ar^+ charge state. Lack of competition from charge transfer would be expected to enhance the probability of proton transfer in the v=0 state with respect to higher vibrational states where charge transfer cross sections are large. The fact that the observed trends are counter to these simple ideas indicates that the reaction dynamics of this system are quite complicated.

Evidence that the proton and charge transfer channels cannot be considered to be independent, can be found in comparing the vibrational dependence of the cross sections for proton and charge transfer. Although the trends are evident at all energies, the similarity in the dependences is particularly strong at higher kinetic energy. This implies that, regardless of the outcome of the collision, proton and charge transfer both involve passing through a common region of the available potential surfaces. Moreover, the major part of the vibrational dependence of either channel appears to be determined in this region, which is most likely to be that of the avoided crossing in the entrance channel. The detailed structure of the intersection region is quite complicated for H_2^+ ($v > 0$) since vibronic surfaces for all accessible states of the system (corresponding to the asymptotic energy levels in Figs. 6 and 7) each generate their own set of avoided crossings. This enables the system to undergo multiple hops between the surfaces, emerging on either the ground or excited PES, with or without substantial vibrational excitation.

This picture may explain the observed similarity of the CT and PT vibrational dependence at high collision energies. CT occurs when the system crosses the seam from the $H_2^+ + Ar$ portion of the potential surface to the $H_2 + Ar^+$ portion. If the collision is one with large impact parameter, then the reagents may separate without a further crossing of the seam. This results in CT. if a second crossing occurs then non-reactive scattering results. For smaller impact parameter collisions the multiple crossings which may occur for $v > 0$ may have the effect of vibrationally exciting the H_2^+. This vibrational excitation may increase the proton transfer cross section, and certainly the reduction of reagent relative velocity upon vibrational excitation will raise the PT probability. Thus we might expect that especially at high collision energies, the same vibrational dependences might be observed for both PT and CT since the reagent vibrational excitation controls the motion of the system through the crossing seam. The fact that the vibrational dependence for PT at low collision energies does not mirror that for CT may be due to the fact that the relative velocity is low and the probability of significant vibrational excitation at the seam is low. Also, at low collision energy, the inherent PT probability may be so high as to mask the effects of any behavior early in the collision.

Conclusion

In summary, cross sections for proton and charge transfer in the H_2^+ and D_2^+ + Ar system have been measured as a function of vibrational and kinetic energy. The data are in qualitative agreement with previous work. Charge transfer proceeds mainly by a long-range mechanism, with transfer of translational energy occurring where necessary to overcome endoergicities. The existence of near-resonant energy levels accounts for the major features of the vibrational dependence. Franck-Condon overlaps appear to play a less important role. Comparison of the vibrational dependences of the two reaction channels indicates that proton and charge transfer are closely linked in this system.

The strong vibrational effects appear to result primarily from the nature of the avoided crossing seam. Detailed trajectory or quantum calculations will be necessary to fully understand the $(H_2 + Ar)^+$ system, and our data should prove to be a sensitive test of theoretical models for non-adiabatic reactions.

Chapter IV

REFERENCES

1. B. H. Mahan, Accts. Chem. Res., 8 55 (1975).
2. P. J. Kuntz and A. C. Roach, J. Chem. Soc. For. Trans. II 68, 259 (1972).
3. S. Chapman and R. K. Preston, J. Chem. Phys. 60, 650 (1974).
4. M. Baer and J. A. Beswick, Phys. Rev. A. 19, 1559 (1979).
5. M. Berta and W. S. Koski, J. Amer. Chem. Soc. 86, 5098 (1964).
6. R. M. Billotta, F. N. Prenninger and J. M. Farrar, Chem. Phys. Lett. 74, 95 (1980).
7. R. M. Billota, F. N. Prenninger and J. M. Farrar, J. Chem. Phys. 73, 1637 (1980).
8. R. M. Billotta and J. M. Farrar, J. Chem. Phys. 74, 1699 (1981).
9. P. M. Hierl, V. Pacak and Z. Herman, J. Chem. Phys. 67, 2678 (1977).
10. W. A. Chupka and M. B. Russell, J. Chem. Phys. 49, 5426 (1968).
11. K. Tanaka, T. Kato and I. Koyano, J. Chem. Phys. (submitted).
12. F. M. Campbell, R. Browning and C. J. Latimer, J. Phys. B. 13, 4257 (1980).
13. R. E. Huffman, Y. Tanaka and J. C. Larrabee, J. Chem. Phys. 391, 902 (1965).
14. H. S. W. Massey and E. H. S. Burhop, Electronic and Ionic Impact Phenomena, Oxford Univ. Press, New York, 1952, p. 478.
15. D. R. Bates, R. H. G. Reid, Proc. Roy. Soc. A 310, 1 (1969).

16. Franck-Condon factors for $H_2^+ \rightarrow H_2$ are from M. R. Flannery, H. Tai, D. L. Albritton Atomic and Nucl. Data Tables 20, 563 (1977). D_2^+ FC factors were calculated from RKR potentials for D_2^+ and D_2 by Dr. Dennis Trevor.

Chapter IV

FIGURE CAPTIONS

Fig. 1. Cut through the $(H_2 + Ar)^+$ entrance channel at infinite reagent separation.

Fig. 2. Collision energy dependence of $h_2^+ + Ar$ charge transfer reactions.

Fig. 3. Vibrational effects on $H_2^+ + Ar$ cross sections.

Fig. 4. Vibrational effects on $D_2^+ + Ar$ cross sections.

Fig. 5. Cross sections for CT from H_2^+ $(v = 0) + Ar$ and D_2^+ $(v = 0) + Ar$.

Fig. 6. Collision energy dependence of $H_2^+ + Ar$ proton transfer reactions.

Fig. 7. Energetics for $H_2^+ + Ar$ CT. Column on the left gives the total energy of the $H_2^+(v) + Ar$ reagents. Columns to the right are the $Ar^+(^2P_{1/2,3/2}) + H_2(v)$ total energies.

Fig. 8. Energetics for $D_2^+ + Ar$ CT. Column on the left gives the total reagent energy, those on the right are the total product energies.

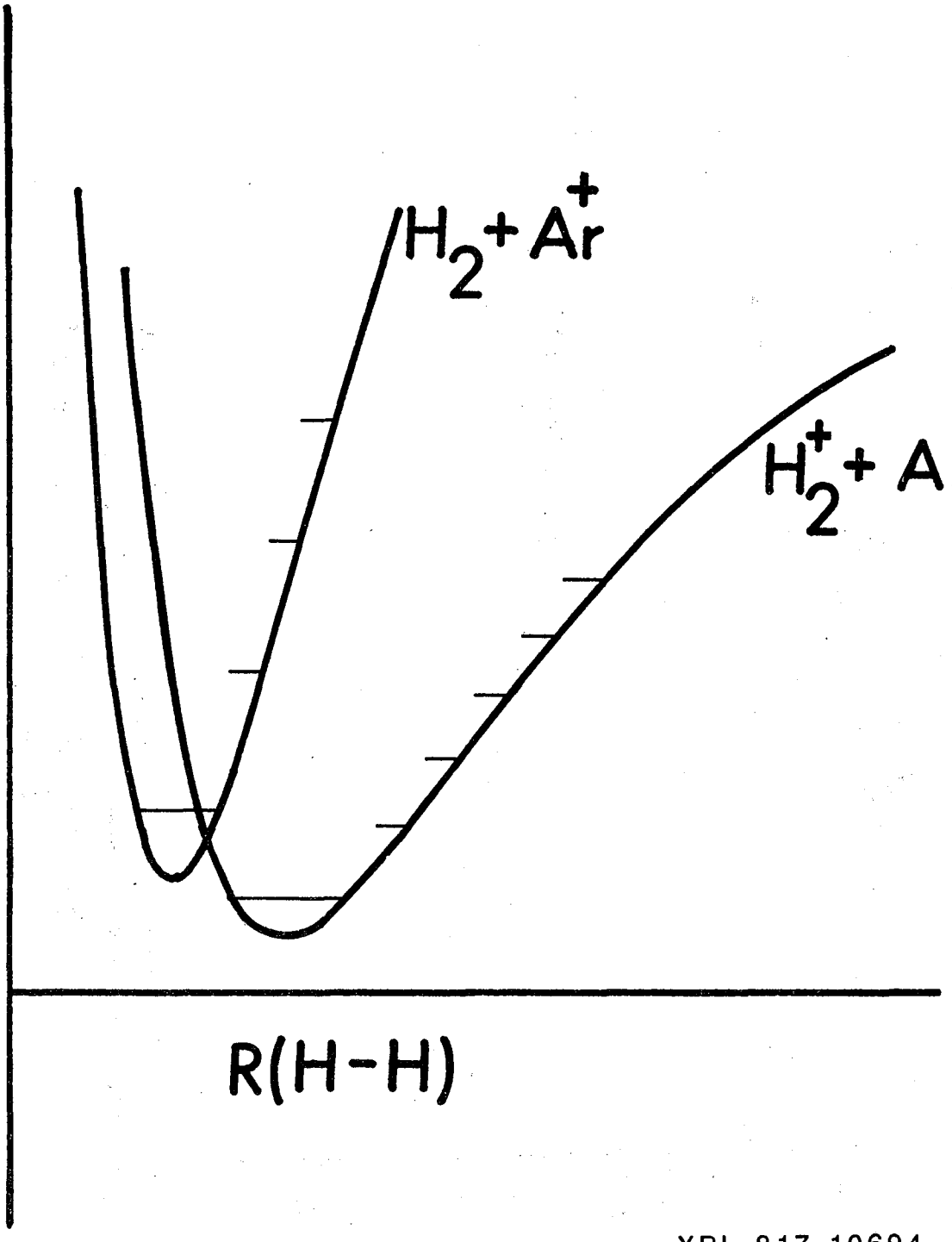

XBL 817-10694

Fig. 1

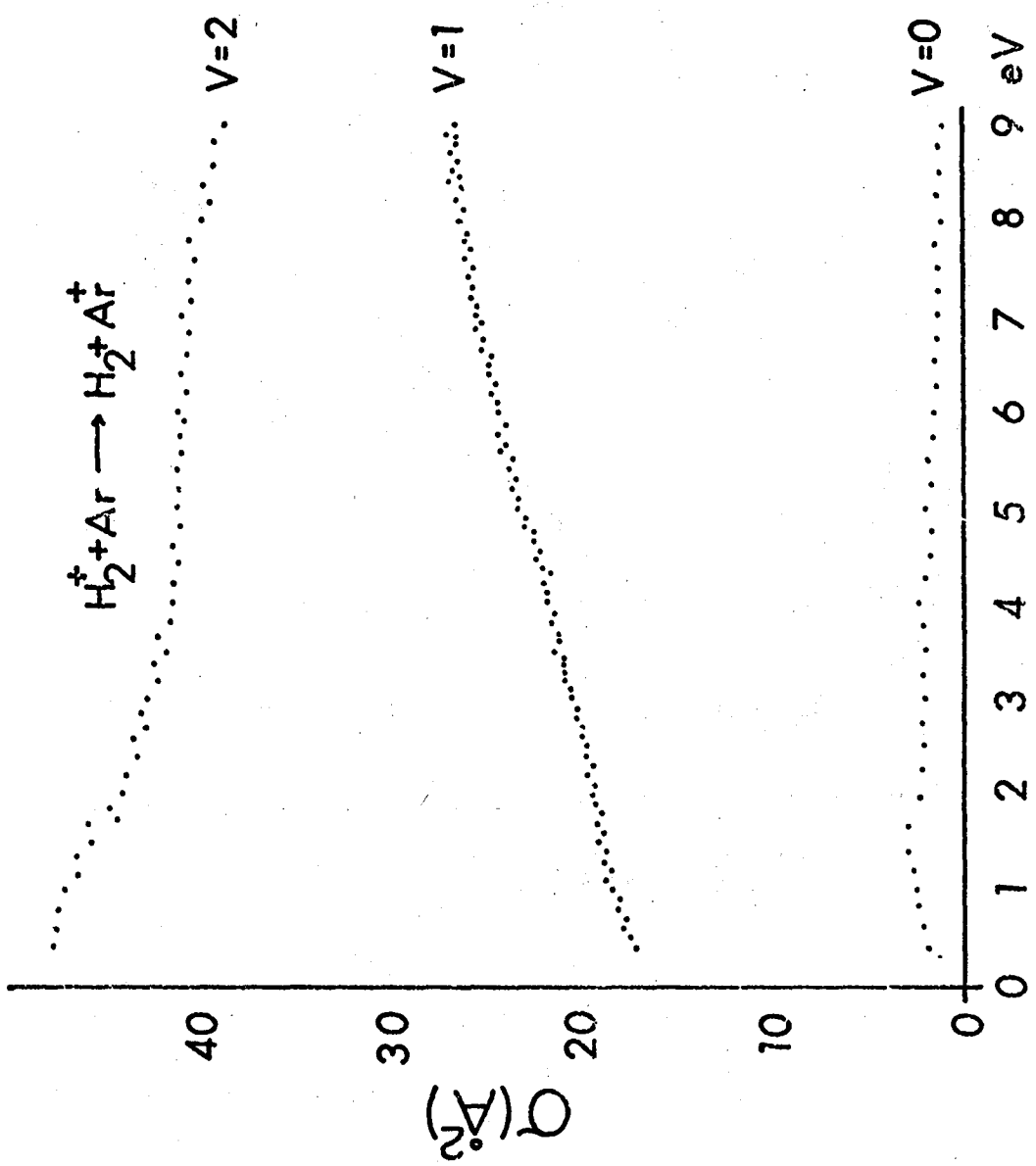

XBL 8111-12345

Fig. 2

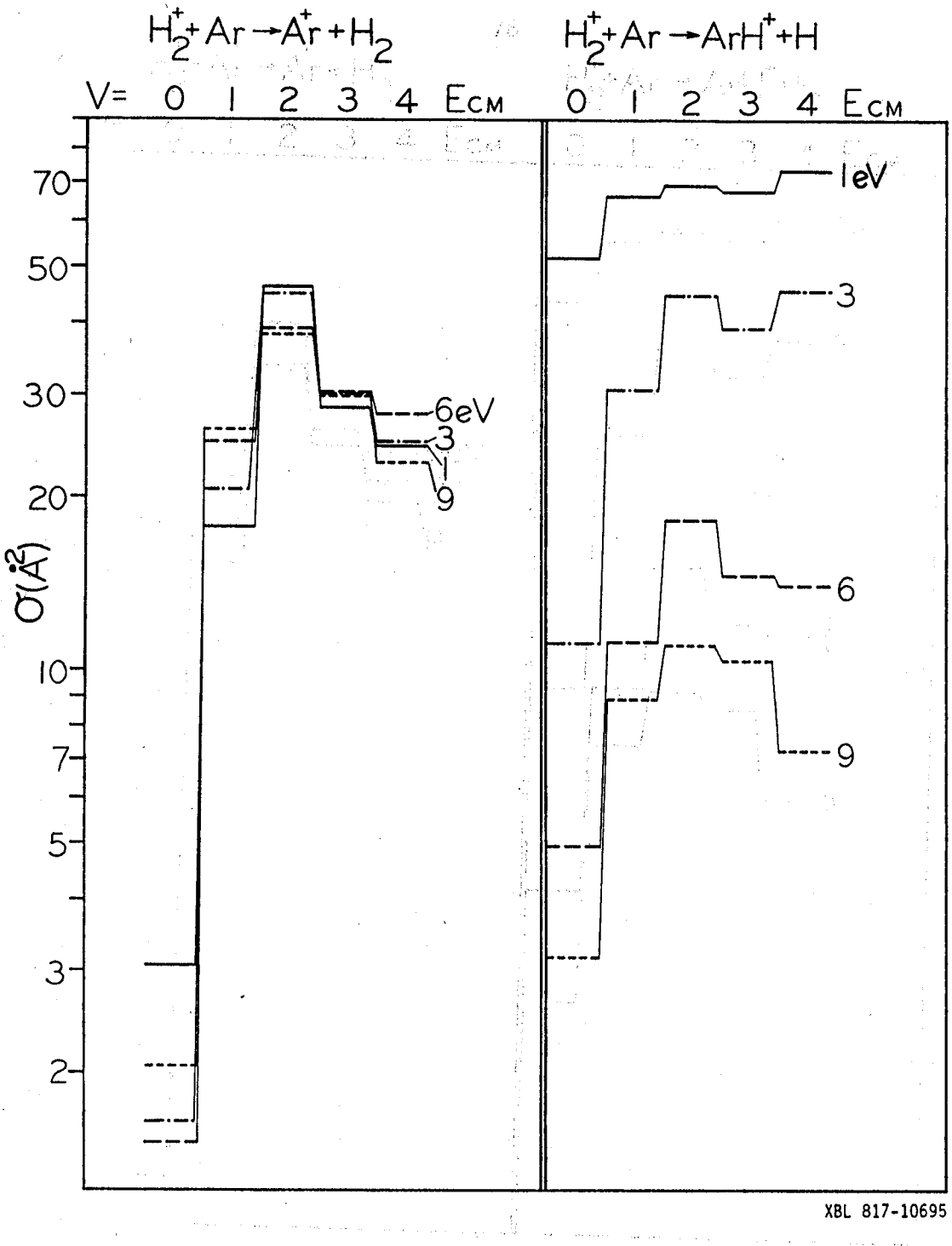
$H_2^+ + Ar \rightarrow Ar^+ + H_2$
$H_2^+ + Ar \rightarrow ArH^+ + H$
V= 0 1 2 3 4 Ecm
0 1 2 3 4 Ecm
70
50
30
20
10
7
5
3
2
σ(Å²)
6eV
3
1
9
1eV
3
6
9
XBL 817-10695

Fig. 3

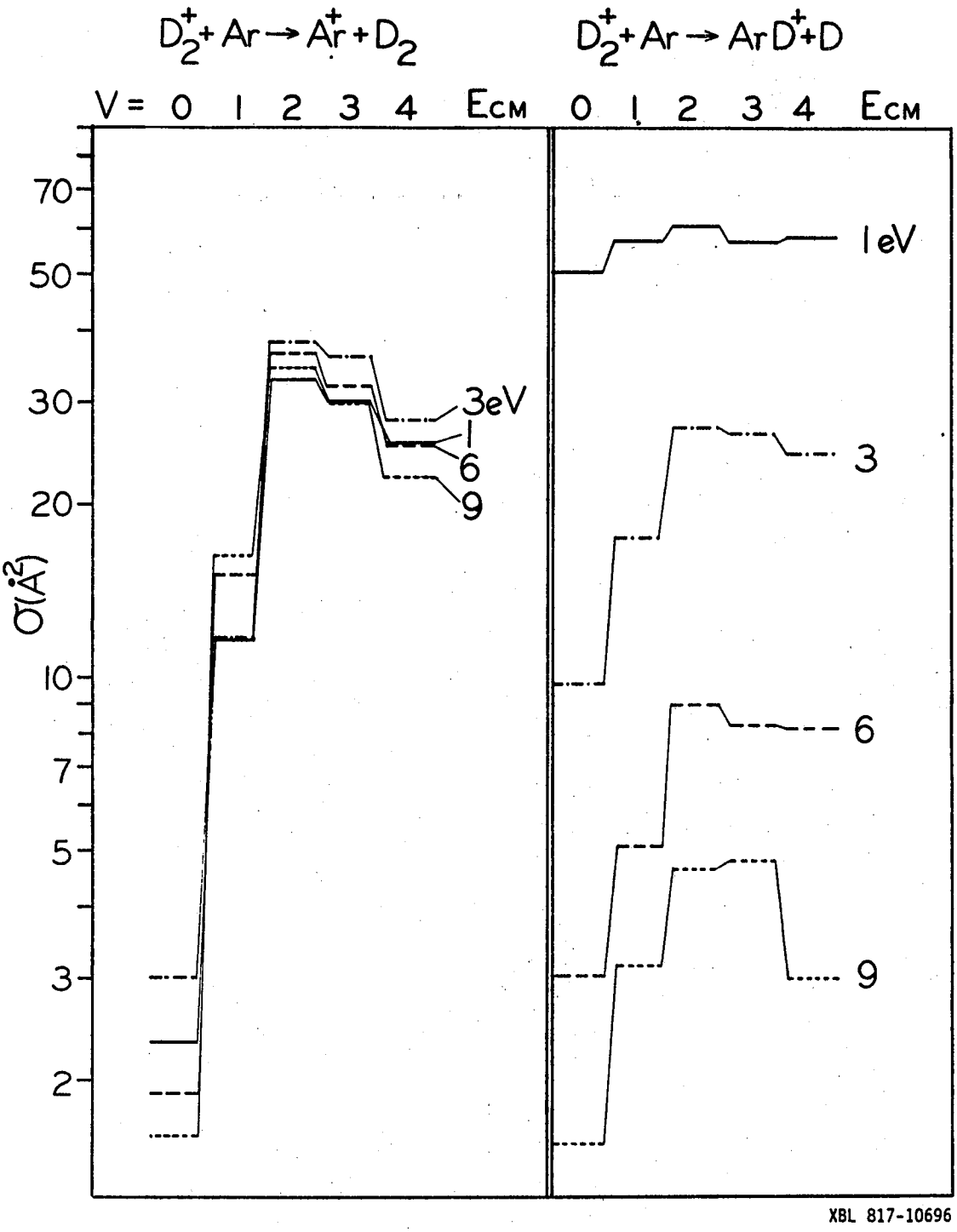
$D_2^+ + Ar \rightarrow Ar^+ + D_2$
$D_2^+ + Ar \rightarrow ArD^+ + D$
V = 0 1 2 3 4 Ecm
0 1 2 3 4 Ecm
70
50
30
20
10
7
5
3
2
σ(Å²)
3eV
1
6
9
1eV
3
6
9
XBL 817-10696

Fig. 4

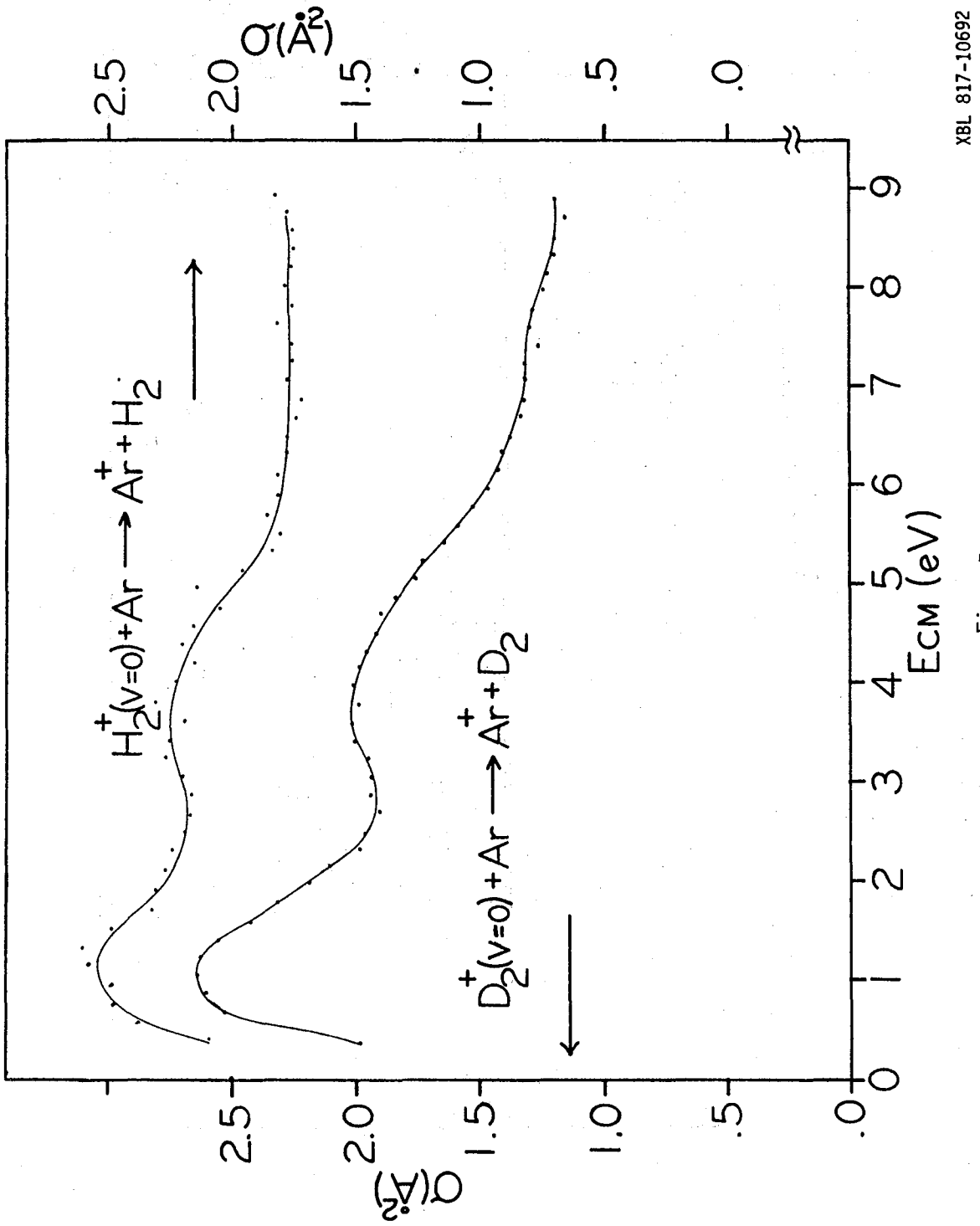

XBL 817-10692

Fig. 5

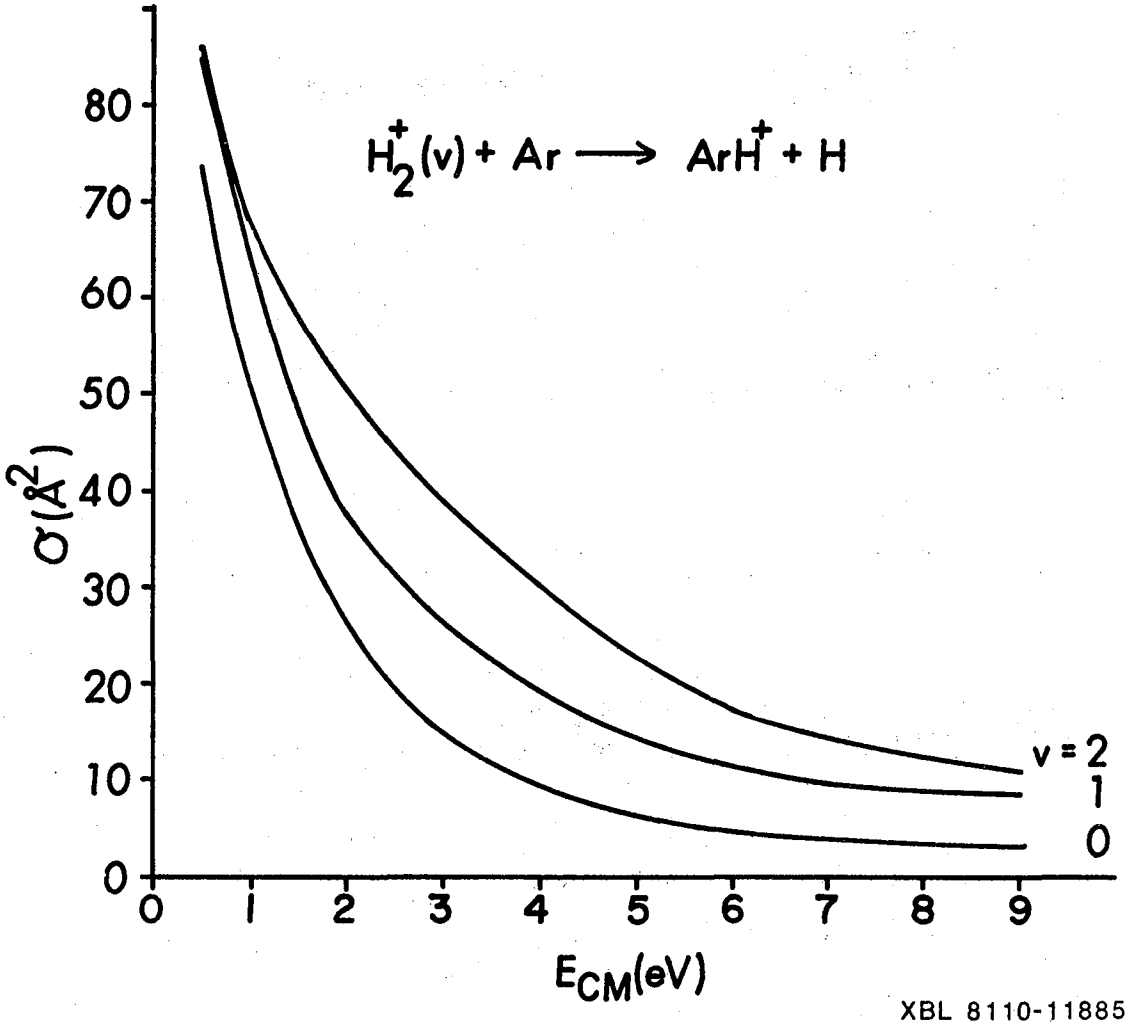
$H_2^+(v) + Ar \longrightarrow ArH^+ + H$
$\sigma(Å^2)$
80
70
60
50
40
30
20
10
0
0 1 2 3 4 5 6 7 8 9
$E_{CM}(eV)$
v = 2
1
0
XBL 8110-11885

Fig. 6

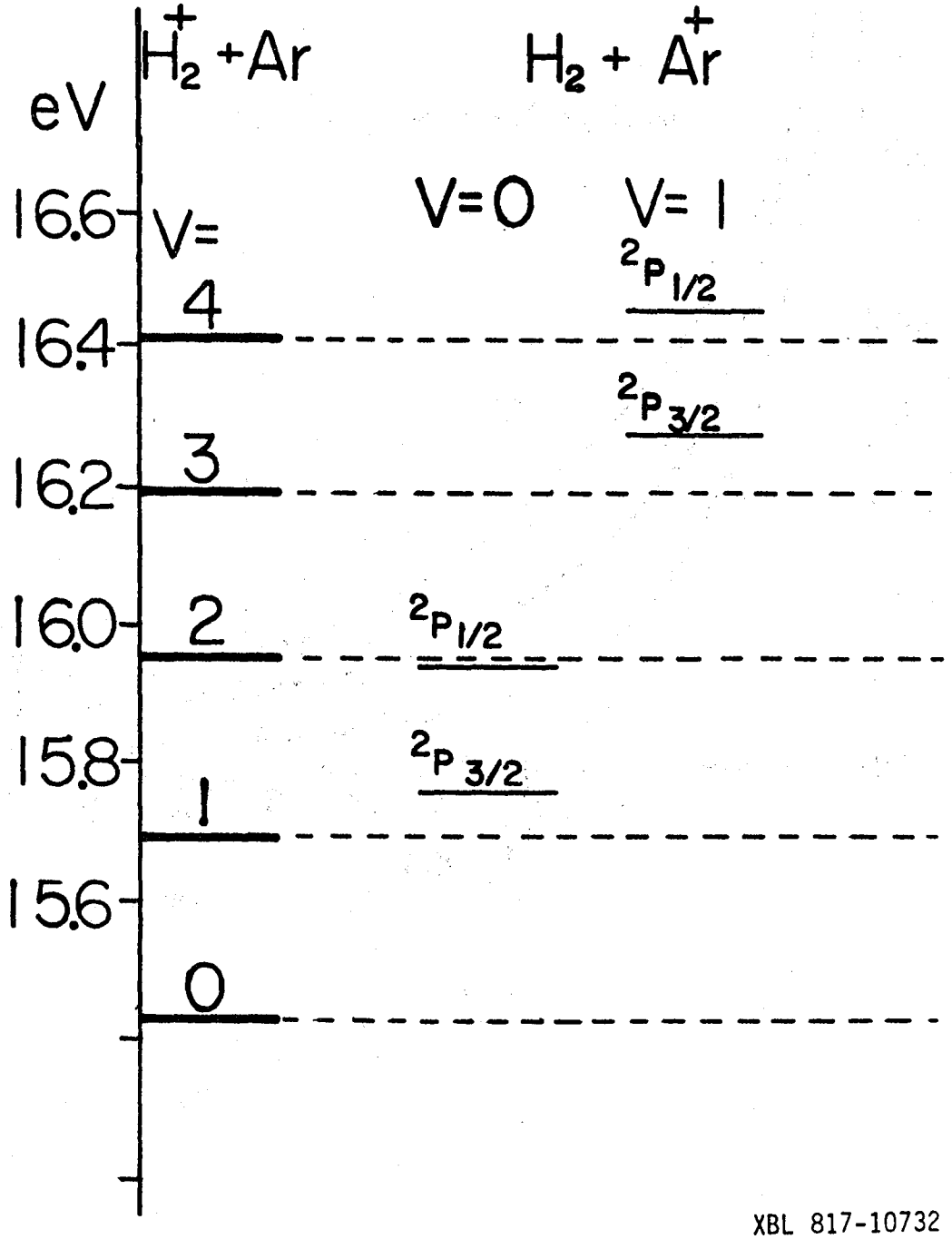
$H_2^+ + Ar$
$H_2 + Ar^+$
eV
16.6
V=
V=0
V=1
$^2P_{1/2}$
4
16.4
$^2P_{3/2}$
3
16.2
16.0
2
$^2P_{1/2}$
15.8
$^2P_{3/2}$
1
15.6
0
XBL 817-10732

Fig. 7

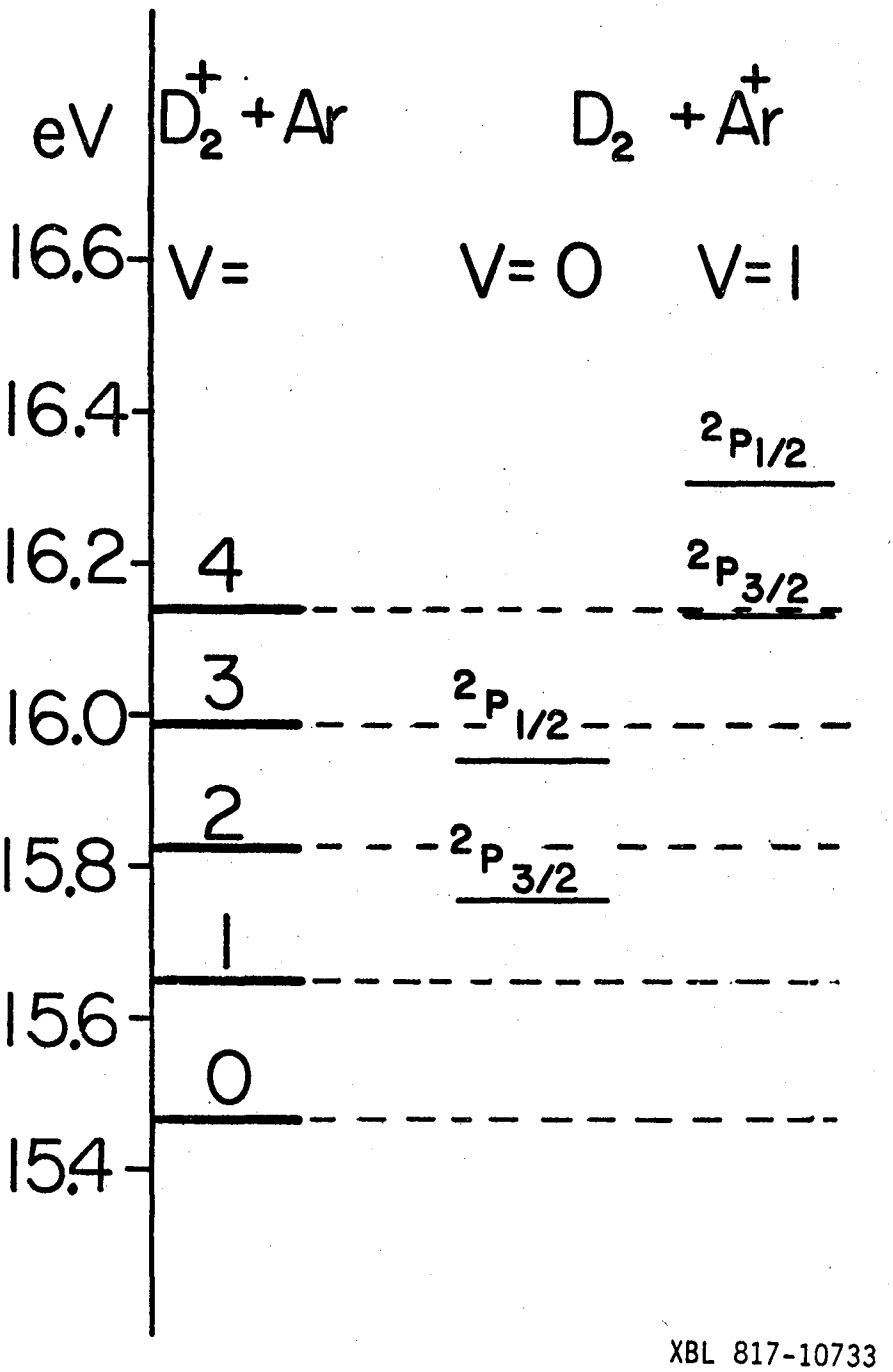

XBL 817-10733

Fig. 8

V. $H_2^+ + N_2$, CO, O_2

Introduction

It is interesting to compare the dynamics of charge and proton transfer of H_2^+ with argon (Chapter IV) with the analogous reactions with N_2, CO, and O_2. The four systems are similar in some ways, but very different in others. The proton and charge transfer reactions and their energetics are summarized in Table 1. The energetics of the various reactions were calculated from data in ref. 1. Since the N_2, CO, and O_2 bonds are quite strong (they might be called pseudo-atoms), no other reactions occur in the collision energy range which our experiments cover, except for collision induced dissociation of H_2^+ (CID), which has a maximum cross section of less than $3Å^2$ for all three systems and will not be considered here.

Examination of Table 1 shows that while all the PT reactions are substantially exoergic, there is a wide variation in the energetics of CT. In particular both $H_2^+ + Ar$ and $H_2^+ + N_2$ are slightly endoergic while both $H_2^+ + CO$ and $H_2^+ + O_2$ are quite exoergic. This would be expected to lead to large differences in the magnitudes of the CT cross sections and in addition has a large effect on the shape of the PES's for the different systems. Figure 1 shows a cut along R(H-H), through the entrance channel of the $H_2^+ + Ar$ system. $H_2^+ + N_2$ will look very similar. Interaction between the two potential surfaces, which begins to occur at $R(H_2\text{-}Ar)$ ~5Å causes an avoided crossing and allows vibration (for v>0) to couple the two reagent charge states.[2] Thus in $H_2^+ + Ar$ we saw large CT cross sections for $v > 0$. This coupling

Table 1. Energetics of the major reaction channels.

$H_2^+ + N_2 \rightarrow N_2^+(X^2\Sigma_g^+) + H_2$	$\Delta E = 0.155$ eV
$H_2^+ + N_2 \rightarrow N_2^+(A^2\Sigma_u) + H_2$	$\Delta E = 1.29$ eV
$H_2^+ + N_2 \rightarrow N_2H^+ + H$	$\Delta E = -2.38$ eV
$H_2^+ + CO \rightarrow CO^+(X^2\Sigma^+) + H_2$	$\Delta E = -1.41$ eV
$H_2^+ + CO \rightarrow CO^+(A^2\Pi) + H_2$	$\Delta E = 1.16$ eV
$H_2^+ + CO \rightarrow HCO^+ + H$	$\Delta E = -3.51$ eV
$H_2^+ + O_2 \rightarrow O_2^+(X^2\Pi_g) + H_2$	$\Delta E = -3.35$ eV
$H_2^+ + O_2 \rightarrow O_2^+(a^4\Pi_u) + H_2$	$\Delta E = 0.73$ eV
$H_2^+ + O_2 \rightarrow O_2^+(A^2\Pi_u) + H_2$	$\Delta E = 1.69$ eV
$H_2^+ + O_2 \rightarrow O_2H^+ + H$	$\Delta E = -1.69$ eV
$H_2^+ + Ar \rightarrow Ar^+(^2P_{3/2}) + H_2$	$\Delta E = 0.33$ eV
$H_2^+ + Ar \rightarrow Ar^+(^2P_{1/2}) + H_2$	$\Delta E = 0.51$ eV
$H_2^+ + Ar \rightarrow ArH^+ + H$	$\Delta E = -1.30$ eV

between the two charge states also seems to strongly influence the proton transfer reaction. Figure 2 shows the same cut through the PES entrance channel for the case where the molecule's IP is substantially lower than that of H_2 (in this case CO). In this case an avoided crossing would allow all H_2^+ vibrational states to charge transfer and we might expect to see very different vibrational effects on both the CT and PT reactions.

A large difference between Ar and N_2, CO, or O_2 is that the diatomics can vibrate and rotate. This means that the number of possible product states is increased. We saw in H_2^+ + Ar CT, that one of the strongest influences on the observed vibrational effects appeared to be energy resonances between the different $H_2^+(v)$ + Ar initial states and the available product states. The differing number and energy spacings of the product states in H_2^+ + Ar, N_2, CO, O_2 provides very different patterns of energy resonances for the four systems.

Since exoergic CT appears to occur through a long range interaction, we might expect that the overlap between an initial state wave function and the various product states - some variety of Franck-Condon factor, would have a large effect on charge transfer probability. Unlike H_2^+ + Ar, the FC factors may play a large role for CT to N_2, CO, and O_2.

In addition, N_2, CO, and especially O_2 have low lying electronic states which may be expected to influence reactivity. If there is sufficient coupling between the ground PES and the PES resulting from the excited states, then additional CT and/or PT

pathways are possible which may be more reactive than the ground PES. Some of the vibrational effects in $H_2^+ + H_2$ were suggested to be the result of increased or decreased reactivity of the first excited surface. The ionization Franck-Condon factors for the excited states of N_2, CO and to a lesser extent O_2 are very different from those of the ground states. To the extent that Franck-Condon factors are important, we would expect this to influence the observed vibrational dependence of CT.

Thus the comparison of the $H_2^+ + Ar$, N_2, CO, and O_2 systems offers a unique test of the effects that the properties of the reactants have on reactivity. This chapter will focus on the dynamical implications of the collision and vibrational energy dependence of proton and charge transfer in $H_2^+ + N_2$, CO, and O_2 and a simple model will be used to assess the relative importance of Franck-Condon factors, energy resonance and excited states on CT.

Before presenting the results, a brief summary of relevant past work on each system will be presented.

$\underline{H_2^+ + N_2}$. Somewhat surprisingly, not a great deal is known about this reaction. Bowers et al.[3] studied reactions in the $(H_2 + N_2)^+$ system at thermal energies using the ICR technique. They determined rate constants for N_2H^+ formation from both $H_2^+ + N_2$ and $N_2^+ + H_2$ (1.95 and 1.4 x 10^{-9} cm^3 $molecule^{-1}$ sec^{-1} respectively) and that the $H_2^+ + N_2 \rightarrow N_2H^+ + H$ rate decreased with increasing collision energy with a concomitant increase in the charge transfer rate. They do not

report the magnitude of the CT rate constant. Ryan[4] studied the $(H_2 + N_2)^+$ system using a space charge trapping technique and obtained rate constants in qualitative agreement with those of Bowers and Elleman. Kim and Huntress[5] report an ICR study of $H_2^+ + N_2$ reactions in which the rate constant for N_2H^+ formation is given as 2.0×10^{-9} $cm^3 molec^{-1} sec^{-1}$ They report no CT under their conditions. The only dynamical studies of $(H_2 + N_2)^+$ have been crossed beam studies of the charge reversed, $N_2^+ + H_2$ system.[6] The reaction was shown to proceed via a direct stripping type mechanism.

$H_2^+ + CO$. The rate constant for the process $H_2^+ + CO \rightarrow$ products was reported to be 2.95×10^{-9} by Ryan[4] and 2.8×10^{-9} cm^3 $molec^{-1}$ sec^{-1} by Huntress et al.[5] Huntress et al. also report the branching between CT and COH^+ production. Unlike $H_2^+ + N_2$, where no CT was observed, the branching was 23 percent CT and 77 percent COH^+ formation. In a crossed beam study, the charge reversed $CO^+ + D_2 \rightarrow COD^+ + D$ reaction was shown to be direct with dynamics very nearly identical to those for $N_2^+ + H_2$.[7] We are fortunate to have in addition, a detailed crossed beam study of the $H_2^+ + CO \rightarrow HCO^+ + H$ reaction, by Farrar et al.[8] They found that the reaction was direct and that at low collision energies most (~90 percent) of the available energy went into internal excitation of the HCO^+ product. As the collision energy was increased, the fraction of the total energy going to product internal excitation dropped to ~50 percent. They attributed this to dissociation of the more highly excited product formed at high

collision energy. The results were interpreted in light of the complex set of potential energy surfaces (PES) which were calculated by Vaz Pires et al.[9]

$H_2^+ + O_2$. Here again very little is known. Huntress et al.[5] studied the CT and H atom transfer reactions at thermal energies. They report a rate constant of 2.7×10^{-9} cm^3 $molec^{-1}$ sec^{-1} for the sum of the two channels and report the branching as 29 percent CT, 71 percent O_2H^+ formation. Again the only dynamical study is of the charge reversed $O_2^+ + H_2 \rightarrow O_2H^+ + H$ reaction.[10] The reaction was found to proceed through a long lived complex mechanism at low energies, switching to a more direct stripping type mechanism as the collision energy is increased above 5 eV. It is quite doubtful that $O_2^+ + H_2$ and $H_2^+ + O_2$ would exhibit the same reaction dynamics since the energy difference between the two charge states is so large (3.35 eV).

Results

$H_2^+ + N_2$. Figure 3 shows our results for the vibrational and collision energy dependence of the two major reaction channels in this system

Proton transfer $\quad H_2^+(v) + N_2 \rightarrow N_2H^+ + H$

and

Charge transfer $\quad H_2^+(v) + N_2 \rightarrow N_2^+ + H_2$.

The analogous data for $D_2^+ + N_2$ is shown in Figure 4. Table 2 contains the same cross sections as the two figures and in addition, presents the data before the vibrational unfolding process (see Chapter 2).

Table 2. Raw and vibrationally corrected data for $H_2^+ + N_2$.

Reaction	E_{cm}	Corrected v=0	Corrected 1	Corrected 2	Corrected 3	Corrected 4	Raw v=0	Raw 1	Raw 2	Raw 3	Raw 4
$H_2^+ + N_2$, CT	0.5	4.86	31.7	15.3	10.8	13.8	4.86	28.7	17.1	14.7	15.4
	1	5.63	35.5	15.0	14.5	17.7	5.63	32.2	17.5	17.4	18.4
	3	5.45	38.0	16.2	14.5	18.8	5.45	34.4	18.8	18.1	19.5
	6	6.3	38.5	18.7	14.5	14.9	6.3	34.9	20.9	18.7	18.2
	9	8.23	40.7	21.5	15.3	17.9	8.23	37.1	23.5	20.2	20.6
$H_2^+ + N_2$, PT	0.5	62.0	80.5	65.5	60.2	72.0	62.0	78.5	67.6	64.8	69.7
	1	47.9	71.8	58.7	52.7	53.7	47.9	69.2	59.9	56.7	56.5
	3	16.6	35.1	27.5	24.2	24.4	16.6	33.1	27.8	26.1	25.8
	6	5.72	15.9	9.12	7.07	7.38	5.72	14.8	9.93	8.85	8.69
	9	2.52	9.10	4.75	3.39	3.44	2.52	8.37	5.27	4.55	4.37
$D_2^+ + N_2$, CT	0.5	3.38	29.1	19.5	29.4	26.5	3.38	26.5	19.9	25.8	25.4
	1	3.44	33.0	19.6	29.0	27.9	3.44	30.0	20.5	26.1	26.5
	3	3.96	35.7	22.1	28.9	28.5	3.96	32.5	22.9	26.9	27.5
	6	4.34	37.1	23.7	28.4	29.0	4.34	33.8	24.4	27.1	28.0
	9	5.29	37.0	25.0	32.5	32.6	5.29	33.8	25.5	29.9	30.9
$D_2^+ + N_2$, PT	0.5	75.6	80.2	79.1	76.3	73.5	75.6	79.7	79.0	77.3	73.3
	1	73.0	70.9	69.8	70.7	60.3	73.0	71.1	71.1	70.7	62.7
	3	16.1	28.4	26.9	28.1	26.8	16.1	27.2	26.5	27.2	26.4
	6	4.16	10.6	8.75	9.14	9.00	4.16	9.93	8.73	8.95	8.87
	9	1.57	3.82	3.72	3.76	3.65	1.57	3.50	2.81	3.43	3.43

The most striking feature of the data for $H_2^+(D_2^+)$ + N_2 is the strong vibrational effect on CT. The cross section increases by about a factor of 6 when the ion is excited from v=0 to v=1. The cross section then decreases by ~50 percent going from v=1 to v=2 and again by about 30 percent from v=2 to 3 followed by a ~25 percent rise from 3 to 4.

For D_2^+ the vibrational pattern for CT is quite different. The D_2^+ v=0 CT cross section is 25 percent lower than that for H_2^+ but rises to approximately the same magnitude when the D_2^+ is in the v=1 state (factor of 9 jump). The decrease from v=1 to 2 is only ~30 percent and the cross section rises from 2 to 3 by ~25 percent, followed by a slight decrease from v=3 to 4. The differences between H_2^+ and D_2^+ seen here are much larger than those for $H_2^+(D_2^+)$ + Ar presented in Chapter IV. As in all the cases of CT studied in our lab so far, there is very little collision energy dependence.

The PT (proton transfer) cross sections show strong vibrational and collision energy dependence. The overall collision energy dependence for PT is a rapid drop from ~70Å^2 at 0.5 eV to between 2 and 4Å^2 at 9 eV. The cross sections at the lowest collision energy are about the same for H_2^+ and D_2^+, which is what is expected from a Langevin type model. Both H_2^+ + N_2 and D_2^+ + N_2 PT cross sections fall off quite a bit faster than the $E_{cm}^{-1/2}$ dependence which legend has it is common for exoergic ion-molecule reactions. Of the two, the D_2^+ PT cross section falls off faster so that at 9 eV it is ~40 percent lower than that for H_2^+ (v=0).

The vibrational effects on PT are quite complex but a comparison between the effects for proton and charge transfer reveal a simple pattern for both H_2^+ and $D_2^+ + N_2$. At low collision energies PT appears to be dominated by a mechanism which is relatively independent of vibrational state. As the collision energy increases however, the vibrational effects for PT begin to mimic those for CT more and more, so that by 6 eV the vibrational effects for the two processes are qualitatively identical. This same effect was observed in $H_2^+(D_2^+)$ + Ar CT (Chap. IV).

$H_2^+ + CO$. Figure 5 shows our vibrational state dependent data for charge and proton transfer of H_2^+ with CO. The analogous data for $D_2^+ + CO$ is shown in Figure 6. Both the raw and vibrationally corrected data for these systems is presented in Table 3. The most obvious effect of vibration in these systems is the large (~45 percent) drop in charge transfer cross section when the ion (H_2^+ or D_2^+) is excited from v=0 to v=1; with little change in cross section as the vibrational excitation is increased further.

For proton transfer the H_2^+ and D_2^+ reactions again show similar vibrational effects; a small overall vibrational enhancement at low collision energy changing to vibrational inhibition at higher collision energy. The degree of enhancement at low energies is larger for D_2^+ than H_2^+ and is reflected in a lesser degree of vibrational inhibition at the higher energies.

Typically, there is virtually no collision energy dependence of the charge transfer reactions, while the proton transfer reaction

Table 3. Raw and vibrationally corrected data for H_2^+ + CO.

Reaction	E_{cm}	Corrected					Raw				
		v=0	1	2	3	4	v=0	1	2	3	4
H_2^++CO, CT	1	53.2	37.4	30.7	26.5	32.7	53.2	39.1	33.6	31.3	33.5
	3	56.3	34.3	32.2	28.5	36.1	56.3	36.7	34.5	32.4	35.5
	6	59.9	33.9	32.5	30.1	33.9	59.9	36.8	34.9	33.6	34.9
	9	62.7	35.6	34.1	32.7	34.9	62.7	38.6	36.6	35.8	36.5
H_2^++CO, PT	1	85.1	82.4	83.8	91.5	39.0	85.1	82.7	83.7	87.9	89.3
	3	42.4	40.6	42.7	42.9	42.1	42.4	20.8	42.3	42.4	42.1
	6	26.0	23.1	22.1	23.3	21.0	26.0	23.4	22.6	23.2	22.2
	9	19.0	14.9	12.0	13.4	8.9	19.0	15.4	13.0	13.8	11.6
D_2^++CO, CT	1	79.0	45.2	47.0	49.5	46.7	79.0	48.6	48.7	50.2	45.7
	3	68.2	34.6	35.1	41.3	34.4	68.2	38.0	37.0	40.8	34.7
	6	63.1	39.4	35.5	38.7	34.6	63.1	41.8	37.7	39.6	34.9
	9	61.0	39.6	33.4	39.5	34.1	61.0	41.7	35.9	39.6	34.4
D_2^++CO, PT	1	74.8	29.5	86.2	98.4	97.8	74.8	90.7	86.4	93.8	92.7
	3	31.9	35.6	33.1	38.6	42.3	31.9	35.2	33.4	36.7	38.4
	6	16.7	17.5	15.3	16.1	16.2	16.7	17.4	15.7	16.2	15.7
	9	6.27	5.74	4.98	5.76	5.10	6.27	5.79	5.16	5.63	5.11

cross sections decrease rapidly with increasing collision energy. Again the D_2^+ PT cross section falls off more rapidly than that for H_2^+. One interesting point is that the magnitudes of the $H_2^+(D_2^+)$ + CO cross sections are ~ 40-50 percent larger than the corresponding $H_2^+(D_2^+)$ + Ar, N_2, O_2 cross sections.

$H_2^+ + O_2$. For this system only the H_2^+ reactions were studied. The CT and PT data are presented in Figure 7 and Table 4. $H_2^+ + O_2$ is unusual in that it is the only case studied so far in which the proton transfer reaction is inhibited by vibration (factor of ~2 drop going from v=0 to 4) at all collision energies. The CT cross sections show monotonic vibrational enhancement which also has not been observed before. The increase in CT is almost a factor of 2.5 going from v=0 to 4. As usual the CT reaction shows little collision energy dependence and the PT reaction cross section decreases rapidly with increasing collision energy.

Error Estimate

As usual the estimated absolute error is 25 percent. The random error is estimated to be 5 percent at the lowest collision energies for the proton transfer (e.g., N_2H^+ product) channels and at all energies for CT. The percent error in the proton transfer cross sections increases as the cross sections decrease and is estimated to be ±10 percent at the highest energies. For CT there is an additional source of error caused by diffusion of the neutral scattering gas into the ion source. For $H_2^+ + O_2$ and $H_2^+ + CO$ the error is estimated to be less than 5 percent. For $H_2^+ + N_2$ this causes no error for v=0 but

Table 4. Raw and vibrationally corrected data for $H_2^+ + O_2$.

Reaction	E_{cm}	Corrected					Raw				
		v=0	1	2	3	4	v=0	1	2	3	4
$H_2^+ + O_2$, CT	0.5	18.9	21.9	32.5	50.5	68.6	18.9	21.6	29.7	39.7	50.1
	1	17.2	22.8	32.2	49.2	63.6	17.2	22.2	29.5	38.9	47.4
	4	24.9	26.2	34.8	45.9	56.7	24.9	26.1	32.6	38.8	45.1
	6	22.4	27.1	31.5	37.4	49.1	22.4	26.6	30.1	33.3	39.6
	9	17.7	19.4	24.9	32.0	40.9	17.7	19.2	23.4	27.4	32.4
$H_2^+ + O_2$, PT	0.5	54.8	56.2	51.6	42.9	32.9	54.8	56.0	52.6	47.8	42.2
	1	42.3	40.8	36.9	26.1	19.6	42.3	41.1	38.0	32.0	27.9
	4	8.33	6.87	5.56	4.70	4.48	8.33	7.03	5.99	5.52	5.29
	6	3.94	3.84	3.67	2.96	3.10	3.94	3.85	3.72	3.32	3.33
	9	2.45	2.22	2.18	2.22	1.99	2.45	2.24	2.21	2.23	2.12

may introduce a ±5 percent error for v=1–4. In addition our correction of the cross sections for the ion vibrational state distribution possibly underestimates the magnitude of the vibrational effects especially for v=3 and 4 where the error may be as high as 20 percent.

Discussion

$H_2^+ + N_2$. Perhaps the most obvious feature of the vibrational and collision energy dependence for the $H_2^+ + N_2$ system is its similarity with that for $H_2^+ + Ar$. For both systems there is a large jump in charge transfer cross section when the $H_2^+(D_2^+)$ is excited from v = 0 to v = 1; with smaller effects for further vibrational excitation. Both systems also show a marked similarity in the vibrational effects for proton and charge transfer at high collision energies. For $H_2^+ + N_2$ this trend is evident to some extent even at very low collision energy. It is not at all surprising that Ar and N_2 are so similar in their reactions with H_2^+. The ionization potentials of H_2, Ar and N_2 are 15.43, 15.77 and 15.58 eV respectively. The CT energetics for $H_2^+(D_2^+) + N_2$ and Ar are shown in Figs. 8 and 9, and in Figs. 7 and 8 of Chapter IV. For both $(H_2 + Ar)^+$ and $(H_2 + N_2)^+$ there are two charge states lying very close in energy. Charge transfer from the reagent charge state (e.g., $H_2^+ + N_2$) is endoergic for H_2^+ (v = 0) and exoergic (N_2) or slightly endoergic (Ar) for H_2^+ (v = 1). For both systems, an avoided crossing (Figure 1) mixes the two charge states, and vibrational motion can cause charge transfer at long range (R ~ 5Å). The differences in CT vibrational effects between $H_2^+ + Ar$ and

$H_2^+ + N_2$ are due to differences in the energetics of the two systems and to Franck-condon effects. This will be discussed below.

Unlike the $H_2^+ + Ar$ case; for the endoergic $H_2^+ (v = 0) + N_2$ charge transfer process, no structure was observed in the collision energy dependence of the cross section from 0.5 to 10 eV. The peaks observed in the $H_2^+ + Ar$ case (Figure 5, Chapter IV) were attributed to peaks in the cross sections for forming various product states. Massey[11] gives a prescription for calculating the energies at which the cross sections for various product channels peak:

$$V_{peak} = \frac{a}{\hbar} |\Delta E| \quad ;$$

where V_{peak} is the relative velocity where the peak occurs, "a" is a parameter related to the range at which the charge transfer occurs, and ΔE is the energy defect for the given product channel. If we use the same "a' factor obtained by fitting the peaks observed for $H_2^+ + Ar$ to calculate the energies where we would expect peaks to appear for $H_2^+ + N_2$ we get a peak at 0.35 eV for $H_2^+ (v = 0) + N_2 \rightarrow N_2^+ (v = 0) + H_2 (v = 0)$. The peak for formation of $N_2^+ (v = 1) + H_2 (v = 0)$ should appear at 2.75 eV and that for $N_2^+ (v = 0) + H_2 (v = 1)$ formation at 6.73 eV. The first peak is below the energy range of our measurements, but the other two are well within our range. The non-observance is not too surprising and probably is due to rather low cross sections for forming either of the two vibrationally excited product channels

and to broadening of the peaks due to the rotational degrees of freedom of the N_2. The low cross sections are expected on the basis of poor Franck-Condon overlap between N_2 (v = 0) and N_2^+ (v = 1) and the rather substantial energy transfer required for formation of the N_2^+ (v = 0) + H_2 (v = 1) product state (0.68 eV). The same effect was seen in D_2^+ + Ar where the peak expected for the $Ar^+(^2P_{3/2})$ + D_2 (v = 1) product channel (Chapter IV, Figure 4 and Table 3) is barely observable, even with excellent data.

Another more sensitive indication that the H_2^+ + N_2 system has essentially identical reaction dynamics to H_2^+ + Ar, is that as the collision energy is raised, the vibrational dependence of the proton transfer channel switches from near independence of the initial vibrational excitation, to a vibrational dependence suggesting strong linkage with the CT channel. In fact, the effect is even more obvious for H_2^+ + N_2. CT in these systems, at least where exoergic, is a long range process, as evidenced by the large, collision energy independent cross sections. The obvious mechanism is vibrational motion induced charge and/or surface hopping at the avoided crossing seam in the collision entrance channel. It is presumably this behavior which gives rise to the strong vibrational effects observed for CT.

The fact that proton transfer and CT show very similar vibrational dependences at high collision energy implies that the same behavior at the crossing seam which promotes CT, greatly enhances the proton transfer probability. What determines the branching of a given collision between PT and CT is presumably the impact parameter; PT

predominating for small impact parameters and CT for the less intimate collisions.

The way in which surface and/or charge hopping in the entrance channel promotes subsequent proton transfer is less clear. One possible explanation is that in crossing and recrossing the seam early on in the collision, the reagents become highly vibrationally excited with concomitant reduction in relative velocity. The reduction in translational energy clearly increases the proton transfer probability (see Figures 3 and 4) and high vibrational excitation may also promote breaking of the H_2^+ bond, thus increasing PT probability. this mechanism should be amenable to testing by Trajectory Surface Hopping[12] or better yet, a non-adiabatic semi-classical type calculation.[13]

$\underline{H_2^+ + CO}$. This system is quite different from $H_2^+ + N_2$. Here, charge transfer from all H_2^+ initial vibrational states is at least 1.4 eV exoergic. The large difference in ionization potential between H_2 and CO also changes the nature of the avoided crossing which occurs in the entrance channel, as Figures 1 and 2 show. While vibrational motion still couples the two reagent charge states ($H_2^+ + CO$, $H_2 + CO^+$), the coupling is to high vibrational levels of the $H_2 + CO^+$ system. In $H_2^+ + H_2$, $H_2^+ + Ar$ and $H_2^+ + N_2$, the initial charge state (e.g., $H_2^+ + Ar$) correlates directly to the proton transfer product. The other reagent charge state ($H_2 + Ar^+$) at least in a diabatic picture, can only scatter non-reactively. In $H_2^+ + CO$, neither the $H_2 + CO^+$ ($^2A_1(1)$) state of H_2CO^+, nor the $H_2^+ + CO$ ($^2A_1(2)$) state correlates to

$HCO^+ + H$. Rather it is the X^2B_2 ground state of H_2CO^+ which correlates to the proton transfer product.[8,9]

There are a number of possible avoided crossings which allow proton and charge transfer to occur for $H_2^+ + CO$. Vibrational motion at the seam in the entrance channel (Figure 2) discussed above can couple $H_2^+ + CO$ ($^2A_1(2)$) and $H_2 + CO^+$ ($^2A_1(1)$). Calculations by Vaz Pires et al.,[9] show that the X^2B_2 state crosses both of the $^2A_1$ states, and in low symmetry collisions may cause not only charge transfer ($^2A_1(2) \rightarrow {}^2A_1(1)$) but also may lead to proton transfer ($^2A_1(2) \rightarrow X^2B_2$). Crossing of these seams, however, is brought about by relative motion of the reagents. Needless to say, the very complicated system of potential surfaces and crossing seams makes it difficult to draw dynamical conclusions from the vibrational and collision energy dependences we observe.

The collision energy dependence of both the proton transfer and charge transfer channels is similar to that observed for $H_2^+ + N_2$ or $H_2^+ + Ar$. The fall off with collision energy observed for proton transfer is nearly universal with exoergic ion-molecule reactions and is just a result of the long range, ion-induced dipole potential. The magnitudes of both channels of the $H_2^+(D_2^+) + CO$ reaction are 40- 50 percent larger than those for $H_2^+ + Ar$ or N_2. This is possibly due to the additional attractive ion-permanent dipole term in the interaction potential.[14]

The magnitude and collision energy independence of the charge transfer cross sections indicate that CT occurs by a long range

process. The fact that there is no collision energy dependence suggests that the coupling between the change states is vibrational rather than translational and occurs via vibration through the seam between the two $^2A_1$ surfaces in the collision entrance channel. If the primary CT pathway was via the X^2B_1 state, then we would expect some collision energy dependence, since the motion through this seam is translational.[8,9]

Further evidence for CT occurring via the seam in the entrance channel is found in its vibrational dependence. The CT cross section is observed to drop by ~45 percent when the ion is excited from v = 0 to v = 1; with relatively little effect from subsequent vibrational excitation. Modeling of the effects of Franck-Condon factors and energy resonance effects on CT has been carried out with fair success for all the systems studied (see below). The modeling of H_2^+ and D_2^+ CT with CO does not predict such a large drop from v = 0 to v = 1, compared with the subsequent vibrational effects. One possible reason for the discrepancy is suggested by Figure 2. It can be seen that the crossing between $H_2^+ + CO$ and $H_2 + CO^+$ occurs right at the classical turning point of the H_2^+ (v = 0) vibration. This should allow CT to occur for H_2^+ (v = 0) at longer range (with higher cross section) than for more highly excited H_2^+ since the classical vibrational velocity at the seam is almost zero for v = 0.

The proton transfer vibrational dependence is quite weak and apparently patternless for $H_2^+ + CO$. This is in strong contrast to the cases of $H_2^+ + Ar$ and N_2. However, the lack of strong vibrational effects is not too surprising in light of the probable mechanism. As

the H_2^+ and CO approach each other in the entrance channel, most of the time the system will vibrate through the avoided crossing between the H_2^+ + CO and CO^+ + H_2 potential surfaces and charge transfer to highly vibrationally excited CO^+ + H_2 states. In CT, the v = 0 state of H_2^+ + CO appears to have a higher cross section. This is because CT samples mainly large impact parameter collisions, where the fact that the H_2^+ + CO v = 0 state begins to charge transfer at longer range, results in higher CT cross sections. For the more intimate collisions which result in proton transfer, this is not important since all the vibrational states will have a high charge transfer probability for small H_2-CO separations. Thus we would not expect the proton transfer vibrational effects to mirror those of charge transfer. That the effects of reagent vibration are quite weak for proton transfer is not surprising, if we consider that the charge transfer in the entrance channel as well as the subsequent transition to the H_2CO^+ X state, where PT actually occurs, will tend to put several eV in the vibrational modes of the system. The small amount of initial vibrational excitation then, would be expected to be fairly insignificant. This is in contrast to the cases of H_2^+ + Ar and N_2 where charge transfer and surface hopping are energetically impossible for the low reagent vibrational states and tend to reduce the vibrational excitation of the system. In those cases the initial vibrational excitation was found to be very important in determining the cross sections for both proton and charge transfer.

$\underline{H_2^+ + O_2}$

This system has quite strong monotonic vibrational enhancement for charge transfer and monotonic vibrational inhibition for proton transfer. Because the IP of O_2 is 3.35 eV less than that of H_2, the $H_2^+ + O_2$ and $O_2^+ + H_2$ electronic potential surfaces do not cross at large internuclear separation. Of course, crossings still occur between the $H_2^+ + O_2$ surface and the higher vibrational levels of the $O_2^+ + H_2$ system. This allows long range CT to occur for $H_2^+ + O_2$, and the $O_2^+ + H_2$ formed is very vibrationally excited. The strong vibrational enhancement for CT is probably mainly due to the increased density of $O_2^+ + H_2$ product states as the energy of the $H_2^+ + O_2$ initial state is increased. The vibrational enhancement is reproduced by the model calculation described below.

The fact that the proton and charge transfer channels show roughly equal but opposite vibrational effects, suggests that maybe competition is occurring between the channels. Unlike cases of $H_2^+ + N_2$ and $H_2^+ + Ar$; when charge transfer occurs in the entrance channel of an $H_2^+ + O_2$ collision, transfer back to the initial reagent state would seem unlikely. This is because the density of states in the $O_2^+ + H_2$ well is much higher than the density of states at the same energy for $H_2^+ + O_2$. It appears from our data that if the system charge transfers in the collision entrance channel, the probability of subsequent proton transfer is reduced, presumably because the $O_2^+ + H_2$ surface is non-reactive. Unfortunately, little is known about the nature of

the $H_2O_2^+$ potential surfaces, and we can only offer this as a speculation. That the total CT plus PT cross section is not constant with varying collision energy is expected on the basis of the long range ion-induced dipole attractive potential which will tend to increase the scattering (elastic + inelastic + reactive) cross section at lower collision energies.

A Simple Model of Charge Transfer

As noted in the introduction, there is some question of what effect things like energy resonance and Franck-Condon factors have on the charge transfer process. Many studies have been performed of CT where emission from excited products is observed.[16,17] The consensus appears to be that energy resonance effects are important at all collision energies; and that Franck-Condon effects are important at high collision energy where the collision time is fast with respect to a vibrational period, and less so at lower collision energies. Effects like curve crossings appear to perturb the distribution of final states significantly.[17] Our 0.5-10 eV collision energy puts us in the range where the collision time is about 2 to 10 vibrational periods. Over our range of collision energy, the collision time clearly has little effect on the observed charge transfer vibrational dependence or cross section magnitude.

While looking at the product state distribution is clearly a better way of assessing the importance of various dynamical effects on charge transfer, modeling of the total CT cross section out of various initial

vibrational states provides some information, as well as being useful in interpreting our data.

A simple model was chosen to attempt to fit the observed vibrational dependences of the charge transfer cross sections. Basically we assume that the charge transfer probability from an initial $H_2^+(v) + M\ (v = 0)$ state is proportional to the sum over all possible product states, of the product of the Franck-Condon (FC) factors for neutralizing H_2^+ ($H_2^+(v) \rightarrow H_2(v')$), and for ionizing the neutral ($M\ (v = 0) \rightarrow M^+(v")$); times an energy gap factor, $f(\Delta E)$ thus:

$$P(H_2^+(v) + M) = \sum_{v'v"} FC(H_2(v',v))\ FC(M(v")\ f(\Delta E) \quad .$$

The Franck-Condon factors for neutralizing H_2^+ were from Flannery et al.[18] Those for D_2^+ were calculated by Dr. Dennis Trevor using RKR-Morse potentials to calculate the D_2 and D_2^+ wave functions. The Franck-Condon factors for ionizing N_2, CO and O_2 are from Gardner and Samson,[19] except that in the case of zero Franck-Condon factors for a given state, the calculation used a value of 10^{-5} just to allow those states to contribute slightly. Several forms of energy gap laws were tried. The best overall seemed to be an exponential form:

$$f(\Delta E) = \exp\left(-\frac{|\Delta E|}{E_o}\right) \quad ,$$

where ΔE is the energy gap between initial and final states, and E_o is a parameter which gives the range of the exponential. The calculation consists of varying E_o and calculating the charge transfer

probability for each initial $H_2^+(D_2^+)$ vibrational state, normalized to 1 for whatever state has the largest probability.

The simplest system, H_2^+ + Ar was used as a test case. For Ar, instead of Franck-Condon factors, we just have the statistical factors for forming Ar^+ in the $^2P_{3/2}$ or $^2P_{1/2}$ states. It was found that it was impossible to reproduce the observed 0.04:0.46:1 ratio of the CT cross sections for H_2^+ v = 0, 1, and 2 unless the energy gap law was changed to make the exponential fall off faster for endoergic channels than for exoergic ones. The form used was

$$f(\Delta E) = \exp\left(-\frac{K|\Delta E|}{E_o}\right)$$

where K is 1.00 for $\Delta E > 0$. With this addition, it was possible to get qualitative fits to the data for all the CT reactions studied. The results are shown in Tables 5-8. What is shown is the experimental vibrationally dependent CT probability (normalized to 1) and the calculated CT probability for two different sets of K and E_o parameters. While it is possible to improve slightly the fit for a given reaction, these two sets provide the best overall fit. The fit is reasonably good qualitatively, reproducing the increases and decreases in probability and the peak vibrational states, with the exception of the $D_2^+ + N_2$ case where the calculated peak is at v = 3 instead of v = 2. Quantitatively, the model tends to overestimate the magnitudes of the vibrational effects. In order to assess the importance of the Frank-Condon factors for H_2^+ (H_2 FC's) and the molecule, calculations were

Table 5. Experimental and calculated vibrational dependence of H_2^+ + Ar charge transfer.

H_2^+ + Ar

				Without H_2^+ FC's		Without Ar Stat. Factors		Without ΔE Law
		Best Fit K = 4	2	4	2	4	2	1
v=	Exp.	E_o = 0.5	0.3	0.5	0.3	0.5	0.3	1000
0	0.04	0.03	0.06	0.05	0.09	0.03	0.05	1.00
1	0.46	0.51	0.67	0.42	0.58	0.04	0.52	0.94
2	1.00	1.00	1.00	0.75	0.84	1.00	1.00	0.89
3	0.67	0.56	0.41	0.79	0.84	0.57	0.41	0.84
4	0.54	0.40	0.28	1.00	1.00	0.39	0.27	0.79

D_2^+ + Ar

				Without D_2^+ FC's		Without Ar Stat. Factors		Without ΔE Law
		Best Fit K = 4	2	4	2	4	2	1
v=	Exp.	E_o = 0.5	0.3	0.5	0.3	0.5	0.3	1000
0	0.05	0.06	0.03	0.10	0.06	0.05	0.02	1.00
1	0.41	0.41	0.30	0.36	0.26	0.35	0.24	0.99
2	1.00	1.00	0.93	0.70	0.61	0.95	0.80	0.99
3	0.88	0.90	1.00	0.81	0.76	1.00	1.00	0.99
4	0.70	0.51	0.60	1.00	1.00	0.55	0.66	0.86

Table 6. Experimental and calculated vibrational effects for $H_2^+ + N_2$ charge transfer.

$H_2^+ + N_2$

v=	Exp.	Best Fit K = 4 E_0 = 0.5	2	Without H_2^+ FC's 4	Without H_2^+ FC's 2	Without N_2 FC's 4	Without N_2 FC's 2	Without ΔE Law 1
			0.3	0.5	0.3	0.5	0.3	1000
0	0.20	0.20	0.27	0.24	0.37	0.08	0.13	1.00
1	1.00	1.00	1.00	0.70	0.76	0.52	0.61	0.94
2	0.53	0.81	0.63	0.70	0.73	0.85	0.89	0.89
3	0.38	0.48	0.31	1.00	1.00	0.92	0.90	0.84
4	0.44	0.52	0.47	0.88	0.96	1.00	1.00	0.79

$D_2^+ + N_2O$

v=	Exp.	Best Fit K = 4 E_0 = 0.5	2	Without D_2^+ FC's 4	Without D_2^+ FC's 2	Without N_2 FC's 4	Without N_2 FC's 2	Without ΔE Law 1
			0.3	0.5	0.3	0.5	0.3	1000
0	0.11	0.22	0.14	0.40	0.29	0.11	0.07	1.00
1	1.00	0.88	0.76	0.74	0.65	0.52	0.41	0.99
2	0.62	1.00	1.00	0.77	0.72	0.99	0.87	0.99
3	0.81	0.66	0.78	1.00	1.00	0.95	0.93	0.99
4	0.80	0.52	0.57	0.91	0.94	1.00	1.00	0.86

Table 7. Experimental and calculated vibrational dependence for H_2^+ + CO charge transfer.

		$H_2^+ + CO$						
				Without H_2^+ FC's		Without CO FC's		Without ΔE Law
		Best Fit K = 4	2	4	2	4	2	1
v=	Exp.	E_0 = 0.5	0.3	0.5	0.3	0.5	0.3	1000
0	1.00	1.00	1.00	0.82	0.81	1.00	1.00	1.00
1	0.57	0.59	0.53	0.73	0.66	0.75	0.72	0.94
2	0.54	0.30	0.21	0.93	0.89	0.68	0.63	0.89
3	0.50	0.38	0.32	0.86	0.82	0.65	0.62	0.84
4	0.56	0.46	0.36	1.00	1.00	0.62	0.60	0.79
		$D_2^+ + CO$						
				Without D_2^+ FC's		Without CO FC's		Without ΔE Law
		Best Fit K = 4	2	4	2	4	2	1
v=	Exp.	E_0 = 0.5	0.3	0.5	0.3	0.5	0.3	1000
0	1.00	1.00	1.00	0.85	0.82	1.00	1.00	1.00
1	0.62	0.72	0.92	0.94	0.82	0.75	0.76	0.99
2	0.56	0.30	0.34	0.85	0.80	0.61	0.59	0.99
3	0.61	0.34	0.39	1.00	1.00	0.57	0.55	0.99
4	0.55	0.26	0.33	0.89	0.86	0.51	0.48	0.86

Table 8. Experimental and calculated vibrational dependence of $H_2^+ + O_2$ charge transfer.

	$H_2^+ + O_2$									
				Including a state		Without H_2^+ FC's		Without O_2 FC's		
v=	Exp.	Best Fit K = 4 E_0 = 0.5	2 0.3	4 0.5	2 0.3	4 0.5	2 0.3	4 0.5	0.3	Without ΔE Law
0	0.46	0.26	0.06	0.15	0.02	0.89	0.92	1.00	1.00	1.00
1	0.57	0.59	0.53	0.73	0.66	0.75	0.72	0.94	0.95	0.94
2	0.54	0.30	0.21	0.93	0.89	0.68	0.63	0.89	0.91	0.89
3	0.50	0.38	0.32	0.86	0.82	0.65	0.62	0.84	0.84	0.84
4	0.56	0.46	0.36	1.00	1.00	0.62	0.60	0.79	0.80	0.79

performed for the best fit K and E_o; leaving out first the H_2 Franck-Condon effects and then the Franck-Condon effects for the neutral reagent. The final column in the tables gives the result when K = 1 and E_o = 1000, which essentially removes the dependence of charge transfer probability on the energy tap. Leaving out any of these factors completely destroys the agreement with experiment.

It is quite obvious from the calculations that at least in the framework of this model:

1. Exoergic CT channels are more probable than endoergic ones for the same energy gap.
2. The CT probability falls of reasonably fast as the energy gap increases.
3. The $H_2^+(D_2^+)$ neutralization, and the neutral reagent's ionization Franck-Condon factors are quite important in determining the CT probability.

It appears, however, that the "Franck-Condon factors" which are active in CT at our low collision energies are too restrictive. For instance, better fits to the H_2^+ + CO and N_2 data can be obtained by increasing the probability of forming vibrationally excited N_2^+ or CO^+. This is not surprising. Even for photoionization, Franck-Condon factors predict narrower ion vibrational state distributions than are observed.[19] The experimental broadening is due to interaction between the molecule's wave function and the departing electron. This effect will be even stronger for charge transfer, where the collision partners separate slowly compared to their vibrational periods.

N_2^+, CO^+, O_2^+ all have low lying electronic states (Table 1). For N_2^+ and CO^+ these are high enough in energy so that at least in the model calculations, they do not contribute more than a few percent to the CT probability. This is borne out experimentally by the fact that the CT cross sections do not change significantly when the collision energy is lowered to the point where CT to the excited state channel is energetically impossible. For $H_2^+ + O_2$ the model shows some dependence on whether or not the first excited state is included. Inclusion (see Table 8) increases the vibrational dependence of the CT cross section substantially. Again experimentally, it appears that CT to the $a^4\pi_u$ state of O_2^+ cannot be very important since CT has very little collision energy dependence, actually dropping off slightly with increased collision energy.

The fact that most of the trends in the vibrational dependence are at least qualitatively reproduced by the model is reassuring and further supports the notion that in all the cases we have studied, exoergic CT is a long range process with little translational-internal energy transfer.

Conclusions

Comparison of the strikingly different vibrational and collision energy dependences for $H_2^+ + Ar$, N_2, CO, and O_2 reactions allows us to examine the changes in charge and proton transfer dynamics brought about by the differences in energetics for the four systems. Charge transfer, at least where exoergic, is observed to be a long range,

collision energy independent process. Modeling shows that both energy resonance and Franck-Condon effects are quite important in determining charge transfer probabilities.

The similarities between $H_2^+ + Ar$ and $H_2^+ + N_2$ reactions demonstrates that they occur by very similar mechanisms. Charge and proton transfer are seen to be strongly coupled at high collision energies and probably both involve vibrationally induced charge and surface hopping transitions in the collision entrance channels.

For $H_2^+ + CO$ and $H_2^+ + O_2$ the linkage between proton and charge transfer is absent. In fact in $H_2^+ + O_2$, PT and CT show opposite vibrational dependences, which may indicate a form of competition between the two channels. For $H_2^+ + CO$, the lack of collision energy dependence suggests that CT occurs by a vibrationally induced mechanism rather than a translationally induced mechanism which is suggested by surface calculations.

Thus from our data and a crude idea of what the reaction potential surfaces look like, we are able to deduce some dynamical information. The many unexplained details of the vibrational dependences will have to await dynamical calculations. In any case, these systems should provide interesting test problems for models of non-adiabatic reactions.

Chapter V

REFERENCES

1. Ray Walder, J. L. Franklin, Int. J. Mass Spectrom. Ion Phys. 36, 85 (1980).

   K. P. Huber, G. Herzberg, Constants of Diatomic Molecules, Van Nostrand Reinhold, New York, 1979.

2. S. Chapman, R. K. Preston, J. Chem. Phys. 60, 650 (1974).

3. M. T. Bowers, D. D. Elleman, J. King, Jr., J. Chem. Phys. 50, 1840 (1969).

   M. T. Bowers, D. D. Elleman, J. Chem. Phys. 51, 4606 (1969).

4. K. R. Ryan, J. Chem. Phys. 61, 1559 (1974).

5. J. K. Kim, W. T. Huntress, Jr., J. Chem. Phys. 62, 2820 (1975).

6. Z. Herman, J. Kerstetter, T. Rose, R. Wolfgang, Disc. Faraday Soc. 44, 123 (1967).

   Z. Herman, J. Kerstetter, T. Rose, R. Wolfgang, J. Chem. Phys. 46, 2844 (1967).

   W. R. Gentry, E. A. Gislason, B. H. Mahan, C. W. Tsao, J. Chem. Phys. 49, 3058 (1968).

7. J. Kerstetter, R. Wolfgang, J. Chem. Phys. 53, 3765 (1970).

8. R. M. Bilotta, F. N. Preuninger, J. M. Farrar, J. Chem. phys. 72, 1583 (1980).

9. M. Vaz Pires, C. Galloy, J. C. Lorquet, J. Chem. Phys. 69, 3242 (1978).

10. M. H. Chiang, E. A. Gislason, B. H. Mahan, C. W. Tsao, A. S. Werner, J. Phys. Chem. 75, 1426 (1971).

11. H. S. W. Massey, E. H. S. Burhop, Electronic and Ionic Impact Phenomena, Oxford Univ. Press, NY, 1952, p. 478.

12. J. C. Tully in Dynamics of Molecular Collisions, Part B, W. H. Miller, ed., Plenum, New York, p. 217 (1976).

13. W. H. Miller, T. F. George, J. Chem. Phys. 56, 5637 (1972).

14. see for instance M. T. Bowers, T. Su; Adv. Electronics, Electron Phys. 34, 246 (1973).

15. W. H. Flygare, Molecular Structure and Dynamics, Prentice-Hall Englewood Cliffs, NJ, p. 408 (1978).

16. A good review is found in Ref. 14, p. 234.

17. T. R. Govers, M. Gerand, G. Marclaire, R. Marx, Chem. Phys. 23, 411 (1977).

18. M. R. Flannery, H. Tai, D. L. Albritton, Atomic Data and Nuclear Data Tables 20, 563 (1977).

19. J. L. Gardner, J. A. R. Samson, J. Elec. Spec. 13, 7 (1978).

Chapter V

FIGURE CAPTIONS

Fig. 1. Cut through $(H_2^+ + Ar)^+$ entrance channel at infinite reagent separation.

Fig. 2. Cut through $(H_2^+ + CO)^+$ entrance channel at infinite reagent separation.

Fig. 3. Vibrational effects on $H_2^+ + N_2$ cross sections.

Fig. 4. Vibrational effects on $D_2^+ + N_2$ cross sections.

Fig. 5. Vibrational effects on $H_2^+ + CO$ cross sections.

Fig. 6. Vibrational effects on $D_2^+ + CO$ cross sections.

Fig. 7. Vibrational effects on H_2^+ cross sections.

Fig. 8. Energetics for $H_2^+ + N_2$ CT, showing reagent total energies (left) and various product state energies.

Fig. 9. Energetics for $D_2^+ + N_2$ CT, showing reagent total energies (left) and various product state energies.

Fig. 10. Energetics for $H_2^+ + CO$ CT, showing reagent total energies (left) and various product state energies.

Fig. 11. Energetics for $D_2^+ + CO$ CT, showing reagent total energies (left) and various product state energies.

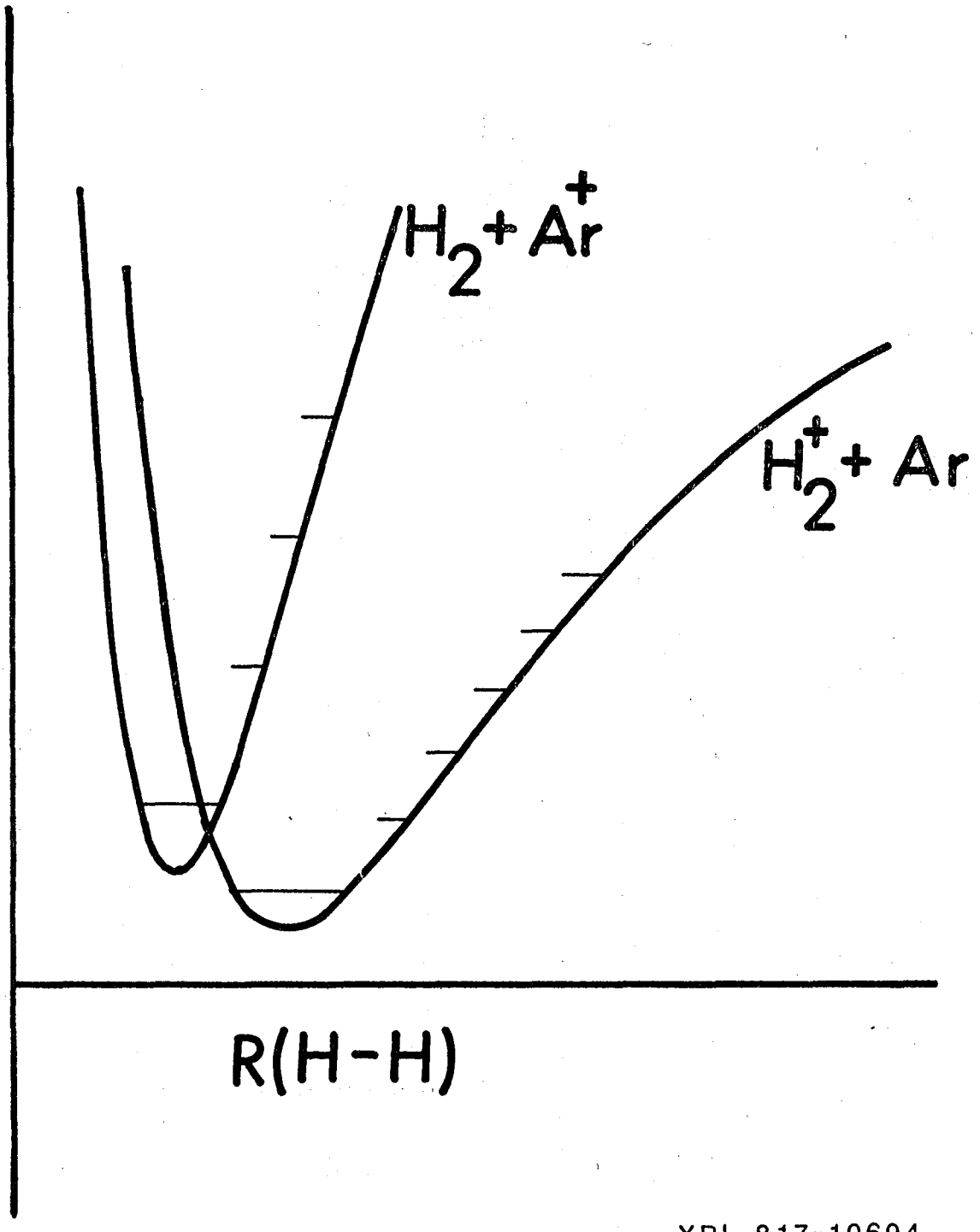

XBL 817-10694

Fig. 1

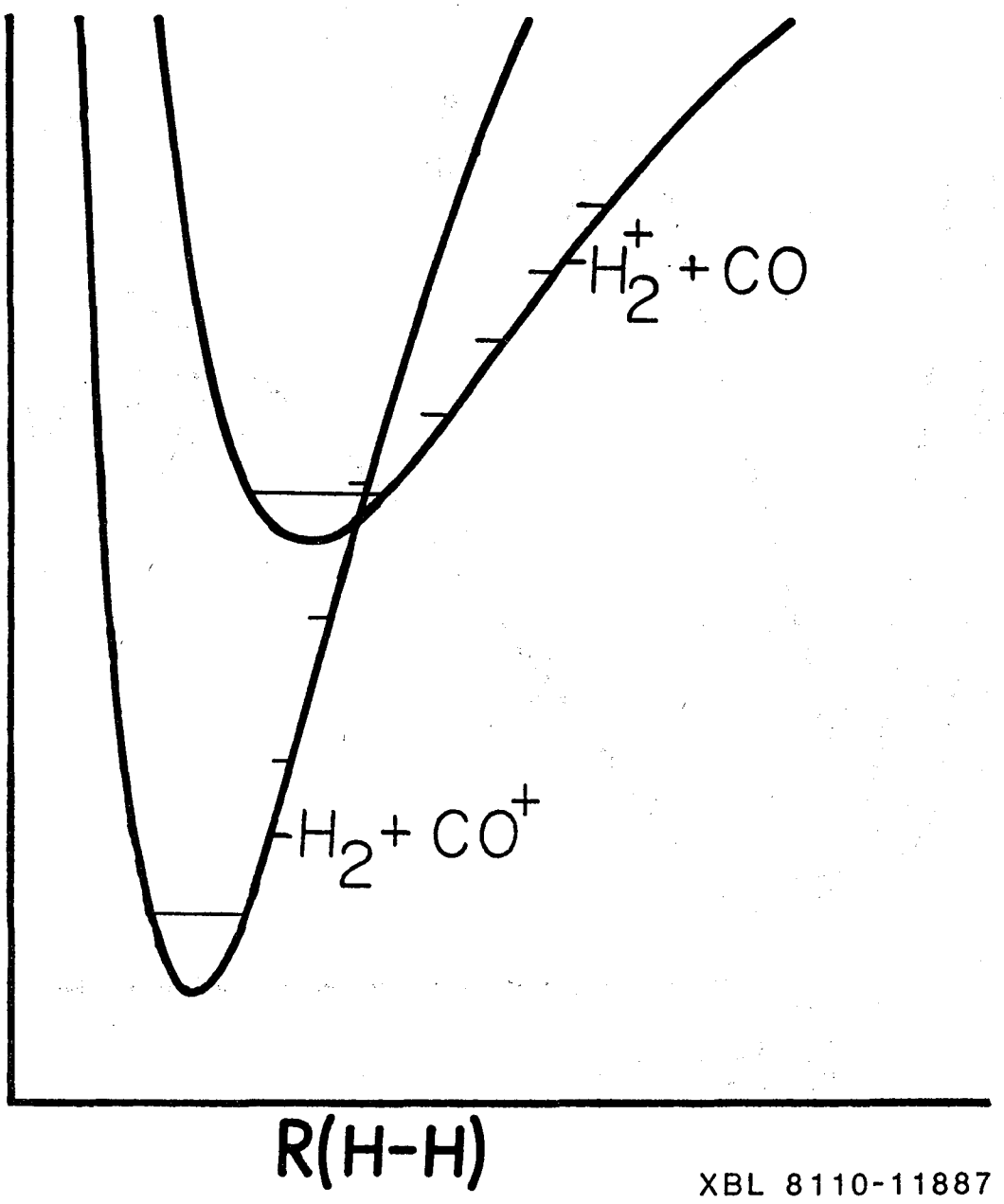

Fig. 2

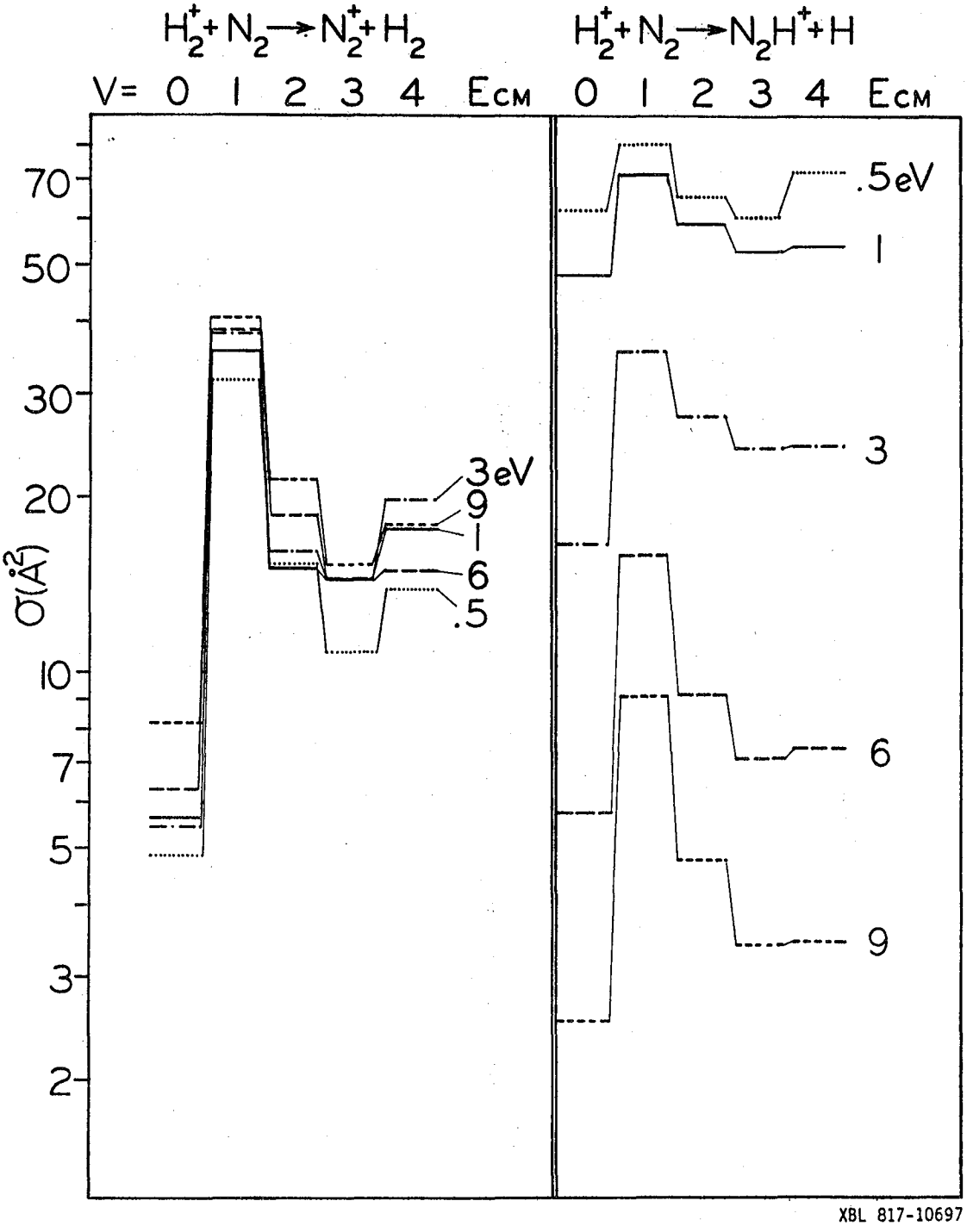
$H_2^+ + N_2 \rightarrow N_2^+ + H_2$
$H_2^+ + N_2 \rightarrow N_2H^+ + H$
V= 0 1 2 3 4 Ecm
0 1 2 3 4 Ecm
70
50
30
20
10
7
5
3
2
σ(Å²)
3eV
9
1
6
.5
.5eV
1
3
6
9
XBL 817-10697

Fig. 3

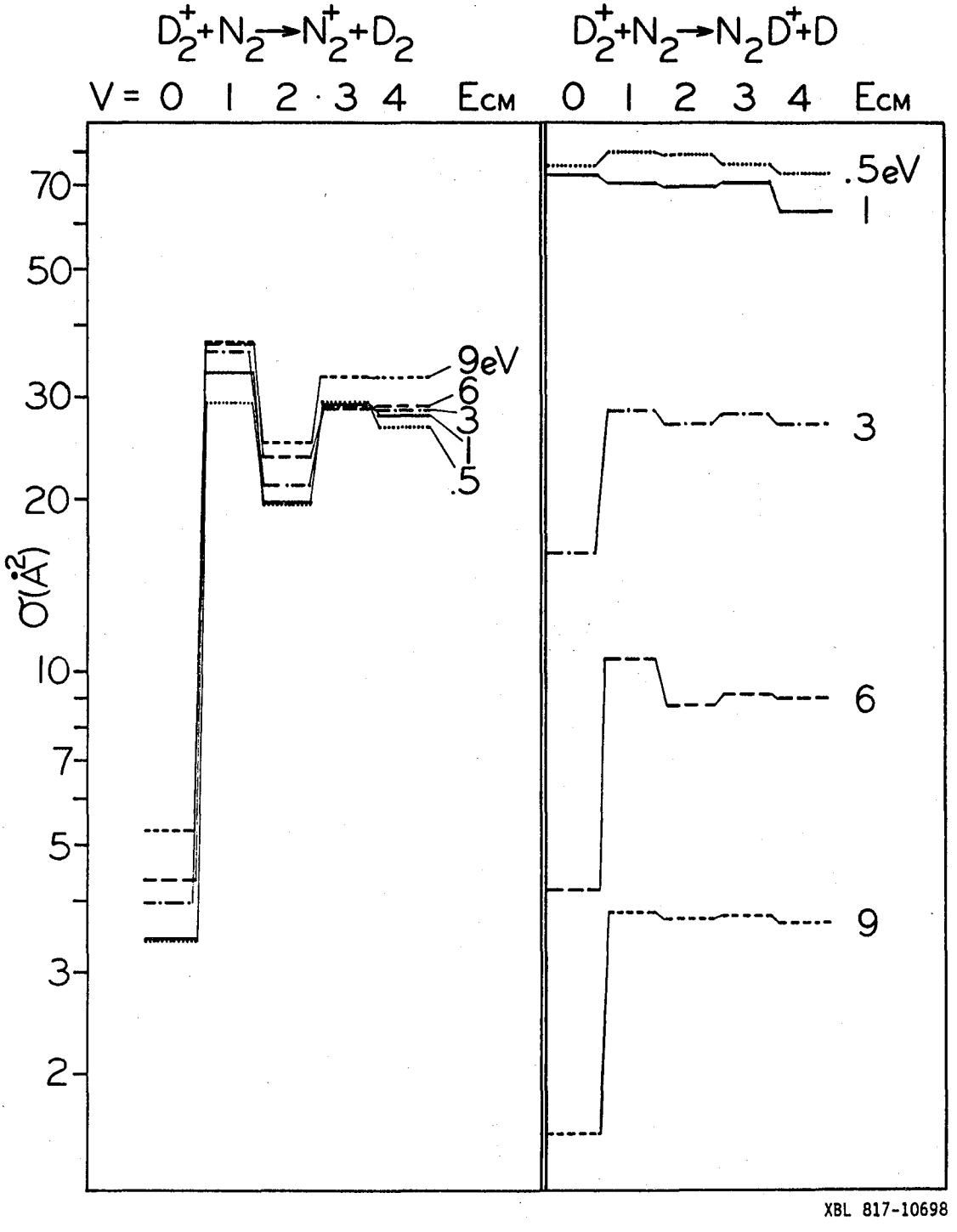
$D_2^+ + N_2 \rightarrow N_2^+ + D_2$
$D_2^+ + N_2 \rightarrow N_2D^+ + D$
V = 0 1 2 3 4 Ecm
0 1 2 3 4 Ecm
70
50
30
20
10
7
5
3
2
σ(Å²)
9eV
6
3
1
.5
.5eV
1
3
6
9
XBL 817-10698

Fig. 4

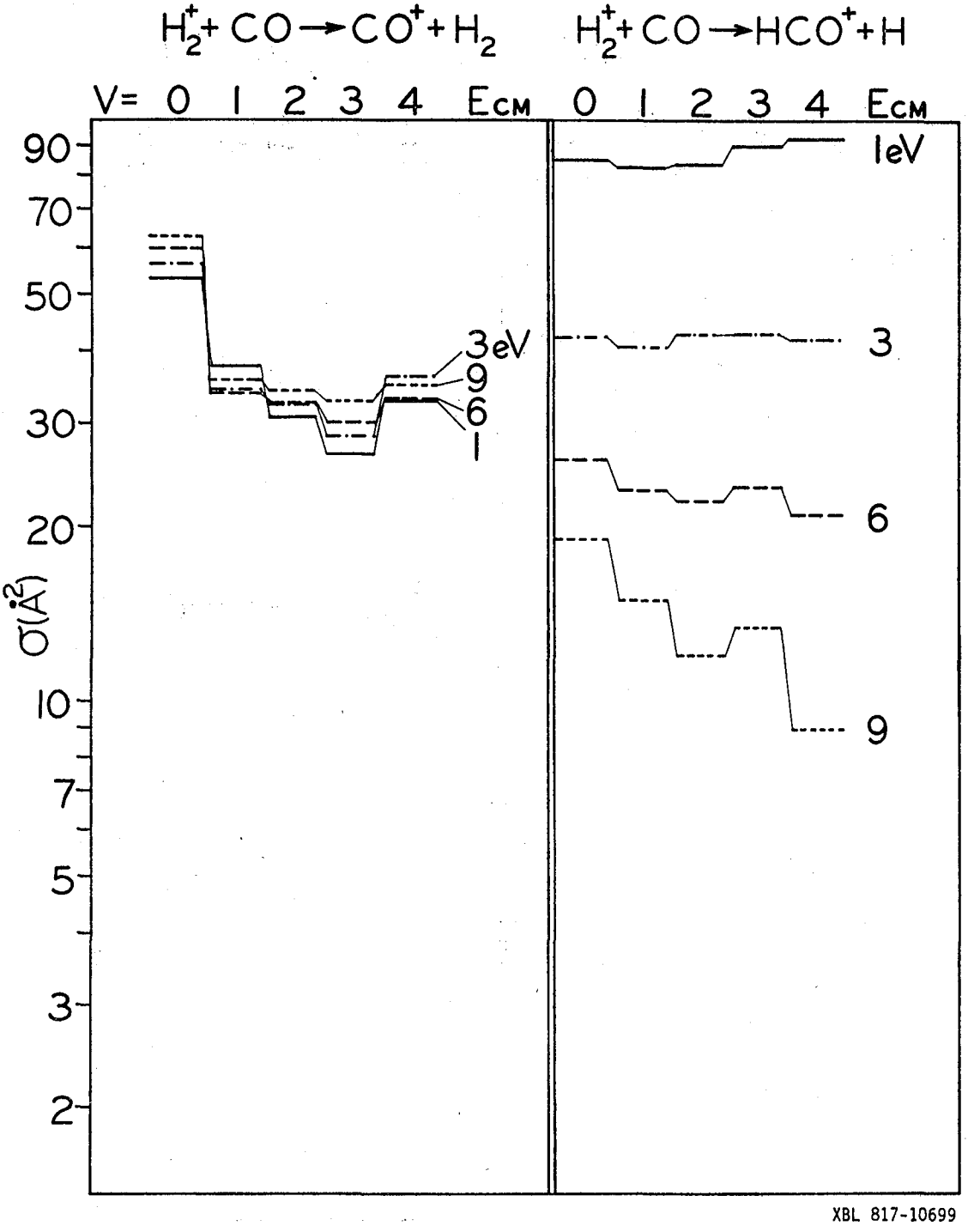
$H_2^+ + CO \rightarrow CO^+ + H_2$
$H_2^+ + CO \rightarrow HCO^+ + H$
V= 0 1 2 3 4 Ecm
0 1 2 3 4 Ecm
90
70
50
30
20
10
7
5
3
2
σ(Å²)
3eV
9
6
1
1eV
3
6
9
XBL 817-10699

Fig. 5

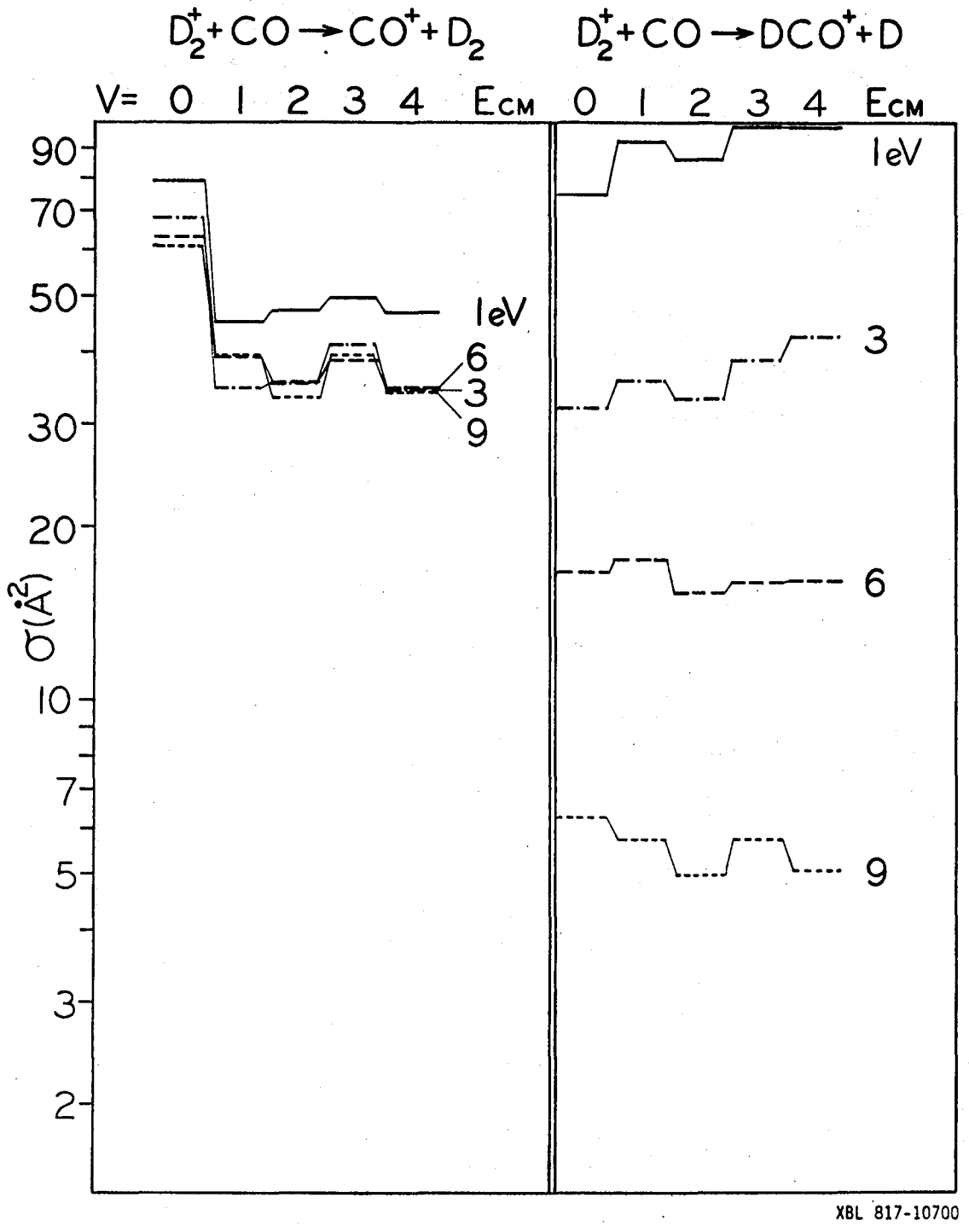
$D_2^+ + CO \rightarrow CO^+ + D_2$
$D_2^+ + CO \rightarrow DCO^+ + D$
V= 0 1 2 3 4 Ecm
0 1 2 3 4 Ecm
90
70
50
30
20
10
7
5
3
2
σ(Å²)
1eV
6
3
9
1eV
3
6
9
XBL 817-10700

Fig. 6

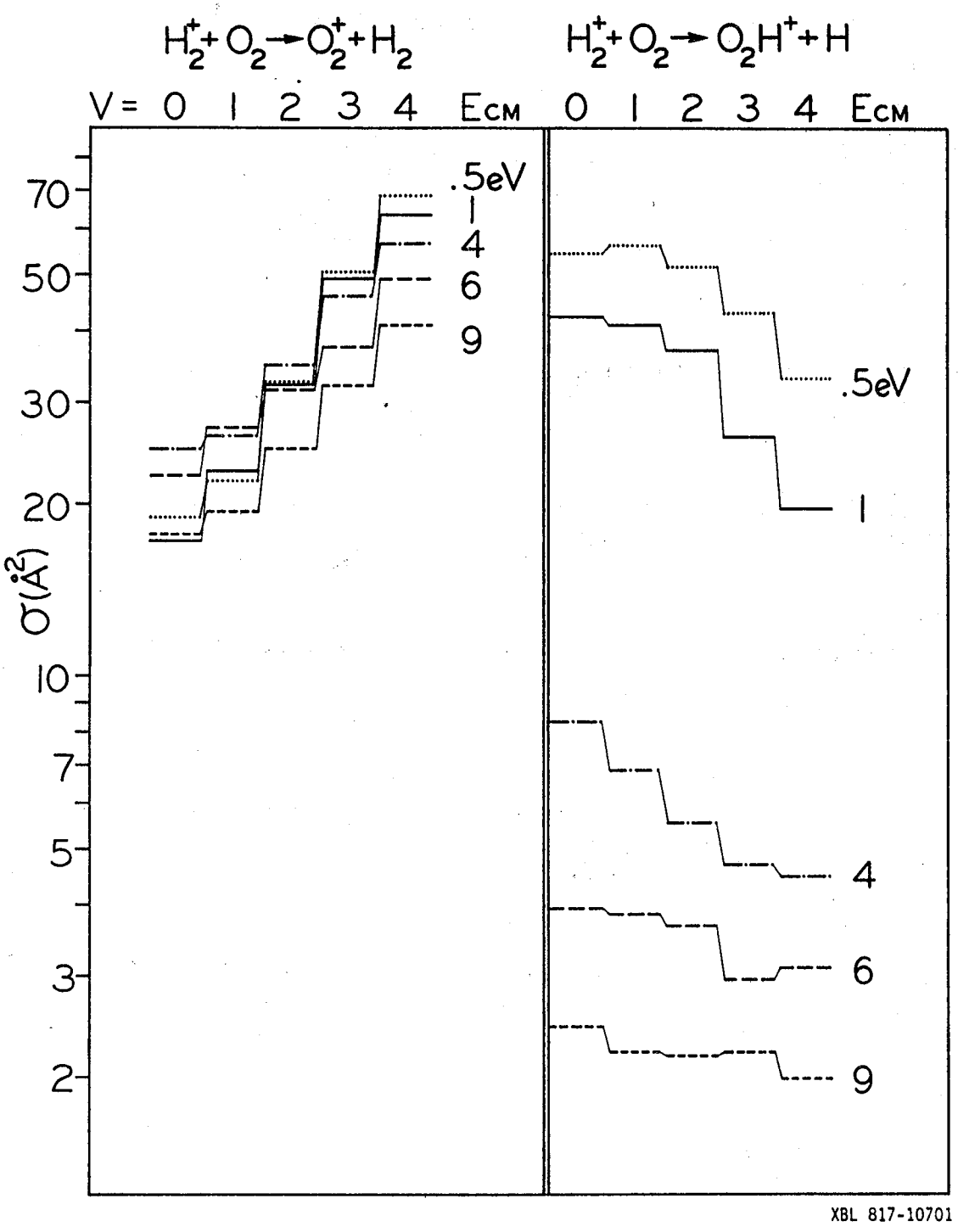
$H_2^+ + O_2 \rightarrow O_2^+ + H_2$
$H_2^+ + O_2 \rightarrow O_2H^+ + H$
V = 0 1 2 3 4 Ecm
0 1 2 3 4 Ecm
.5eV
1
4
6
9
70
50
30
20
10
7
5
3
2
σ(Å²)
XBL 817-10701

Fig. 7

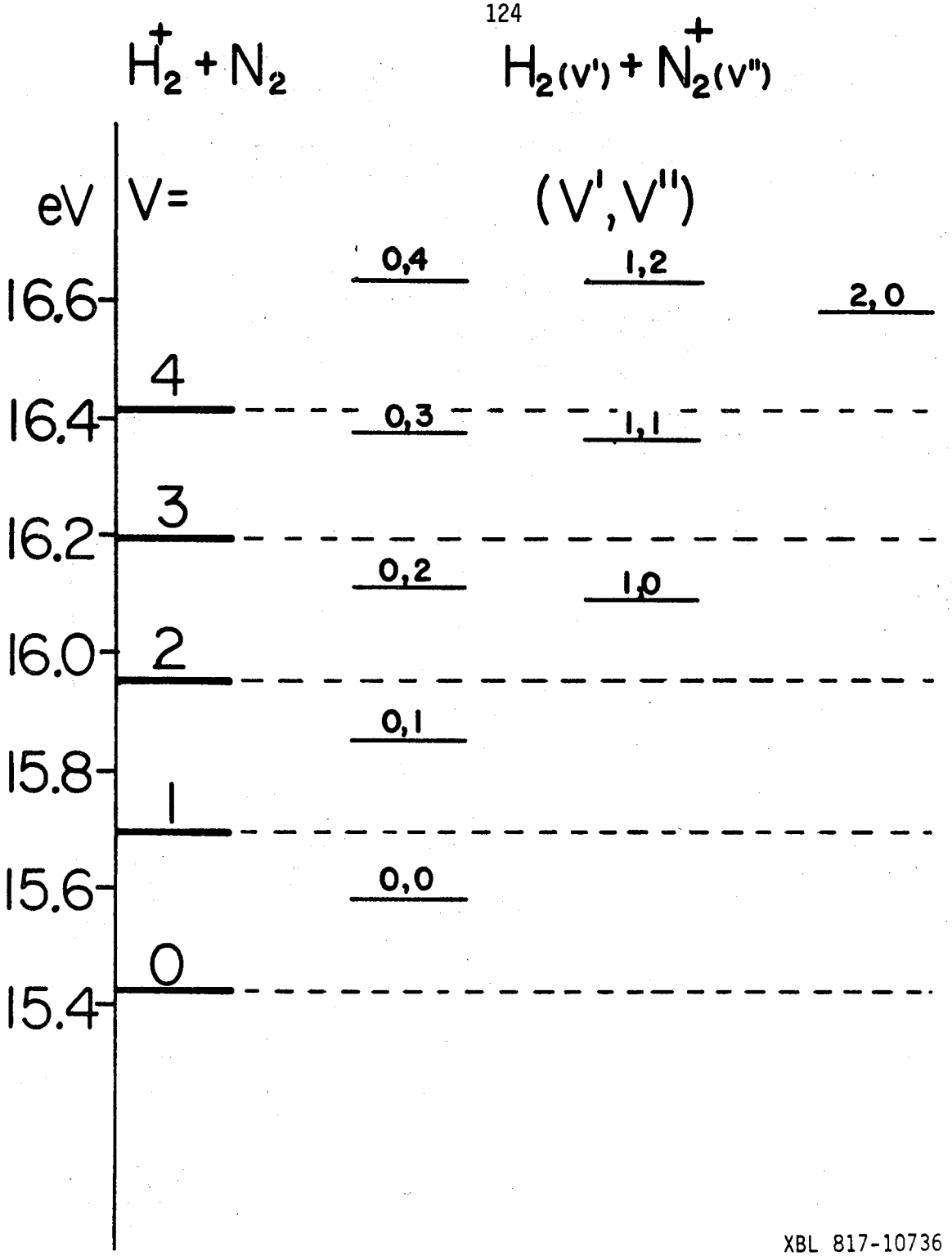
$H_2^+ + N_2$
$H_{2(V')} + N_{2(V'')}^+$
eV
V=
(V', V'')
16.6
16.4
16.2
16.0
15.8
15.6
15.4
4
3
2
1
0
0,4
1,2
2,0
0,3
1,1
0,2
1,0
0,1
0,0
XBL 817-10736

Fig. 8

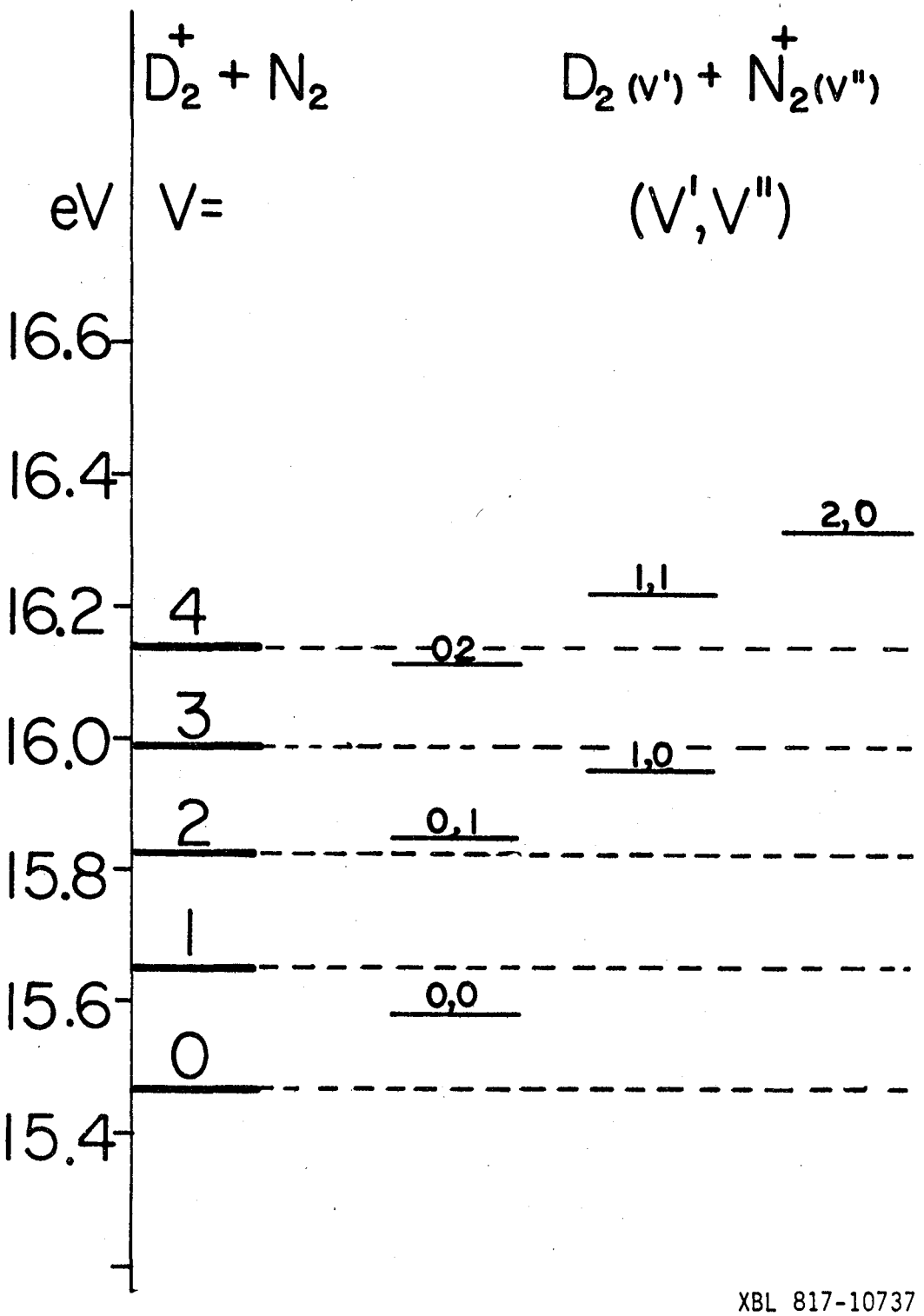
$D_2^+ + N_2$
$D_{2(v')} + N_{2(v'')}^+$
eV
V=
(V',V'')
16.6
16.4
16.2
16.0
15.8
15.6
15.4
4
3
2
1
0
2,0
1,1
0,2
1,0
0,1
0,0
XBL 817-10737

Fig. 9

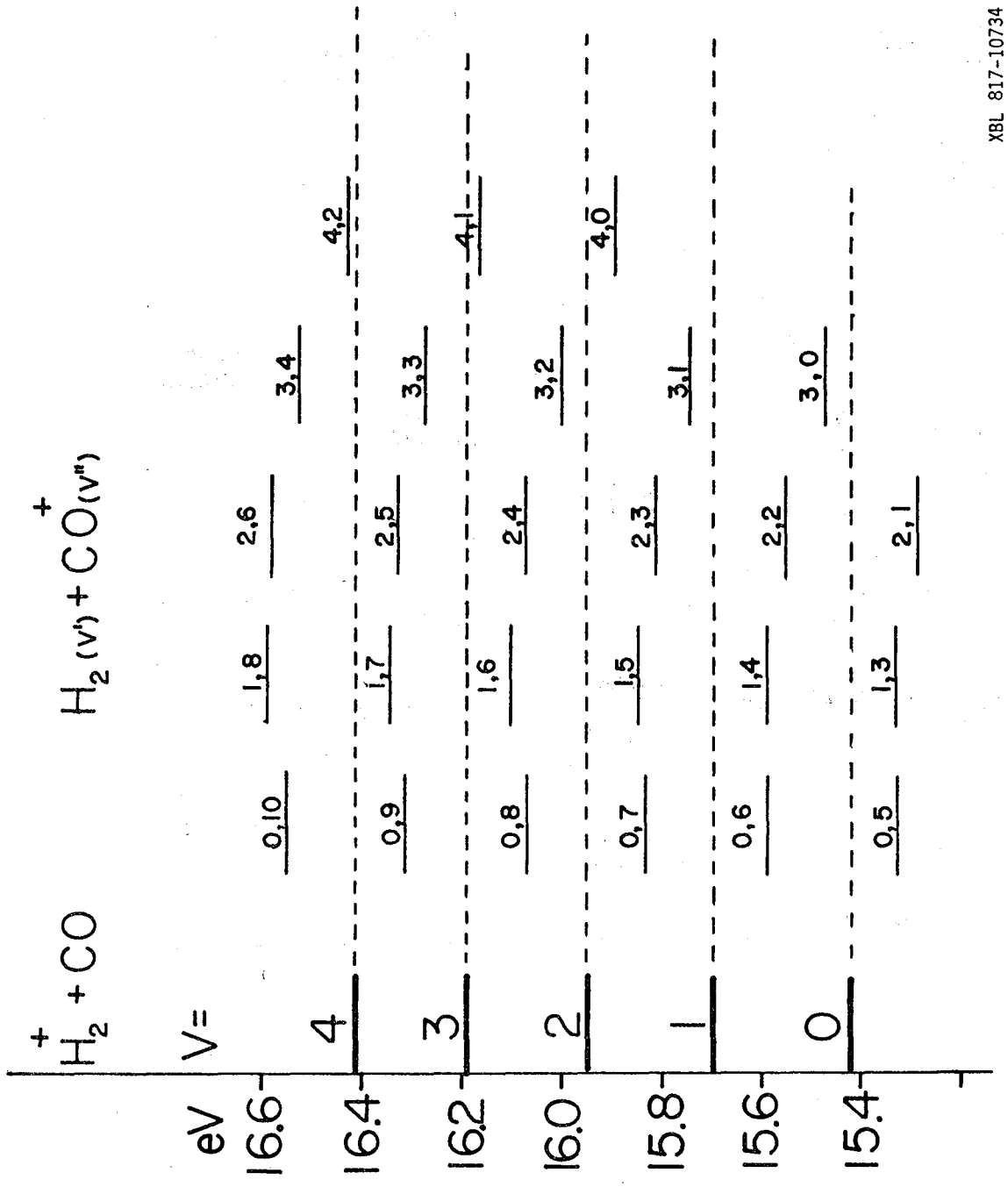

XBL 817-10734

Fig. 10

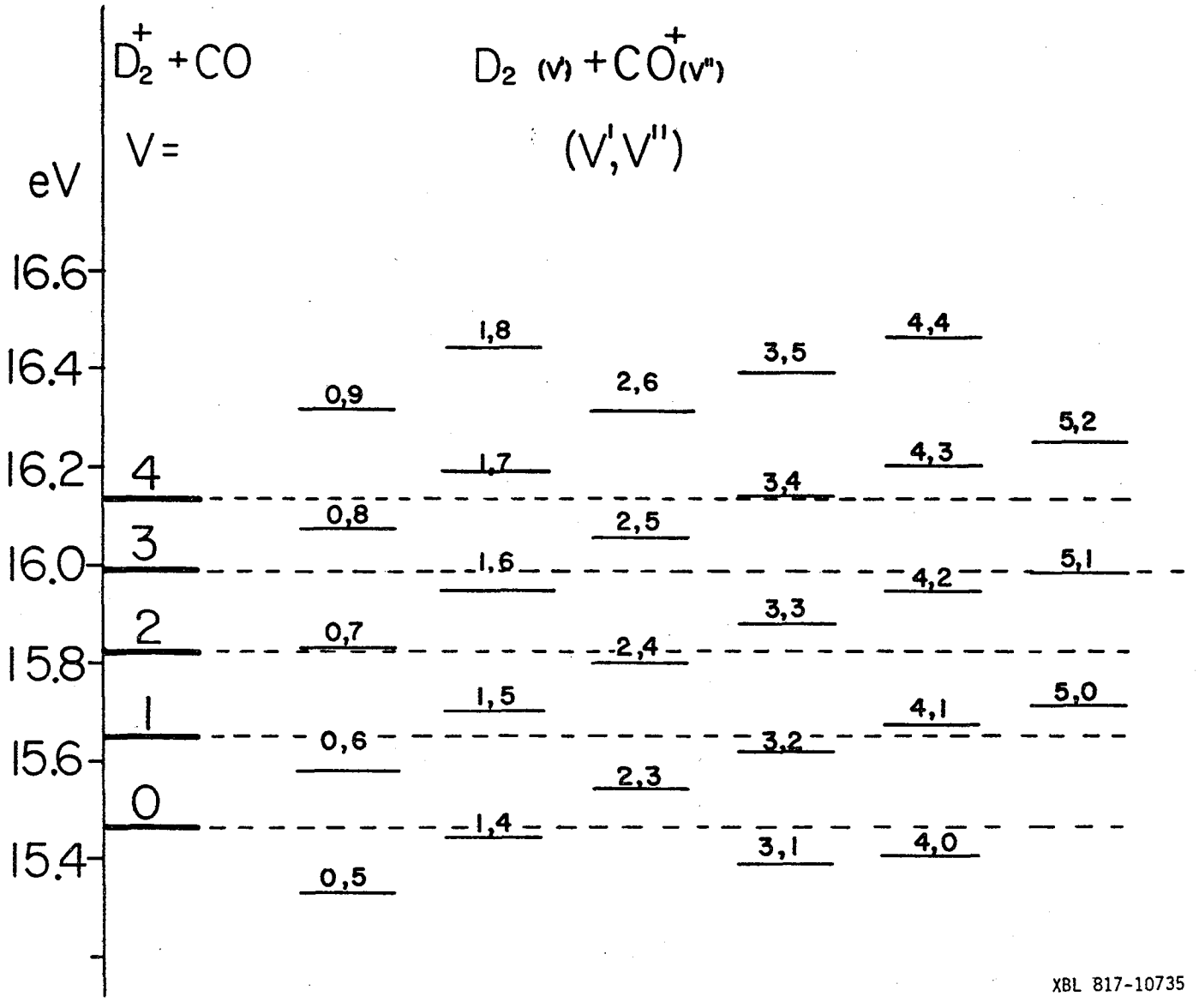
$D_2^+ + CO$
$D_2\ (V) + CO^+_{(V'')}$
V =
(V', V'')
eV
16.6
16.4
16.2
16.0
15.8
15.6
15.4
4
3
2
1
0
0,9
1,8
2,6
3,5
4,4
5,2
0,8
1,7
2,5
3,4
4,3
0,7
1,6
2,4
3,3
4,2
5,1
0,6
1,5
2,3
3,2
4,1
5,0
0,5
1,4
3,1
4,0
XBL 817-10735

Fig. 11

This report was done with support from the Department of Energy. Any conclusions or opinions expressed in this report represent solely those of the author(s) and not necessarily those of The Regents of the University of California, the Lawrence Berkeley Laboratory or the Department of Energy.

Reference to a company or product name does not imply approval or recommendation of the product by the University of California or the U.S. Department of Energy to the exclusion of others that may be suitable.

TECHNICAL INFORMATION DEPARTMENT
LAWRENCE BERKELEY LABORATORY
UNIVERSITY OF CALIFORNIA
BERKELEY, CALIFORNIA 94720